Investigating the role of PTPN13 and ENTR1 in apoptotic cell death and proliferation

The University Of Sheffield.

By:

Antonio Carmona Serrano

A thesis submitted in partial fulfilment of the requirements for the degree of:

Doctor of Philosophy

The University of Sheffield
Faculty of Science
Department of Biomedical Sciences

March 2019

Table of contents

List of figures and tables

Main figures

Supplementary Figures

Abstracts

Chapter I: ENTR-1/PTPN13 complex regulates post-endocytic sorting of the death receptor Fas

Death receptor Fas/CD95 is a crucial component in the regulation of ligand induced apoptosis in many cell types. It is well known that several cancers exhibit a decreased cell surface expression of Fas and consequently escape the control of Fas-mediated apoptosis, although underlying mechanisms are unclear.

PTPN13, a multi-PDZ domain phosphatase, directly interacts with Fas and low surface levels of Fas have been previously correlated with increased levels of PTPN13 in a wide variety of tumour cell lines. Here we report that ENTR-1, an established interacting partner of PTPN13, also regulates cell surface levels of Fas. ENTR-1 forms a novel endocytic complex with PTPN13 that controls Fas-mediated apoptotic signaling by regulating the delivery of internalized Fas receptors from the early endosomes to the endolysosomal degradation pathway. The complex mediates the endosome-to-lysosome sorting of Fas via Dysbindin-Hrs1 axis thereby controlling termination of Fas signal transduction.

Taken together, our data provide novel insights into the molecular mechanism of Fas post-endocytic trafficking and signaling. As downregulation of any component of the complex increases Fas receptor levels at the cell surface and affects the sensitivity of the cells to Fas-mediated apoptosis, our findings open possible explanations on how cancer cells regulate cell surface levels of death receptors

Chapter II: Investigating the role of PTPN13 in the Hippo pathway and cell proliferation

Recent evidence suggests that PTPN13 might be involved in the Hippo signaling pathway. The Hippo signaling pathway plays an essential role in development, tissue homeostasis and carcinogenesis and is highly dependent on external signals such as cell density or mechanical forces. Given the involvement of the Hippo cascade in processes such as cell proliferation and growth control, it is currently considered as a key pathway in the regulation of tumour progression and aggressiveness. The connection of PTPN13 with a cancer-related signaling pathway such as Hippo cascade could provide a better understanding of the physiology of cancer disease.

Strikingly, our data indicated that ENTR1, rather than its interacting partner PTPN13, is directly binding to LATS2. Thus, we hypothesize that PTPN13 might be part of a complex formed by ENTR1 and LATS. Whether this complex acts in a Hippo-dependent or independent manner still needs further investigation.

Furthermore, we found that PTPN13 has a similar behaviour to YAP, central effector of the Hippo pathway, and shuttles from the nucleus to the cytoplasm in response to an increase in cell density. The description of PTPN13 cell density-dependent shuttling together with the potential interaction of ENTR1 with LATS kinases open an interesting line of research as these results suggest that PTPN13 might be an alternative effector to the Hippo pathway that could control cell proliferation in response to external signals such as cell density.

Acknowledgement

First of all, I would like to express my most sincere gratitude to my supervisor Kai Erdmann. Not only he gave me the chance to undertake a PhD in The University of Sheffield, but he also supported and guided me in the right direction during all my PhD. Since the very beginning he always pushed me to work harder, to go beyond my comfort zone (scientifically speaking) and to be a good scientist. Every step of the way he had a constructive comment to share or a different approach to help me getting out of the disenchantment of scientific research. I really admire his enthusiasm and ethics. He definitely set a model for what I aspire to be as a scientist. Again, thank you very much for everything.

I would also like to acknowledge the help and support of my advisors Andrew Peden and Ivana Barbaric throughout my PhD. There was always a very good atmosphere during our advisory meetings and of course very helpful feedback that helped shaping my project. Special thanks to Andrew for not only providing countless constructs, antibodies, reagents and protocols used in this study but also with his valuable comments and feedback on my work.

A huge thank you to both Shruti and Aga, who patiently taught me most of the lab techniques/protocols and showed me how a real lab works. Furthermore, their excellent work set the foundations of this PhD project, which wouldn't be possible without them. Their help has been invaluable, and I am very grateful for that.

I would also like to express my gratitude to the rest of the members of the Erdmann lab, undergrads and master students that also contributed in a scientific and personal way to the project. Finally, I would like to acknowledge all the help and advice that I have received from all the people on the D and E floor of the Florey Building.

However, a PhD is not “just” science. There is a big emotional component that is essential to keep the mental strength you need to always carry on. It is a long road that you have to walk patiently by yourself, especially when the PhD it’s done far away from home. But I never walked alone this road. That is why I want to thank my closest friends back in Spain that supported me all along the way despite the distance. That is a massive contribution to this PhD and probably the reason why I never gave up and always had passion and motivation to keep going even in the darkest hours. This PhD thesis also goes for them.

Finally, I want to thank my family, particularly my parents and my sister, for supporting me emotionally (and financially) and giving me the opportunity to fulfil my ambitions since I was a kid.

Now, show must go on!

Cheers,

Gracias,

Declaration

I declare that the work presented in this thesis is my own composition and has been carried out by myself unless otherwise stated. I confirm that this work was done while in candidature for a research degree at The University of Sheffield. Most of this work has been published before submission.

Figures and consulted work from other publishers have been clearly acknowledged. Where I have quoted from the work of others, the source is always given. I have acknowledged all main sources of help.

Where the thesis is based on work done by others, I have described it clearly in the introduction sections and did not present it as my results. Where the work was done in collaboration, I have acknowledged clearly exactly what was done by others and what I have contributed myself.

Antonio Carmona Serrano

March 2019

1. Objectives

Chapter I. PTPN13/ENTR-1 complex regulates post-endocytic sorting of the death receptor Fas

As described in the introduction, PTPN13 is a negative regulator of Fas receptor mediated apoptosis although the exact molecular mechanisms remain unclear. The revelation of ENTR1 as a key regulator in the endocytic trafficking of Fas led us to further investigate the potential existence of a PTPN13/ENTR1 complex that modulates levels of Fas at the cell surface and sensitivity to Fas-mediated apoptosis. Thus, the main objectives of this project are:

- To determine if ENTR1 and PTPN13 form a novel endocytic complex and are involved in the regulation of Fas receptor trafficking and apoptotic signaling.
- To unveil key aspects of ENTR-1 dependent post-endocytic trafficking of Fas receptors and how this is mediated by the sorting/recycling machinery.
- To understand how Fas-induced caspase activity can regulate ENTR1-dependent Fas receptor trafficking.

Chapter II. Investigating the role of PTPN13/ENTR1 in the Hippo pathway and cell proliferation

Recent evidence suggests that PTPN13 might be involved in the Hippo signaling pathway. The Hippo signaling pathway plays an essential role in development, tissue homeostasis and carcinogenesis and is highly dependent on external signals such as cell density or mechanical forces. Given the involvement of the Hippo cascade in processes such as cell proliferation and growth control, it is currently considered as a key pathway in the regulation of tumour progression and aggressiveness. Accordingly, the main objectives of this project were:

- First, to validate the potential interaction between PTPN13 or/and ENTR1 and LATS kinases, central kinases of the Hippo pathway.
- Second, to determine if PTPN13 subcellular localization can be influenced by cell density, in a similar fashion to YAP, central effector of the Hippo pathway.

1. Introduction

I. Fas-mediated apoptosis

1. Apoptosis: basic concepts

Programmed cell death, also known as apoptosis, is an essential process that keeps the homeostasis of living organisms and the correct growth and development of embryo or tissues by selectively terminating cells and maintaining cell populations balanced[1]. Apoptosis can also be triggered as a defensive mechanism (for example in immune reactions or upon damage by disease or noxious agents)[2]. The term "apoptosis" (derived from the Greek "apo-" which means "off" and "-ptosis" which means "falling") was used for the first time back in 1972 by Kerr, Wyllie and Currie[3]. It was described as a "morphologically distinct form of cell death and a mode of programmed cell death which involves the genetically determined elimination of cells". Apoptosis is a fine-tuned physiological process that implies several morphological changes in the cell, namely blebbing, rounding up and shrinkage, eventually leading to DNA fragmentation and subsequent cell death.

Apoptosis is a key element in the immune surveillance, and defective apoptotic signaling is partially responsible of autoimmune-related diseases and cancer. Apoptosis eliminates autoreactive lymphocytes or those which are not able to recognize external antigens, assuring the selection of non-defective lymphocytes[4, 5].

Depending on the activation components and the involvement of mitochondrial effectors two major apoptotic signaling mechanisms have been described: the intrinsic and the extrinsic apoptosis signaling pathways[6-8]. External stress (UV radiation) and cellular stress (DNA damage, oxidative stress, growth factor withdrawal) can elicit the intrinsic pathway which involves the Bcl-2 proteins and mitochondrial outer membrane permeabilization (MOMP). On the other hand, the extrinsic pathway is mediated by a family of transmembrane receptors, the death receptors (DR) that require binding of specific ligands to induce the apoptotic signaling[1, 6-8].

2. Death Receptors

Death receptors are part of the tumour necrosis factor receptor superfamily (TNFRSF) and play a cardinal role in the extrinsic apoptotic signaling, but also participate in the intrinsic apoptotic signaling. DRs are characterized by a homologous sequence located in their cytoplasmic tail, the so-called death domain. Highly conserved and found in nearly all mammalian cells, they are involved in other signaling pathways such as inflammation, lymphocyte homeostasis and tissue development[1, 9-12]. Death receptors were initially recognized as potent inducers of apoptotic cell death upon binding of specific ligands. To date, the following death receptors have been described: Fas, TRAIL-R1 or DR4 (TNF related apoptosis inducing ligand receptor-1), TNFR1 (tumour necrosis factor receptor 1), TRAIL-R2 (TNF related apoptosis inducing ligand receptor-2), DR3 (death receptor 3), DR5 (death receptor 5), DR6 (death

receptor 6), Nerve growth factor receptor (NGFR) and ectodysplasin A receptor (EDAR)[11].

The main common feature of DR is the recruitment of intracellular adapter proteins upon ligand binding and the formation of multiprotein complexes. DRs associate with death domain containing adaptor molecules such as FADD (Fas-associated death domain) and TRADD (TNF-receptor associated death domain), which are able to initiate different but not mutually exclusive apoptotic and non-apoptotic responses.

DR signaling is not only inducing apoptotic cell death, but also activates pro-inflammatory and pro-tumour pathways. The outcome of DR responses is highly dependent on the cellular context, cell type or the particular DR receptor involved[1, 13]. Consequently, there has to be an exquisite spatiotemporal regulation of the receptor-associated signaling complexes and downstream effectors. In particular, receptor trafficking and recruitment in specialized endocytic compartments are potential regulatory elements that guarantee the proper functioning of DR signaling[13].

2.1 The role of caspases in DR-mediated apoptosis

Caspases (cysteine-aspartic proteases) are the key effectors in the DR-mediated apoptotic signaling and represent an important family of proteases. Caspases mediate the cleavage of target proteins in aspartate residues within their C-terminus[14].

There are two types of caspases in the apoptotic pathway, which are categorized according to their activation mechanism. On one hand, initiator pro-caspases (e.g. caspases 8 and 9) are able to recruit other pro-caspases and undergo dimerization. Upon dimerization, both pro-caspases are autoproteolytically cleaved and subsequently activated. On the other hand, executioner caspases (e.g. caspases 3, 7 and 6) are activated by cleavage by the initiator caspases[15].

In particular, activated executioner caspases cleave a wide range of substrates resulting in membrane blebbing, DNA degradation and nuclear/cytoskeleton fragmentation[16]. Moreover, they generate a positive feedback loop by cleaving other executioner/initiator caspases, which eventually leads to a massive dysfunction in cell functions and death.

Despite of being highly homologous, the activity of the different executioner caspases has been shown to be not redundant. Slee and collaborators demonstrated that caspase 3 is the leader executioner caspase whereas caspase 6 and 7 play more specialized roles[17]. Caspase 3 was found to be necessary for most of the proteolytic events that lead to mitochondrial and nuclear fragmentation, whereas caspase 6 and 7 did not target most of caspase 3 substrates. Strikingly, depletion of either caspase 6 or 7 had a minimal effect in these final apoptotic events[17].

Interestingly, caspases are not only essential in apoptotic cell death. New studies are suggesting their active involvement in other cellular processes like cell cycle, proliferation, migration and receptor internalization[18].

3. Fas receptor mediated apoptosis

We have provided a basic overview of death receptors and their effectors, the caspases. Next, we will describe a particular cell death receptor, Fas, which constitutes the main subject of the present thesis.

Fas (FS7-associated cell surface antigen), also known as APO-1 (apoptosis antigen 1) or CD95 (cluster of differentiation 95) was discovered in 1989 and is considered a member of the tumour necrosis receptor family. In humans, Fas gene is located on chromosome 10q24.1, contains 9 exons (for a total 26 kb of DNA) and encodes a 335 amino acid protein, with 157 extracellular amino acids and 145 amino acids in the intracellular domain. There are at least 7 variants of mRNA transcripts generated by alternative splicing that encode soluble forms of the receptor[13, 19, 20].

Fas is a type-I transmembrane glycoprotein that exhibits extracellular, transmembrane and intracellular domains. On one hand, the extracellular part contains three cysteine-rich domains (CRDs) required for ligand binding and a pre-ligand assembly domain (PLAD) necessary for receptor multimerization and subsequent signaling conduction. The binding with Fas ligand is mediated by the CRD2 and the first loop of the CRD3[21, 22]. PLAD mediates the trimerization of Fas receptors by homotypic interactions when they are localised to the cell surface[23]. On the other hand, the C-terminal half of the intracellular domain contains a conserved death domain, responsible for the actual apoptotic signaling[24] (Figure 1).

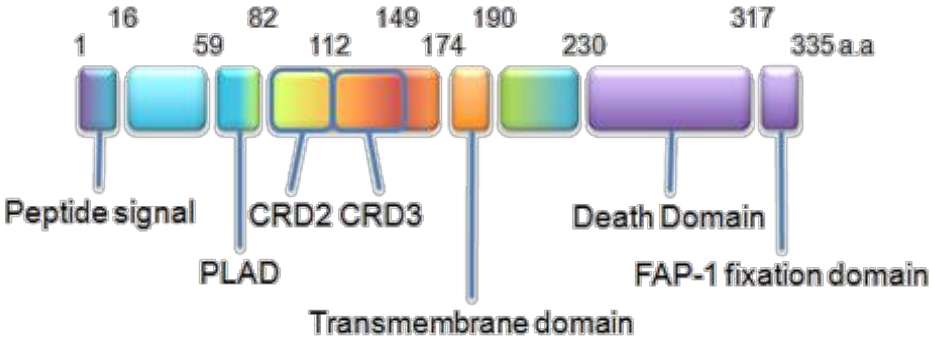

Figure 1. Scheme of the modular structure of Fas receptor. The N-terminal region contains a signal peptide followed by a pre-ligand assembly domain (PLAD) and cysteine rich domains (CRD). The cytoplasmic domain contains an 87 amino acid long death domain followed by C-terminal FAP-1 (Fas associated phosphatase-1) binding domain. Figure adopted from Atlas of Genetics and Cytogenetics in Oncology.

In the plasma membrane, Fas receptors can be found as pre-associated trimers that form stable microaggregates upon ligand binding. Extensive evidence supports the translocation of these Fas micro-aggregates into lipid rafts, specialized areas of the plasma membrane rich in cholesterol and sphingolipids. This results in the formation of higher molecular Fas structures and coalescence into large signaling platforms in a highly ordered lipid environment[25, 26].

Fas-ligand binding to Fas receptors in the cell surface induces a conformational change that allows its cytoplasmic death domain to engage with other proteins and begin the formation of DISC complex (death-inducing signaling complex)[27, 28]. Key to the formation of DISC is the association of Fas with FADD (Fas associated death domain protein), which contains a death effector domain (DED) that rapidly recruits the proteases procaspase-8 and 10[7, 29, 30].

These are considered the early steps of Fas-induced apoptosis, as they occur 5 - 10 minutes after Fas activation.

Subsequently, Fas undergoes internalization into the endosomal compartments, where DISC is accumulated[31]. High levels of DISC trigger autoproteolytic cleavage of pro-caspase 8 into active caspase 8[32]. More specifically, homo-oligomerization or hetero-oligomerization with c-FLIPL is responsible of the autoproteolytic activation of pro-caspase 8 within the DISC complex[33-35]. Activated caspase 8 initiates a protease cascade involving executioner caspases 3, 6 and 7 further downstream leading eventually to apoptosis. Executioner caspases carry out the actual process of apoptosis resulting in nuclear and cytoskeleton fragmentation[1, 7, 9] (Figure 2).

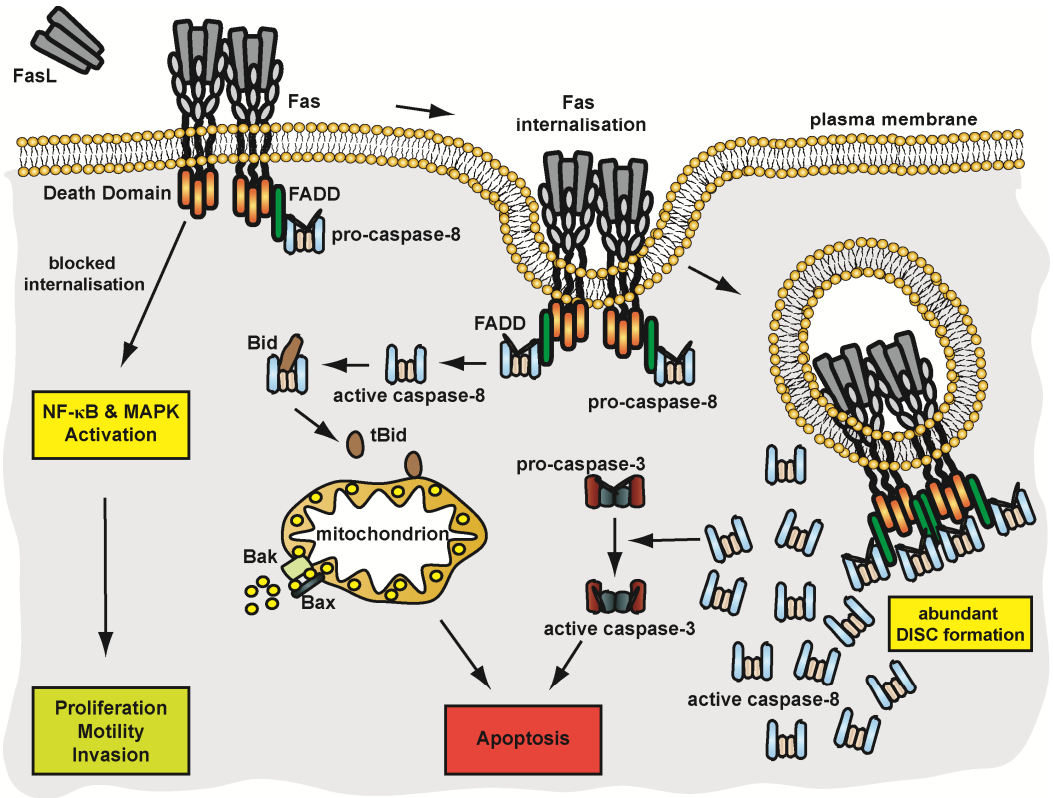

Figure 2. Fas-mediated apoptosis, the bigger picture. Fas ligand binds to Fas receptor and induces the assembly of DISC complex and Fas internalization. Once in the endosomal compartment, abundant DISC complex is recruited and cleaves pro-caspase 8. The activated caspase 8 launches the apoptotic events by initiating a cascade of executioner caspases. Type II cells require the intervention of the mitochondrial pathway to induce the intrinsic apoptotic signaling, also mediated by caspase 8. Figure adopted from Schneider-Brachert et al. (2013)[13].

Cells can be categorized into two different types depending on the mode of transition from apoptosis initiation to the execution phase. Type-I cells have a rapid and efficient DISC assembly which potently activates the initiator caspases to trigger cell death via executioner caspases. In the case of type-II cells, DISC signaling is weak and delayed leading to an insufficient activation of initiator caspases. That is why type-II cells have to rely on a mitochondrial amplification loop to efficiently activate executioner caspases and induce cell death[6, 13, 30, 36]. In brief, effective killing does not require mitochondrial involvement in type-I cells, such as SKW6.4, BJAB or H9, but does in type-II cells, such as Jurkat, hepatocytes and CEM[30, 36].

As it is shown in Figure 3, type-II cells cleave Bid (BH3-interacting domain death agonist) via activated caspase 8, producing truncated version of Bid that are translocated to the outer mitochondrial membrane. There, truncated Bid activates Bak (Bcl-2 homologous antagonist/killer), which oligomerizes with Bax (Bcl-2 associated X-protein) to form pores in the mitochondrial membrane, losing its permeability and allowing pro-apoptotic proteins (cytochrome c, SMAC/DIABLO, HtrA2/Omi) to be released into the cytoplasm. Subsequently,

cytochrome c forms a complex with Apaf-1, forming the apoptosome, responsible of caspase 9 activation. Caspase 9 is then able to potently activate executioner caspase 3 and induce cell death, converging at this step with the type-I apoptotic pathway[6, 13, 37, 38] (Figure 3).

Two studies provided further evidence on the mitochondrial pathway importance in type-II cells, as overexpression of inhibitors of the mitochondrial pathway Bcl-2/Bcl-xL blocked Fas-mediated apoptosis in type-II cells and not in type-I cells[30, 39]. However, mitochondrial activation occurs in both type-I and type-II cells, highlighting that the difference between both types does not reside in the mitochondrial activation itself but in other factors such as the efficiency of the DISC complex assembly and signaling. For instance, cellular location where the DISC complex is assembled might affect the quality of the DISC formation and therefore potentiate or weaken the signaling downstream[31].

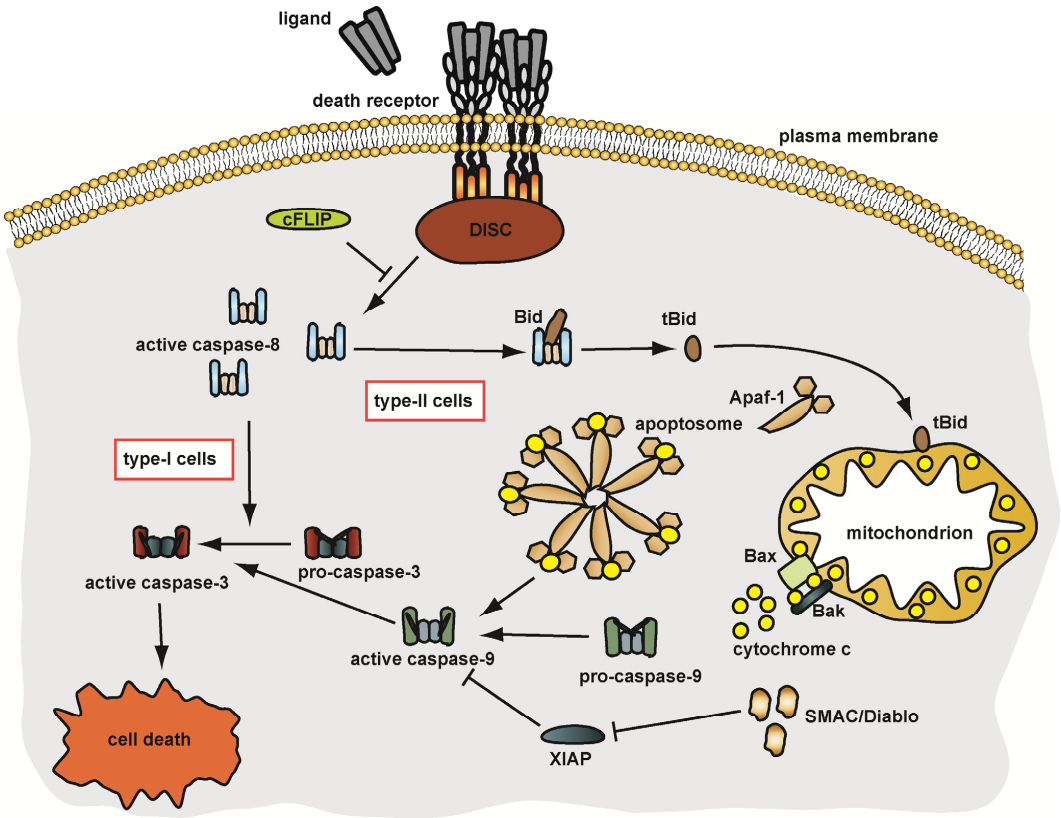

Figure 3: Types of DR-mediated apoptosis induction. Figure adopted from Schneider-Brachert et al. (2013)[13].

Finally, it is also necessary to mention Fas ligand (FasL) characteristics. Gene encoding FasL is localized on chromosome 1q23 and has a length of 8 kb[40]. The extracellular region of FasL contains a TNF homology domain, whereas the intracellular domain has an extended proline-rich region, tyrosine phosphorylation sites and a casein kinase phosphorylation motif, implicated in FasL sorting and reverse signaling[41, 42]. FasL can be found in two functional forms: the soluble version is generated from the cleavage of the membrane bound version but only membrane bound or artificially immobilised FasL stimulates strong receptor activation[43].

3.1 Fas mediated apoptosis: physiological and pathophysiological implications. Relevance in cancer disease

The Fas/FasL duo was long viewed as a system that mediates apoptosis induction to maintain immune homeostasis. At present, it is clear that Fas-mediated signaling goes beyond that and is of great relevance in many physiological systems and in cancer disease[44]. Notably, FasL activation of Fas signaling has revealed multiple non-apoptotic activities: it is essential in liver regeneration upon partial hepatectomy[45], stimulates renal tubular epithelial cell migration[46], provides a mitogenic signal in quiescent hepatic cells through EGFR[47] or plays a fundamental role in neurite outgrowth[48].

Extensive literature has reported that Fas-mediated apoptosis plays a critical role in the immune system acting as a guardian against autoimmunity and keeping immune cells homeostasis. FasL is predominantly expressed in activated T lymphocytes and natural killer cells and is constitutively expressed in tissues of immune-privilege sites such as the testis and eye[9]. Experiments with mutant mice have demonstrated the importance of Fas-mediated apoptosis in the maintenance of cell homeostasis and in the deletion of dysfunctional or autoreactive T cells. As a matter of fact, mice with FasL dysfunction exhibit a phenotype of generalized lymphoproliferative disease (lpr). Consequently, these mice are more sensitive to autoimmune diseases and display symptoms such as lymphadenopathy, production of auto-antibodies, hypergammaglobulinemia and accumulation of $CD4^{-}CD8^{-}$ T-cells[49, 50]. Moreover, CD8+ and CD4+ T-cells use Fas

receptor mediated apoptosis to eliminate virus-infected cells as well as cancerous cells by infiltrating the tumour site[51].

Fas has also been extensively studied in the context of cancer and is considered a fundamental regulatory element in carcinogenesis and tumour development. Fas receptor expression is highly elevated in many cancer cells (e. g. hepatocellular, renal, ovarian and pancreatic)[52]. However, most cancer types are relatively resistant to Fas-mediated apoptosis. Several studies have shown that this resistance might be achieved through multiple ways. First, the apoptotic signal can be inhibited at the level of DISC by reducing the expression of FADD and pro-caspase 8[53, 54], as well as at the level of downstream signal proteins via promoting the degradation of anti-apoptotic proteins such as Bcl-2 family proteins[55]. Furthermore, cancer cells also regulate the expression of cell surface Fas in order to survive. The expression of Fas in the cell surface is required for effective apoptosis and consequently cancer cells have developed strategies (such as reduction of cell surface Fas) to escape the immune surveillance[51, 56, 57]. Lastly, several studies have suggested that once cancer cells acquire resistance to Fas-mediated apoptosis, further stimulation of Fas is tumourigenic[58-61].

Given the fact that almost all types of cancers are resistant to Fas-mediated apoptosis, stimulating Fas might not be an effective approach to killing cancer cells. Moreover, administration of recombinant FasL to enhance apoptosis stimulation cannot be used therapeutically, as major side effects such as massive apoptosis induction in the liver have been observed[62].

Besides its obvious pro-apoptotic effects, Fas signaling has also been recognized to have cancer-relevant non-apoptotic and tumour-promoting activities. FasR and FasL were found to be critical survival factors for cancer cells, protecting and promoting cancer stem cells (CSCs)[45, 48, 58, 63]. Remarkably, recent publications have identified several tumour-promoting FasR/L activities that could serve as potential targets for cancer therapy (summarized in Figure 4)[51]. Consequently, inhibiting FasL activity or targeting FasL mRNA to induce DICE (death induced by CD95R/L elimination)[64] instead of using FasL to induce apoptosis in cancer cells represents a potential therapeutic approach, alone or in combination with standard chemotherapy or immune therapy[51, 65-67].

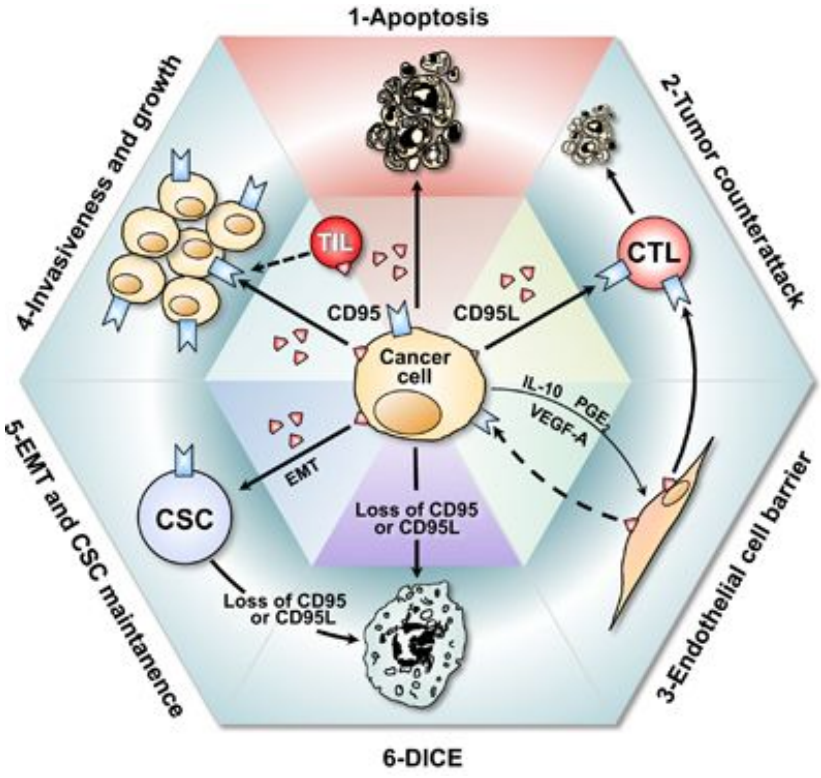

Figure 4. The multiple functions of Fas/FasL system in cancer: the yin and the yang. Apoptosis-sensitive cancer cells can be eliminated by triggering the canonical Fas-mediated apoptosis signaling pathway (tumour supressing activity) (1). On the other

hand, FasL carries out several tumour promoting activities: indirect, such as suppression of immune response in cancer micro-environment by FasL generated by either tumour cells (2) or by the surrounding endothelial cells (3); or direct, like the promotion of tumour growth and invasiveness (4) or the acquisition of CSC phenotype (5). Finally, the elimination of Fas signaling leads to an irreversible and effective type of cell death, DICE, which predominantly affects CSCs (6). Adopted from Peter et al. (2015)[51]

Fas-mediated apoptotic and non-apoptotic signaling constitutes a promising target for development of therapeutic strategies against cancer. However, its dual tumour suppressing/promoting activity opens many questions that need to be addressed first.

3.2 Trafficking of death receptor Fas

Cell surface receptors such as Fas are transported back and forth to the plasma membrane by the two major intracellular trafficking mechanisms: exocytosis and endocytosis. On one hand, receptors are synthesized in the cytoplasm and transported to the cell surface through secretory vesicles via the exocytic pathway. On the other hand, upon ligand activation the receptors present in the cell surface are internalized and trafficked within the cell via endocytic pathways.

The endocytic pathway comprises the internalization of cell surface receptors from the plasma membrane (in a clathrin dependent or independent fashion) into the early endosomes, where sorting into recycling or degradation pathway occurs[68] (Figure 5). If recycled, receptors are sorted into recycling endosomes and directed back to the plasma membrane. On the contrary,

receptors destined for degradation are transported from sorting to late endosomes and finally transported to the lysosomes, where degradation of the majority of internalized proteins takes place[68, 69].

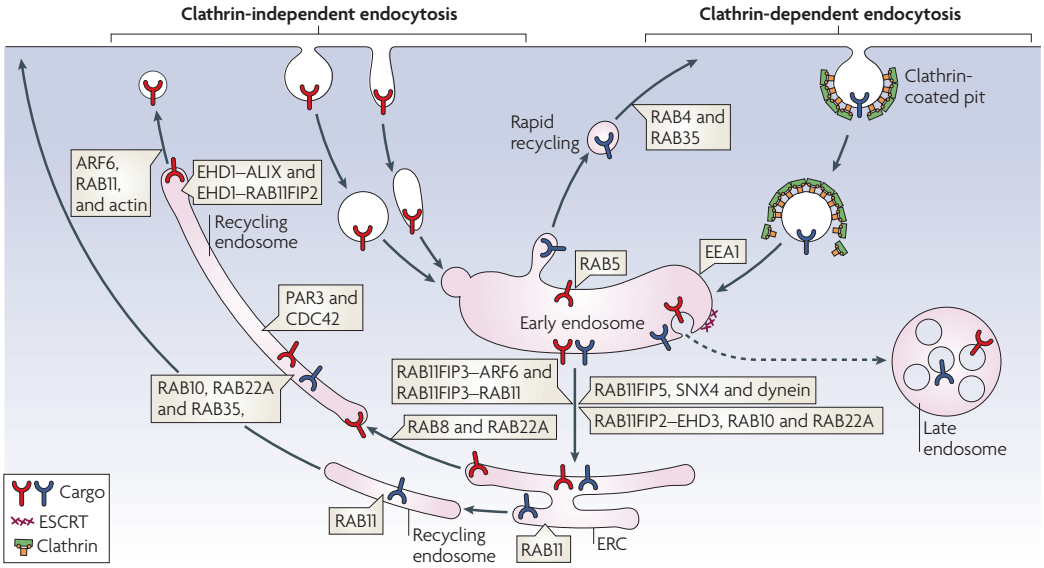

Figure 5. Pathways of endocytosis and endocytic recycling. Itinerary of cargo proteins entering cells by clathrin-dependent (blue cargo) and clathrin-independent (red cargo) endocytosis. Subsequent routing of cargo to the early endosome, juxtanuclear endocytic recycling compartment (ERC) and the recycling endosome is shown. Figure adopted from Grant & Donaldson (2009)[69].

The balance between cell surface receptor degradation to the endolysosomal pathways and recycling back to the plasma membrane is exquisitely regulated and essential to preserve homeostasis in the cell. Dysfunctional sorting of these receptors alter the delicate balance required in a wide variety of signaling pathways leading to several diseases[70].

Fas is regulated at different steps of the endocytic pathway (Figure 6). First, internalization of Fas is crucial for the initiation of the signaling and proper formation of DISC complex. Upon internalization, post-endocytic sorting controls the fate of internalized Fas receptor localised to the endosomes and further attenuates or intensifies apoptotic signalling.

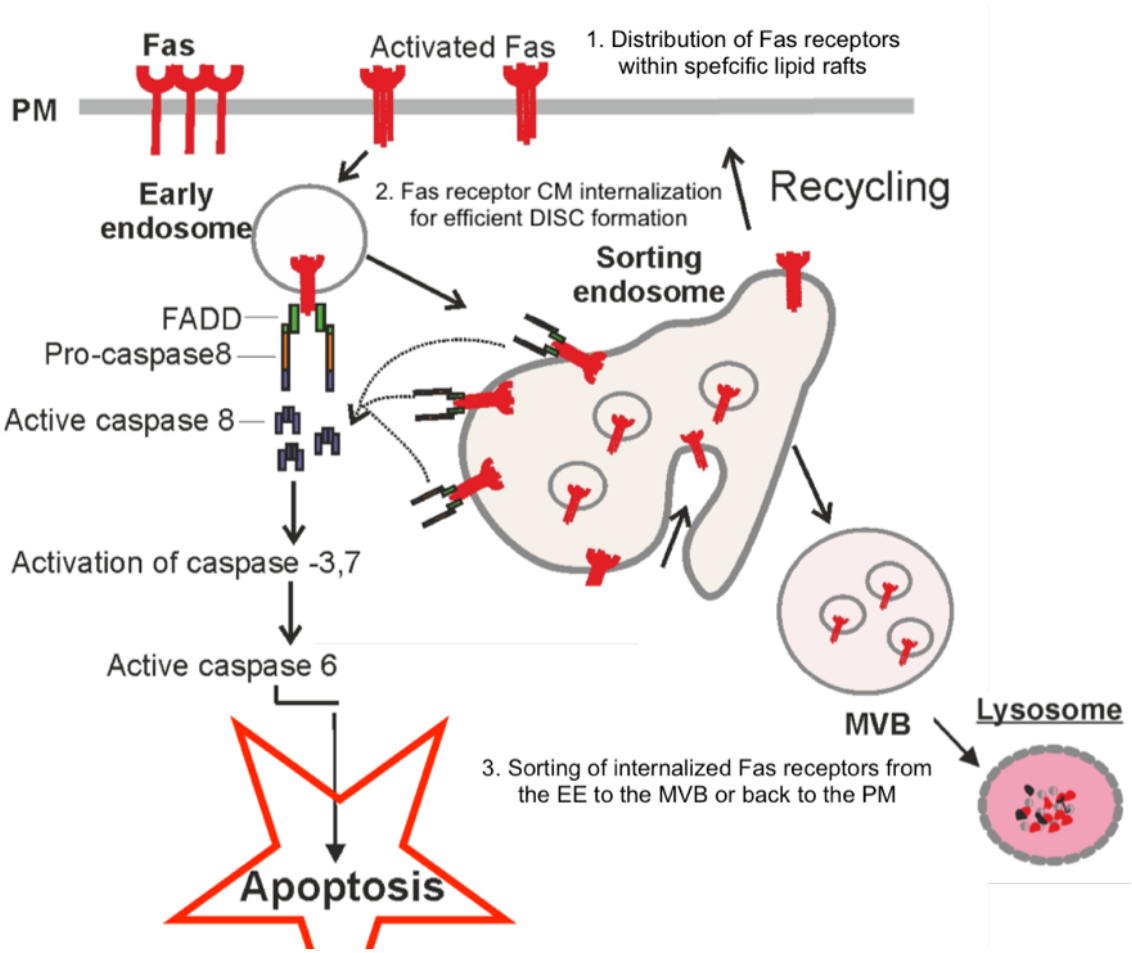

Figure 6. Membrane trafficking plays a crucial role in Fas mediated apoptosis. Regulation of the distribution of Fas receptors within lipid rafts by PTMs (1), clathrin mediated internalization of Fas receptors upon ligand binding (2) and internalized Fas sorting from early endosomes to late endosomes and lysosomes or back to the cell surface (3) are membrane-dependent processes that regulate Fas-mediated apoptosis.

3.2.1 Fas internalization

Internalization plays a key role in signaling of death receptors and affects the intensity and length of the signaling itself by limiting the availability of receptors in the cell surface.

The majority of DRs undergo clathrin-mediated endocytosis by being recruited by adaptor proteins (e.g. AP-2) straight into clathrin coated pits. After recruitment, clathrin coated pits are budded into clathrin coated vesicles (CCVs) by BAR-domain proteins such as SNX9 (sortin nexin 0) or endophilin, which are able to sense the curvature of the CCVs and accordingly adapt to the shape of vesicle. Subsequently, CCVs are excised by dynamin rings and transported into the cytoplasm, where vesicles are uncoated and finally fused to early endosomes[71].

Both Fas apoptotic and non-apoptotic signaling pathways share a starting point at the plasma membrane[13]. Fas non-apoptotic signaling is independent of receptor internalization. However, Fas apoptotic signaling heavily relies on the internalization of Fas receptors from the cell surface to the endosomal compartments[31, 72].

Fas receptors in particular are internalized into clathrin coated vesicles via clathrin-mediated endocytosis[31]. In vitro studies take advantage of anti-Fas monoclonal antibodies that act as agonists of Fas receptors. Anti-Fas agonistic antibodies are pentameric IgMs that are able to crosslink with Fas receptor. In other words, they mimic the activity of the FasL by specifically binding to Fas and

stimulating the activation of apoptotic events in a similar fashion to the physiological Fas ligand[73]. Treatment of cells with agonistic, Fas-specific antibodies induces receptor internalization within 5 to 15 minutes whereas binding of FasL elicits an even faster internalization[31, 72].

Fas receptors are internalized in vesicles positive for endocytic markers such as Rab4, EEA1 and Cathepsin D[31, 74]. At this early time point, low levels of FADD and active caspase 8 are detectable, but it is after approximately 30 minutes post-stimulation when the abundance of these two proteins peak. Even 3 hours after ligand binding, both FADD and active caspase 8 can be detected[72].

Several studies highlighted the importance of the internalization in Fas-mediated apoptosis. For instance, mutations on the Fas internalisation motif (YDTL, aa 291-294) or knockdown of AP-2 (adaptor protein 2, key in clathrin-mediated endocytosis) significantly inhibited DISC assembly and Fas-mediated apoptosis while other non-apoptotic signaling pathways such as NFkB and ERK remained intact[31]. Moreover, abolishment of the glycosphingolipid-binding motif in the extracellular domain of Fas (cardinal for internalization) blocked apoptotic Fas signaling but did not affect non-apoptotic signaling pathways[75].

As mentioned before, in vitro studies make use of crosslinking agonistic antibodies or recombinant soluble Fas ligand, which do not entirely resemble the physiological stimulus for Fas-mediated apoptosis, a membrane-bound form of FasL. Consequently, Fas internalization was assessed after co-culturing cells with cells expressing a non-cleavable form of membrane-bound FasL. In this

"physiologically relevant" scenario, Fas receptor internalization was found to be comparable to experiments using the soluble forms of FasL[31].

Upon internalization, post-endocytic sorting is the main mechanism that will determine the fate of Fas and will dramatically influence the apoptotic signaling process.

3.2.2 Endosomal sorting of Fas

Following internalization, Fas sustains the apoptotic signaling within early endosomes unless sorting machinery reinitiates or terminates the signaling by delivering Fas back to the plasma membrane (recycling) or to the endolysosomal pathway, respectively.

Early endosomes (also known as sorting endosomes) are the key players in the sorting of internalized proteins, including cell surface receptors. The classic definition of early endosome is "the first endocytic compartment to accept incoming cargo internalized from the plasma membrane" and they act as a sorting station within the cell[76]. Early endosomes are highly dynamic membrane structures composed of large vesicles (~400 nm diameter) and thin tubular extensions (~60 nm diameter) that undergo homotypic fusion[68, 77]. Early endosomes are compartmentalized in different structural and functional subdomains within the limiting membrane and each subdomain contains specific proteins that regulate different endosomal functions.

The endocytic sorting per se starts in the mature endosomes and the localisation of cargo within different endosomal compartments is key to the

correct sorting. For instance, DRs targeted to be recycled are translocated into structures of tubular morphology that subsequently separate from the endosome and fuse with endocytic recycling compartments (ERC) or are transferred back to the plasma membrane[69]. On the other hand, DRs targeted for degradation are sent to the late endosomes (also known as multi-vesicular bodies or MVB) to eventually be degraded in the lysosomes

Post-endocytic sorting of DRs: recycling pathways

Recycling plays a crucial role in keeping the balance between internalized and cell surface receptors. In particular, the abundance of DRs at the cell surface determines the sensitivity of cells to DR-mediated apoptosis so impairment of the recycling pathways can dramatically affect the ability of cells to undergo apoptosis. Sorting of DRs from the early endosomes to the plasma membrane is mediated by two major recycling pathways commonly known as the slow and fast recycling pathways. Recycling represents the "default" route for DRs once they are internalized: if they are not marked for degradations (e.g. ubiquitin), they will undergo recycling and replenish the pool of cell surface receptors[69, 78].

Internalized DRs are directed towards the recycling compartments via Rab GTPase effectors. These low-molecular-mass GTP-binding proteins function as molecular switches to regulate key recycling processes by cycling between a GDP-bound 'off' state and a GTP-bound 'on' state, in which they are able to interact with and activate other effector proteins. The so-called slow or classic recycling pathway is mainly dependent on Rab11, whereas the fast recycling pathway is Rab4 dependent[69, 79].

Many other effectors are also vital in the endosomal recycling of cell surface receptors (Figure 5). On one hand, different members of the Rab family of proteins have been also implicated in regulating recycling of cell surface receptors: Rab 35, Rab 22, Rab 8[69]. On the other hand, sortin nexins (SNXs) have also been found to be essential in regulating the sorting of cell surface receptors such as transferrin to the recycling compartments. As a clear example, downregulation of SNX3 missorted transferrin receptors to lysosomal compartments instead of being recycled back to the plasma membrane[80]. However, little is known about the specific mechanisms that govern Fas recycling and how recycling influences the attenuation or intensification of apoptotic signaling.

Post-endocytic sorting of Fas: degradation pathways

Receptor-mediated signaling starts at the plasma membrane, is sustained at the endosomal compartments and terminates by incorporation of the receptor into the degradation pathways[81]. Thus, DR degradation is tightly regulated by the endocytic pathway and modulates the apoptotic signaling.

The presence of several sorting signals determines the fate of the cell surface receptors and effectively sort them for lysosomal degradation[82]. Ubiquitination is a post-translational modification that targets proteins destined for degradation and involves the attachment of one or more ubiquitin groups to the targeted proteins. Ubiquitination is a reversible process, as it can be reversed by deubiquitinating enzymes (DUBs). Proteins that contain ubiquitin-binding domains (UBDs) are usually localised in the limiting endosomal membrane and

are able to recognize ubiquitinated proteins. UBDs identify target ubiquitinated proteins and directly sort them to the late endosomes and multi-vesicular bodies[83].

The formation of multi-vesicular bodies, the first step in the degradation pathway, is initiated by the ESCRT-0 (endosomal sorting complex required for transport). ESCRT-0 is recruited by cargo containing the proper sorting signals in the early endosomes. This complex helps in the recruitment of clathrin coats that will be formed on the endosomal membrane and also facilitates the grouping of cargo specifically targeted for degradation in specific regions of the endosomal membrane[84, 85] (Figure 7). As a key member ESCRT-0 complex, Hrs (hepatocyte growth factor-regulated tyrosine kinase substrate) is vital in the endosomal core sorting machinery. Hrs is recruited to the endosomal membrane via interaction with PI3P and contains both ubiquitin interaction motif (UIM) and VHS domains that aid the recognition of ubiquitinated proteins and subsequent sorting to the endolysosomal pathway[86].

Once ESCRT-0 has recruited cargo targeted for degradation at these specific microdomains, ESCRT-1 and 2 complexes mediate the membrane deformation and budding to form the intraluminal vesicles (ILVs). The membrane deforms into a bud and ESCRT-1 plays a fundamental role in its stabilization by localizing to the neck of the budding vesicle. Upon bud formation, ESCRT-3 assembles transiently, excises the membrane and recruits deubiquitanases such as USP8 (ubiquitin specific protease 8) in order to deubiquitinate cargo and recycle ubiquitin before sorting to the forming intra-luminal vesicles. ESCRT-3

contributes to the stabilization and constriction of the neck of the vesicle with the aid of Vps4 ATPase and finally releases the vesicle from the limiting membrane[84-88] (Figure 7).

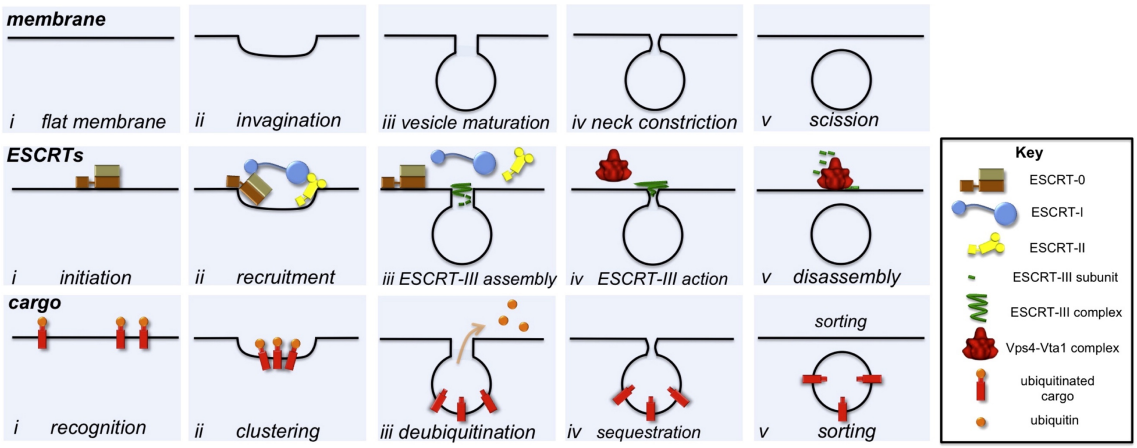

Figure 7. Model for ESCRT-mediated vesicle budding. The cartoon is showing the formation of ILV from the perspectives of the membrane (top), the ESCRT machinery (middle) and the cargo (bottom). The five stages mediated by the ESCRT complexes are: invagination of the flat membrane (i and ii), vesicle maturation (iii), neck constriction (iv) and final scission (v). Adopted from Henne et al. (2011)[88].

The previous model was established for mammalian EGFR but the precise mechanisms by which Fas is sorted to the endolysosomal pathways remain largely unclear. It is also not understood how sorting of Fas to the degradation or recycling pathways can influence the apoptotic signaling. The present thesis will provide further details on the molecular mechanisms of post-endocytic sorting of Fas receptors and the effects of altered trafficking of Fas in apoptosis and cancer.

II. The Hippo pathway and the regulation of cell proliferation

1. The Hippo pathway: context

The Hippo cascade represents a cardinal signaling pathway involved in development, tissue homeostasis and cancer[89]. Research interest in the Hippo pathway began in 1995 with the identification of the key kinase of the pathway, encoded by the *warts* gene in a search for tumour suppressor genes using genetic mosaics of Drosophila melanogaster[90]. However, the specific function of warts, which is the Drosophila ortholog of LATS (central kinase of the Hippo pathway in mammals), was not deeply investigated until 2003 when the other core components of the Hippo cascade were described by similar screens. For example, Yorkie (ortholog of the mammalian YAP/TAZ in flies) was isolated in 2005 as a warts-interacting protein and placed downstream of Hippo cascade by epistasis experiments[91]. These findings helped to the functional and biochemical description of the 'Salvador-Warts-Hippo' in Drosophila, ortholog to the Hippo signaling pathway present in mammals (see Figure 8 for details).

In several studies it was shown that inactivating mutations in these genes invariably induce hyperproliferation and reduced apoptosis in several tissues, causing overgrowth of Drosophila larval tissues and the emergence of tumours. Altogether, suggested the role of Hippo pathway as a potential tumour suppressor in flies. Furthermore, mouse knock-outs of specific proteins of the Hippo pathway exhibited phenotypes characterized by organ overgrowth, an

increased content in stem cells and less cellular differentiation [89, 92]. At present, Hippo cascade is not only related to organ size determination and growth control but also has been described to be implicated in many other functions, like cell cycle progression, apoptosis, stem cell renewal and differentiation as well as mechanotransduction [93].

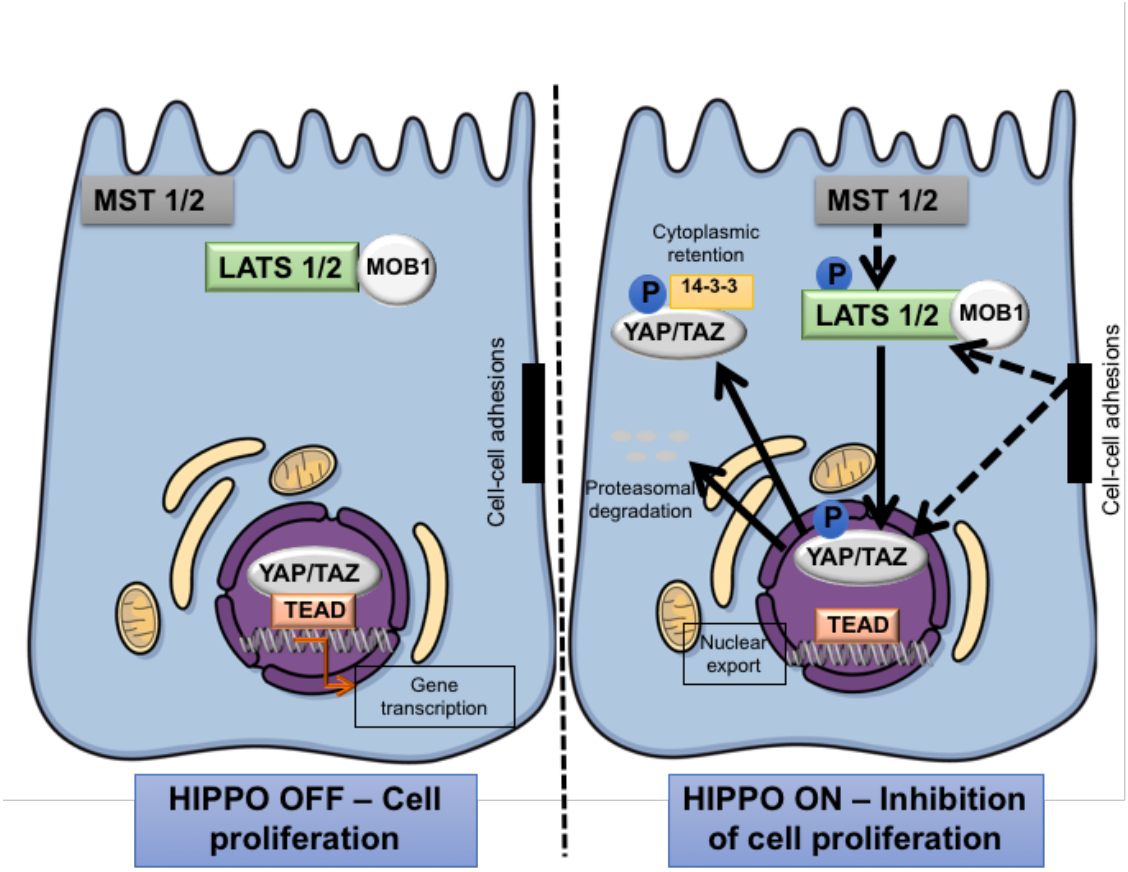

Figure 8. General model of the canonical mammalian Hippo pathway. The canonical Hippo cascade is initiated by NF2 activating MST1/2 kinases, which bind to co-activator protein SAV. MST1/2 kinases are responsible of the activation of LATS1/2 by phosphorylation. The following step of the cascade involves activated LATS1/2 kinases, which in complex with MOB1 phosphorylate YAP and TAZ at serine/threonine residues (defined by consensus HxRxxS). Therefore, YAP/TAZ are inhibited after LATS1/2 phosphorylation by nuclear exclusion, sequestration in the cytoplasm and/or proteasomal degradation (Hippo ON).

Otherwise, non-phosphorylated YAP and TAZ are translocated to the nucleus, where they interact with TEAD and regulate gene transcription, activating specific genes responsible of cell-proliferation (Hippo OFF)[89].

2. YAP and TAZ: effectors of the Hippo pathway

YAP and TAZ are the central effectors in the Hippo pathway, acting as transcriptional co-activators of several genes that control cell proliferation[89]. Moreover, YAP/TAZ play a key role in mechanotransduction, acting as a primary sensor of the cells own physical nature (cell structure, shape and polarity) and external mechanical cues that the cell receives from tissue architecture and surrounding extracellular matrix (cell density, ECM stiffness...)[89, 92, 94]. It has also been described that YAP/TAZ crosstalk with Wnt[95-97], Notch[98] and TGF-β[99] pathways and are also regulated by Rho-GTPases[94], GPCRs[100, 101] and mevalonate metabolism[102, 103].

The Yes-associated protein (YAP) was first described by Mario Sudol in 1994, but its connection with the Hippo pathway was not defined back then[104]. The YAP1 gene cloning allowed the identification of a WW domain, vital in YAP protein-protein interactions and known for preferentially binding particular proline motifs in proline-rich proteins[105, 106]. Besides the WW domain, YAP contains a proline-rich region at the N-terminus, which is followed by TEAD binding domain (TBD)[107] and a 14-3-3 binding domain. In the C-terminal region there is a Src Homology 3 binding motif (SH3-BM)[104, 108], the transcription activation domain (TAD)[107] and a PDZ domain-binding motif (PDZ-BM)[104, 109] (Figure 9).

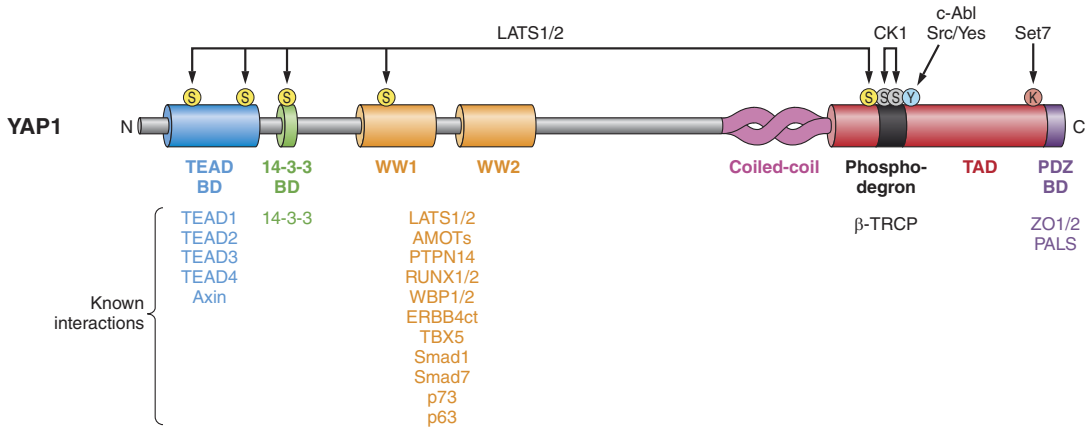

Figure 9. Schematic representation depicting the multiple domains of YAP and mapped interactions with other proteins. In yellow, serines that are targeted by LATS kinase phosphorylation. Adopted from From Piccolo et al. (2014)[89].

YAP can be found in the nucleus and/or the cytoplasm and undergoes a tightly regulated nucleocytoplasmic shuttling. Given YAP's role as transcriptional co-activator, the regulation of its nuclear accumulation is crucial. Phosphorylation by LATS represents a main input for YAP subcellular localisation, leading to its sequestration in the cytoplasm[110, 111]. Although phosphorylation by LATS is important for YAP nuclear exclusion, is not necessarily the main inactivating event. Other serine kinases such as AKT and JNK[110, 112] or tyrosine kinases such as c-Abl[113] have also been identified as potential YAP regulators.

3. LATS kinases

NDR/LATS (Nuclear Dbf2-related / Large Tumour Suppressor) family of kinases is a subgroup of the AGC (protein kinase A (PKA)/PKG/PKC-like) group of protein kinases and are highly conserved from yeast to humans (Figure 10). LATS kinases act as tumour suppressor proteins and regulate a diversity of

physiological processes such as mitotic exit, morphological changes, cell proliferation and apoptosis[114].

Overexpression of LATS1/2 has been found to be sufficient to suppress EMT and tumour growth of cancer cells[115-117], whereas loss of LATS1 and LATS2 leads to cellular transformation of MCF-10A cells[116] and cell overgrowth[118] respectively. As a matter of fact, generation of LATS2 knockout animals has been unsuccessful as loss of LATS2 is embryonic lethal[119]. In humans, loss of function of LATS1/2 leads to several tumour types such as soft tissue sarcomas, leukemia as well as breast, prostate, lung and esophageal cancers[120].

The investigation of LATS kinases role in the Hippo pathway has drawn major attention in recent years. LATS are the main upstream kinases in the Hippo pathway and require phosphorylation of conserved Ser/Thr residues to be activated. Once activated, LATS phosphorylate YAP and TAZ at serine threonine residues (defined by consensus HxRxxS) and inhibit their activity by nuclear exclusion, sequestration in the cytoplasm and/or proteasomal degradation. Both YAP and TAZ bear 5 potential serines targeted for LATS phosphorylation. When LATS1/2 are inactivated, YAP and TAZ remain non-phosphorylated and are translocated to the nucleus, where they interact with TEAD and regulate gene transcription, activating the transcription of several oncogenes [89, 94, 114] (Figure 8).

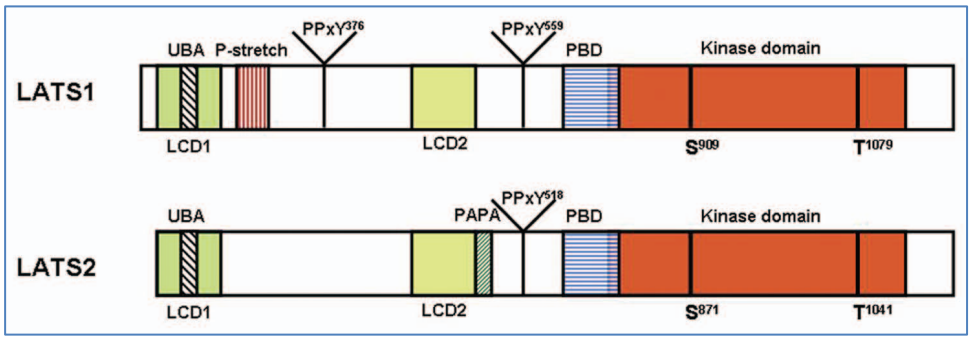

Figure 10. Structure of LATS1 and LATS2 kinases. Both LATS1 and LATS2 share several conserved domains including the C-terminal Ser/Thr kinase domain, a protein binding domain (PBD), two LATS conserved domains (LCD1 and LCD2) and ubiquitin binding domain (UBA). LATS1 has two PPxY motif for interaction with the WW domains of YAP, whereas LATS2 only has one. Adopted from Visser & Yang (2010)[120].

The regulation of LATS kinases involves, on one hand, the interaction with the co-activator MOB1 (human Mps-1 binder-1), which is responsible for efficient auto-phosphorylation of LATS on the activation segment. On the other hand, phosphorylation of the C-terminal hydrophobic motif of LATS1/2 is required for their complete activation, which is carried out by MST kinases (mammalian serine/threonine Ste20-like kinase), upstream members of the Hippo signaling [89, 121]. Nevertheless, upstream regulation of LATS kinases is a complex process that can be fine-tuned at different molecular levels (transcription, post-transcription, protein, conformational changes)[114].

4. The role of YAP and TAZ in mechanotransduction

Cells are able to effectively perceive their microenvironment through physical and mechanical cues. Mechanotransduction is a cellular process by which cells translate external stimuli into biochemical signals that regulate the

fate of the cell and influence on cell behaviour (growth, differentiation and even cancer malignant progression)[94]. Interestingly, mechanical cues represent a second pillar for YAP/TAZ activation, apart from the canonical Hippo activation via LATS kinases.

YAP and TAZ are able respond to mechanical cues such as cell density, cell polarity or ECM stiffness (Figure 11 a). Consequently, the subcellular localisation of YAP/TAZ can also be regulated by these upstream signals through complex mechanisms that require further investigation[89, 92, 94]. For example, when the cells are at low density, the Hippo pathway is OFF and the localisation of YAP/TAZ is nuclear, so it becomes transcriptionally active and stimulates proliferation. However, when cells become confluent, proteins involved in mechanotransduction (cell-cell contact proteins in collaboration with elements of the Hippo pathway) transmit this information to YAP/TAZ. Hence, Hippo pathway is activated and YAP/TAZ is excluded from the nucleus, with a predominant cytoplasmic localisation, which stops further proliferation (Figure 11 b and c).

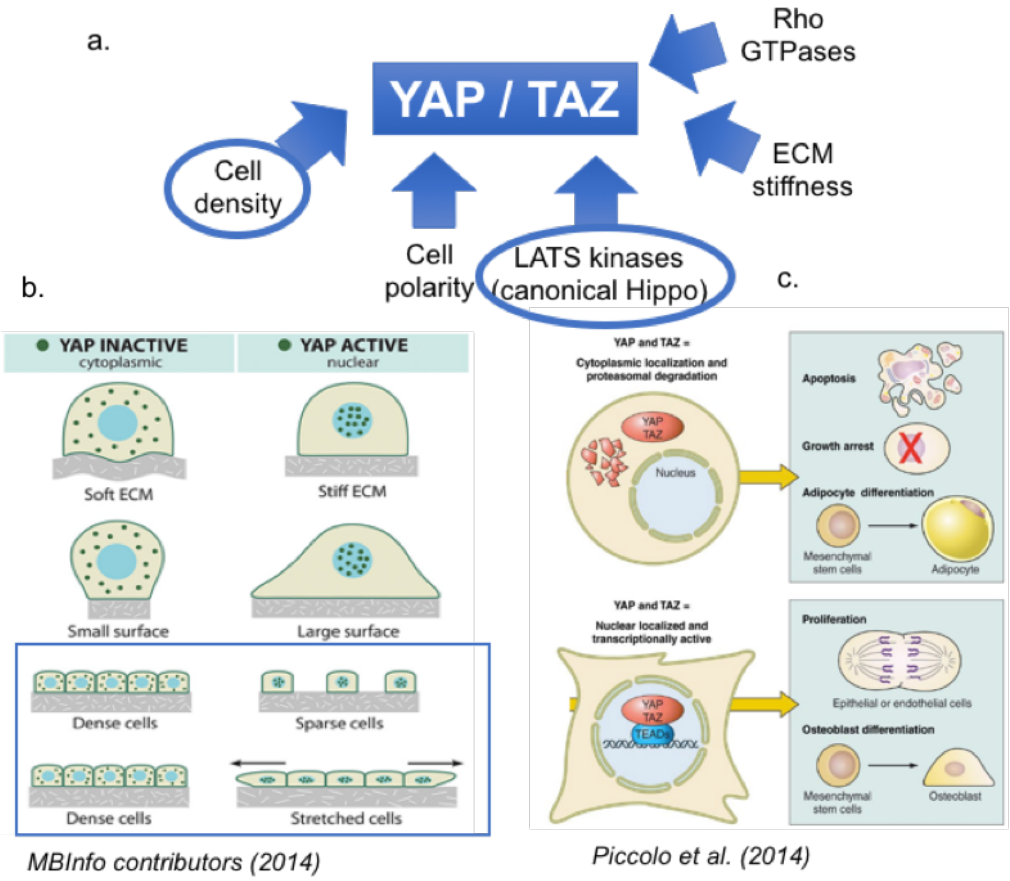

Figure 11. YAP/TAZ is regulated by different upstream signals. (**a)** The Hippo pathway can be switched ON or OFF not only by LATS kinases phosphorylation, but also in response other external signals such as cell density, cell polarity or ECM stiffness **(b)** Scheme representing the localisation and activation status of YAP/TAZ in different mechanical conditions (**c)** The changes in subcellular localisation of YAP/TAZ trigger different physiological processes partially dependent on the activation/deactivation of the Hippo pathway. Adapted from different sources indicated in the Figure.

Among these external signals, cell density is of special interest, as we suggest that PTPN13 might be a cell density sensor itself that acts similarly to YAP. YAP/TAZ play an important role in the regulation of the contact inhibition of proliferation (CIP) by which cells stop dividing when they reach full confluence[122]. This is especially important in epithelia, where loss of CIP control is considered a

hallmark of cancer. In the present thesis we will study the potential role of PTPN13 as an alternative effector of LATS kinases that similarly to YAP is shuttling from nucleus to cytoplasm in response to mechanical cues such as cell density.

III. PTPN13, a multi-PDZ domain phosphatase

The previous sections have provided a background on the functions which we hypothesize that PTPN13 is involved in and that will be discussed in the results and discussion parts of the present thesis. However, this section is going to focus on the protein itself, the tyrosine phosphatase PTPN13.

Protein phosphorylation is considered a paramount post-translational modification that is involved in the regulation of the activity, subcellular localisation and interacting properties of proteins. More specifically, the phosphorylation of tyrosine residues in the proteins is one of the most important regulators in higher eukaryotic cells[123]. Among the protein tyrosine phosphatases (PTPs), the non-receptor subtype PTPs are characterized by the presence of 4.1/Ezrin/Radixin/Moesin (FERM) domain and the lack of a transmembrane domain. Consequently, non-receptor PTPs are cytosolic or membrane-associated phosphatases[124-126].

The non-receptor protein tyrosine phosphatase 13 (also known as PTP-Bas, PTPL1, hPTP1E and FAP-1; mouse homolog is named PTP-BL) is a multi-PDZ domain protein that serves as a central scaffolding element facilitating the assembly of many different proteins. PTPN13 maps to the human chromosomal

locus 4q21, encoding a high molecular weight protein of 270 kDa and 2490 amino acids length [124, 127].

1. Subcellular localisation

PTPN13's mouse homolog PTP-BL is localised in the apical membrane in MDCKII epithelial cells[128] and is accumulated in axons and growth cones of sympathetic and sensory neurons[129]. Furthermore, Erdmann et al. demonstrated that PTP-BL displays a dynamic localisation during cell cycle, as it localises at the centrosomes during both the interphase and metaphase, but at the spindle midzone during anaphase. Strikingly, PTP-BL is accumulated at the midbody during cytokinesis[130].

Whereas PTP-BL is located in a punctuate pattern mostly in the cytosol, with enrichment at the centrosome and spindle poles, PTPN13 visualization in pancreatic cells carried out by Ungefroren et al. revealed a predominant juxtanuclear staining. These results suggested that PTPN13 is also localised at the Golgi apparatus and in the nucleus[131].

2. Structure

PTPN13 is a highly modular protein that contains multiple domains, providing an excellent base for potential interactors (Figure 12 and 13)[124]. The extreme N-terminus consists of a 200 amino acid putative Kinase Non-catalytic C-lobe (KIND) domain, which was recently identified by sequence homology to the regulatory C-lobe of protein kinases. KIND domain function has not yet been experimentally addressed and the absence of catalytic and activation loops

suggests that this domain lacks catalytic activity but might mediate protein/protein interactions[132].

The next amino terminal domain is a 4.1/Ezrin/Radixin/Moesin (FERM) domain. FERM domains are found in peripheral membrane proteins that play an important role in connecting plasma membrane receptors to the cytoskeleton[133]. These domains have a length of about 300 amino acids and are also known to bind 1-phosphatidylinositol 4,5-biphosphate [PtdIns (4,5)P2 or PIP2]. The FERM domain interaction with PIP2 is of great importance as it allows the localization of PTPN13 to the plasma membrane[134].

The core of the PTPN13 comprises five PSD-95/Drosophila discs large/Zonula occludens (PDZ) domains. PDZ domains are able to interact selectively with the C-terminus of their target proteins, so they have an essential role in protein-to-protein interaction and in the assembly of supramolecular protein complexes[135, 136]. PDZ domains have a length of 90 amino acids and, as the FERM domain, are also able to bind PIP (PtdInsP)[137]. There are a growing number of proteins interacting with one or more of the PDZ domains of PTPN13, and these domains represent the principal binding sites of the protein (Figure 13).

As the final component of PTPN13, the protein tyrosine phosphatase domain is located at the extreme C-terminus of the molecule [124, 138].

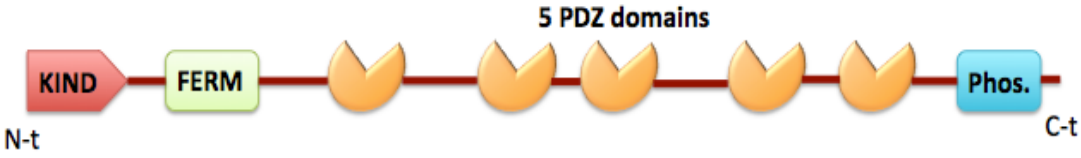

Figure 12: Scheme of PTPN13 modular structure. PTPN13 is composed of an N-terminal KIND domain, FERM domain, Protein tyrosine phosphatase domain and 5 PDZ domains.

It has been previously described that PTPN13 exhibits alternative splicing variants in the N-terminus between the FERM domain and the first PDZ domain and within the second PDZ domain[139, 140]. Further minor alternative splicing products have been identified, predicting C-terminal truncated versions of PTPN13[141].

3. PTPN13 functions

PTPN13 comprises a considerable number of protein-to-protein interaction domains. As mentioned before, many proteins have been identified as interactors of PTPN13 via one or two of its five PDZ, FERM or KIND domains (Figure 13). Other studies have demonstrated that PTPN13 interacts with F-actin and microtubules as well as to PIP2 in the cell membrane[130, 137]. The identification of PTPN13 substrates and interactors is critical in discovering the common mechanism underlying the diversity of physiological systems and signaling pathways that PTPN13 regulates.

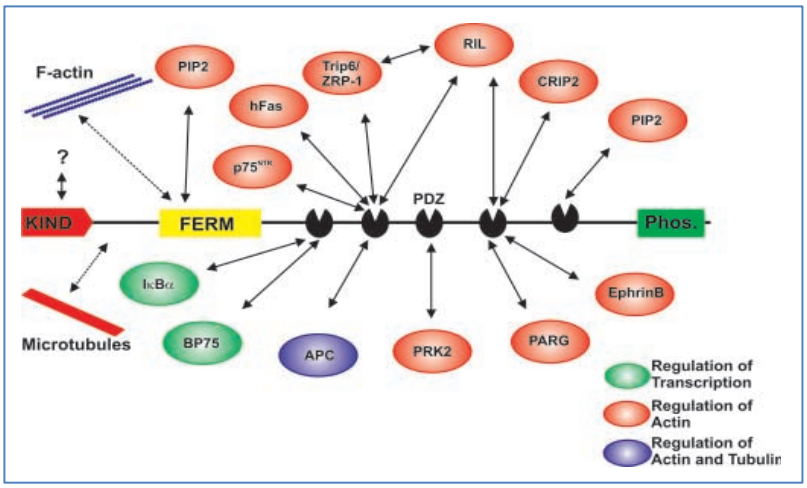

Figure 13. Scheme displaying PTPN13 interacting proteins in a domain-specific organization. Adopted from Erdmann (2003)[124].

Both the complex domain structure and the huge number of interactors provide clear evidence on PTPN13 involvement in a wide range of physiological processes. So far, PTPN13 plays major roles in many different biological systems such as Fas receptor trafficking, cytokinesis regulation, adipocyte differentiation, ephrinB signaling or in the aggressiveness of specific tumours (Table 1).

	Structure	Functions
PTPN13 Non-receptor Protein tyrosine phosphatase also known as PTPL1, hPTP1e, PTP-Bas, FAP-1 *Mouse homologue: PTP-BL*	Large macromolecular protein complex, highly modular multi-PDZ domain protein: • N-terminal KIND domain • FERM domain • 5 PDZ domains: protein-to-protein interaction, regulation of phosphatase activity • Tyrosine phosphatase domain Molecular mass: 276,906 kDa *Saras et al. (1994), Erdmann (2003)*	- Regulation of cell surface expression of cell death receptor Fas (role in membrane trafficking and vesicular transport). *Saras et al. (1997), Ungefroren et al. (1998), Li et al. (2000)* - Regulation of the cytokinesis and actin cytoskeleton. *Herrmann et al. (2003)* - Regulation of cell/cell adhesion. *Erdmann et al. (2000), Huang et al. (2013).* - Regulator of ephrinB phosphorylation. *Lin et al. (1999), Palmer et al. (2002)* - Adipocyte differentiation. *Glondu-Lassis et al. (2009)* - Role in tumour progression and aggressiveness, as well as metastasis. *Freiss & Chalbos (2011), Abaan & Toretsky (2008)*

Table 1. Summary of the essential characteristics of the PTPN13 protein in terms of structure and function, as well as corresponding bibliography.

The following sections will highlight the two functions which are relevant to understand the context of the results presented in this thesis.

3.1 PTPN13 in Fas-mediated apoptosis

Since its early cloning and characterization, PTPN13 has been intimately linked to Fas receptor mediated apoptosis. As a matter of fact, Sato's lab named PTPN13 as FAP-1 for Fas-associated phosphatase-1 due to evidence of its ability to interact with the death receptor Fas[142]. A considerable amount of literature has been published on the role of PTPN13 conferring resistance to Fas-mediated apoptosis, but it still remains controversial[143-145].

First evidence pointing out to a relation between PTPN13 and apoptosis came with the description of the interaction of PTPN13 with the carboxy terminal of Fas receptor via its PDZ2 domain[142]. They also showed that only three aminoacids of the C-terminal (SLV) of Fas are necessary to establish the interaction with PTPN13. However, this is not evolutionarily conserved, as mouse Fas lacks the SLV peptide and is not able to interact with PTPB-L[146]. Later on, it was shown that PDZ4 domain of PTPN13 was also able to interact with high affinity with peptides derived from Fas C-terminus[145].

When overexpressing PTPN13 in Jurkat cells the apoptotic effect of Fas agonistic antibody was 50% reduced, increasing the resistance to Fas-induced apoptosis[143]. Moreover, direct cytoplasmic microinjection of the SLV peptide resulted in the induction of Fas mediated apoptosis in colon cancer cell line[147]. Finally, downregulation of PTPN13 expression by siRNA or expression of PTPN13

dominant negative mutants enhanced the sensitivity of cells to Fas-mediated apoptosis as increased levels of Fas in the cell surface were observed[57, 148].

PTPN13 phosphatase activity has been demonstrated to also be cardinal in regulating of Fas-induced apoptosis:

- First, treatment of cells with orthovanadate (a blocker of tyrosine phosphatase activity) resulted in a decreased cell viability. This result indicated that PTPN13 may dephosphorylate Fas at specific tyrosine residues and consequently regulate its activity[131].
- A deeper look into the impact of Fas dephosphorylation by PTPN13 in glioma cells revealed that PTPN13 was co-immunoprecipitated with endogenous Fas upon treatment with Fas ligand. Fas receptor also exhibited an increased phosphorylation at tyrosine 275 upon stimulation. However, a point mutation in tyrosine 275 (corresponding to the cytoplasmic death domain of Fas) resulted in higher levels of cell surface Fas expression and reduced PTPN13/Fas association[148].

Altogether, these studies supported the idea that PTPN13 may dephosphorylate cell surface Fas in its cytoplasmic tail to inhibit apoptotic signaling.

The subcellular localisation analysis of PTPN13 and Fas in pancreatic cell lines revealed that unstimulated cells showed limited co-localisation of PTPN13 and Fas, but upon treatment with Fas ligand the co-localisation was significantly increased, with a specific strong co-localisation in the intracellular

compartments. The increase of intracellular co-localizing PTPN13/Fas was accompanied by a decreased presence of Fas in the cell surface[131, 144]. These studies pointed to a role of PTPN13 as a negative regulator of cell surface Fas.

The potential molecular mechanisms by which PTPN13 might modulate cell surface Fas can be summarized in two different hypotheses (Figure 14)[124]:

1. The internalization of Fas receptor from the cell surface to the intracellular reservoirs is increased by PTPN13 interaction, leading to the reduction of Fas levels in the cell surface.
2. PTPN13 affects the trafficking to the degradation pathways and/or recycling of Fas receptor from the intracellular reservoirs to the cell surface. This would also result in the decrease of Fas receptor in the cell surface and inhibition of Fas-induced apoptosis.

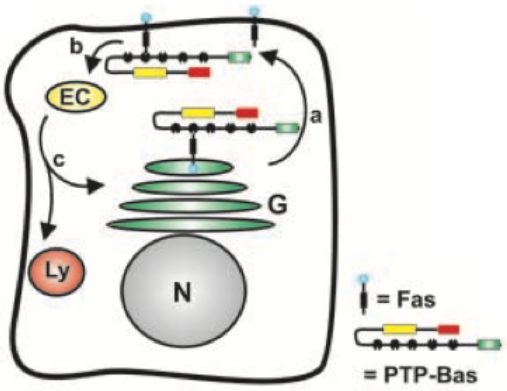

Figure 14. PTPN13 regulates the cell surface expression of the human Fas receptor. PTPN13 could regulate transport from endosomal compartments/Golgi apparatus to the cell surface (a), increase the transport of Fas from the cell surface to the endosomal compartments (b) or from endosomal compartments to the degradation pathways/Golgi apparatus (c). Adopted from Erdmann (2003)[124].

Gump and collaborators suggested an alternative molecular mechanism by which PTPN13 may be regulating Fas-induced apoptosis. In this study, autophagy adaptor protein p62 interacted with PTPN13 upon stimulation with Fas ligand, targeting PTPN13 for degradation in the lysosomes and increasing the expression of Fas at the cell surface[149]. In summary, the identity of PTPN13 as a negative regulator of Fas level in the cell surface is well established and partially explains the inhibitory action of PTPN13 in Fas-induced apoptosis.

3.2 PTPN13 and the Hippo pathway

The potential involvement of protein tyrosine phosphatases such as PTPN13 in the Hippo pathway has not been at all investigated and constitutes a promising research niche awaiting to be exploited. As a matter of fact, PTPN14 (a tyrosine phosphatase from the same family as PTPN13) has been described as a negative regulator of the oncogenic function of YAP, central effector of the Hippo pathway[150]. PTPN14 directly interacts with YAP via its PPxY domain and also forms a complex with Kibra that interacts with LATS1, activating its kinase activity and negatively regulating YAP by phophorylation[93]. Interestingly, two studies support the idea of a potential role of PTPN13 in the regulation of LATS kinases and the Hippo pathway:

- First, Couzens *et al.* defined the Hippo cascade protein-protein interaction network and among 749 interactions identified both LATS 1 and LATS 2 (Figure 15). Whereas LATS1 interaction with PTPN13 was only predicted by BioID proximity label mass spectroscopy, LATS2 interaction was determined by both proximity label-MS and affinity capture-MS[151]. In the same study,

LATS1 and LATS2 were also predicted to interact with the serologically defined colon cancer antigen-3 (ENTR1, previously known as SDCCAG3), a well-known interacting protein for PTPN13[152].

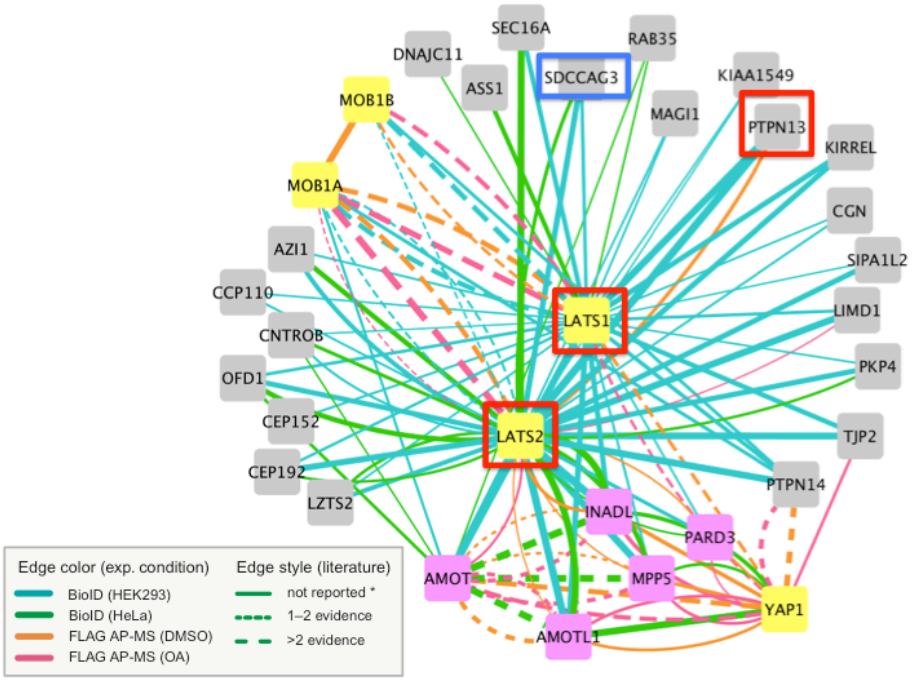

Figure 15. Hippo pathway interactome. Proteomic screening results predicted potential interactions for LATS1 and LATS2 proteins and defined the protein interaction network of the mammalian Hippo pathway. On one hand, BioID (proximity label MS) takes advantage of a mutated biotin ligase which is fused to a bait of interest, allowing for the local activation of biotin and subsequent biotinylation of proteins in the bait vicinity. Thus, BioID identifies which proteins are in close proximity to the bait protein but does not necessarily mean that they are directly interacting. On the other hand, in affinity capture MS a single bait protein is affinity captured in a matrix. A protein mixture is passed through the matrix and interacting partners are retained by interaction with the bait. Hence, it gives a more solid indication that prey proteins are interacting with the bait protein and forming a protein complex[153]. Adopted from Couzens et al. (2013)[151].

- Cai et al. proved that APC, another previously established interacting protein for PTPN13, functions as a scaffold protein that facilitates the Hippo kinase cascade regulation by interacting with Sav1 and LATS1[154].

All the previous evidence points out to a potential interaction between PTPN13 and the central kinases of Hippo cascade, which will be further investigated in the present thesis. The potential role of PTP1N3 in the Hippo pathway might have a great impact in understanding how YAP/TAZ can promote tumour development.

4. ENTR1, interacting partner of PTPN13, is involved in endocytic trafficking

Former Serologically defined colon cancer antigen 3 (SDCCAG3), recently renamed as Endosome associated trafficking regulator 1 (ENTR1) is a 45 KDa protein identified as an antigen recognized by serum extracted from colon cancer patients[155]. It was first isolated from cDNA expression libraries obtained from these patients and it has four different splicing variants[155]. ENTR1 has a simple protein structure, comprising a coiled-coil domain in the C-terminal with no catalytic activity described up to date[152, 156]. Analysis of ENTR1 by Western Blot has revealed that is highly phosphorylated and multiple bands corresponding to ENTR1 are detected around 55 KDa in HeLa cell line[152].

Interestingly, ENTR1 has been described as an interacting partner of PTPN13. The N-terminus region of ENTR1 interacts with the FERM domain of PTPN13 and both the proteins co-localise at the midbody during cytokinesis[152].

ENTR1 role in endocytic trafficking

Several pieces of evidence point to a potential role of ENTR1 in endocytic trafficking. First, partial co-localisation of ENTR1 with EEA-1, a marker for early endosomes, suggested the presence of ENTR1 in early endosomal compartments[152]. ENTR1 is interacting with Arf-6, a well-established regulator of trafficking[157]. Another study confirmed that ENTR1 is interacting with Vps35 in the endosomes[158]. Vps35 is a component of the retromer complex, implicating ENTR1 in the sorting of retromer-dependent cargo from the endosomes to the trans-Golgi network (e.g. CIMPR receptor sorting) and from the endosomes to the plasma membrane (e.g. GLUT1 receptor sorting)[158]. Furthermore, ENTR1 interacts with FAM21, a member of the actin nucleating Wiskott-Aldrich syndrome and SCAR homolog (WASH) complex[159]. As a matter of fact, the interaction of ENTR1 with FAM21 mediates the recruitment of ENTR1 to the retromer complex[159].

Last but not least, ENTR1 was described to regulate tumour necrosis factor receptor 1 (TNFR1) trafficking, modulating its abundance in the cell surface[156]. Expression of an ENTR1 truncated version made NIH3T3 and HeLa cells resistant to TNF-specific apoptosis by decreasing the presentation of TNFR1 in the cell surface[156]. Thus, ENTR1 represents a promising candidate in a potential therapeutic modulation of cell sensitivity to TNF-induced apoptosis.

Given the interaction of ENTR1 with PTPN13 and its involvement in the regulation of a cell surface receptor such as TNFR1, we considered ENTR1 as a very promising candidate to associate to PTPN13 and regulate Fas trafficking, modulating the expression of Fas in the cell surface.

5. PTPN13 role in cancer, a double-edged sword

Cancer cells use several strategies to survive in the harsh environment present in tumours. It is known that the phosphorylation of diverse proteins in their tyrosine residues is responsible for the transduction of signals for cellular stress-response pathways that control cell survival. Consequently, the reverse process catalysed by phosphatases like PTPN13 might also have a key role in cell survival[126].

As a highly modular scaffolding protein, PTPN13 interacts with a number of proteins involved in different steps of tumour progression. The connection of PTPN13-interacting partners with cancer-related signaling pathways suggests multiple and diverging roles for PTPN13 in cancer and metastasis[138]. PTPN13 can be considered as a double-edged sword: several studies suggest that PTPN13 acts as a tumour promoter that exerts a positive effect on progression and aggressiveness, whereas other studies indicate that PTPN13 might function as a tumour suppressor. Unfortunately, a conclusive confirmation of the positive or negative effects of PTPN13 on tumourigenesis is still elusive, as the role of PTPN13 in cancer cells is likely to be complex and context-dependent[126].

1) PTPN13, a tumour promoter

PTPN13 cannot be considered an oncogene itself, but its implication in several oncogenic pathways, such as regulation of cell growth, cell motility or stress-responses is already demonstrated. PTPN13 has a positive role in cancer cells survival by negatively regulating Fas receptor and increasing the resistance of

cancer cells to Fas-mediated apoptosis. As a matter of fact, there is a large volume of published studies reporting the inhibition of Fas-induced apoptosis by PTPN13 in pancreatic adenocarcinoma[131, 144], melanoma[57], ovarian cancer[160], colon cancer[161], head and neck cancer[162], hepatocellular carcinoma[163] and in hepatoblastoma cell lines[164].

Furthermore, another study provided an explanation on how the increased PTPN13 expression in cancer cells correlates with reduced cell surface Fas. mir200c is a microRNA known for inhibiting epithelial to mesenchymal transition (a key feature of cancer cells) by downregulating transcriptional factors ZEB1 and ZEB2. The study revealed that PTPN13 is a target for mir200c. Thus, this microRNA regulates PTPN13 expression by translational repression. Cancer cell lines displaying mesenchymal characteristics changed their morphology from mesenchymal to epithelial after transfection with mir200c. In addition, a decreased expression of PTPN13 and increased sensitivity towards apoptosis was observed[165].

Thus, interaction with Fas receptor is the first evidence of PTPN13 participation in anti-apoptotic and oncogenic pathways. However, this is not the only one, as Abaan et al. found that PTPN13 is also a direct transcriptional target of EWS-FLI1, a fusion protein expressed in Ewing's Sarcoma Family of Tumours (ESFT) which promotes cell growth and oncogenesis[166].

Moreover, the characteristics of other PTPN13 interactors such as ENTR1[152], $p75^{NTR}$, TRPM2 (Transient receptor potential M2) and NFκB might also be supporting the survival of cancer cells within tumours[126]. Given that PTPN13

interacts with both proteins and lipids that are able to modulate cell shape and motility it might also act as a promoter of cancer metastasis. These interactors include PIP2[167], TAPP1/2[168], EphrinB1[169] and PARG1[170].

2) PTPN13, a tumour suppressor

In spite of the studies mentioned above, a negative impact of PTPN13 on cell growth and survival has also been reported. PTPN13 substrates have been identified in the majority of pathways that either prevent or reverse oncogenic transformation[126].

- First evidence was the involvement of PTPN13 in the pro-apoptotic effects of anti-estrogens in breast cancer cell lines. PTPN13 was identified as an up-regulated transcript in breast cancer cells after tamoxifen treatment and reduction of PTPN13 levels were shown to partially protect breast cancer cells from tamoxifen-induced apoptosis[171].
- Castilla et al. found that PTPN13 in collaboration with PKCδ contribute to pro-apoptotic signaling in prostate cancer cells[172].

Finally, PTPN13 might also reduce metastatic potential by reducing cell motility via interaction with the thyroid receptor interacting protein 6 (TRIP6, also named Zyxin-related protein 1, ZRP-1)[173]. The reduction of cell motility limits the invasiveness of tumour cells and consequently, decreases the risk of metastasis.

In conclusion, PTPN13 opposite regulatory roles in tumour progression depend on the context and tissue, as both tumour promoter (anti-apoptotic,

increase of cell proliferation) and tumour suppressor (pro-apoptotic, reduction of cell growth and invasiveness) have been documented in previous literature.

3. Materials and methods

I. Materials

1. Devices

3D gyratory rocker SSM3	Stuart Equipments
AE2000 Inverted Microscope	Motic
Analogue tube rollers SRT6	Stuart Equipments
Avanti J-26 XP Centrifuge	Beckmann Coulter
BD FACSAria IIu cell sorter	BD Biosciences
BD LSR II Flow Cytometer	BD Biosciences
Class II Biological safety cabinet	ESCO
Dry block heating system QBD2	Grant Instruments
Entris analytical balance	Sartorius
Fast Gene Blue LED Illuminator	Nippon Genetics Europe
FLUOStar OPTIMA Absorbance Reader	BMG Labtech
Galaxy 170S CO_2 incubator	New Brunswick Scientific
Gel DOC EZ System	Bio-Rad Laboratories
Incubator (Heratherm)	Thermo Fisher Scientific
Innova 44 incubator Shaker	New Brunswick Scientific
Jenway 3510 Bench pH/mV meter	Jenway
Mini Trans-blot Electrophoretic transfer cell	Bio-Rad Laboratories
Mini-Protean Tetra Cell	Bio-Rad Laboratories
NeoLab rotator with Vortx RM-2M	NeoLab
Neubauer counting chamber	Labor Optik

Nikon A1 TIRF Confocal microscope	Nikon
Nucleofector 2b Device	Lonza
Odyssey Sa Infrared Imaging system	LI-COR
Olympus BX61 Epifluorescence Microscope	Olympus
PefectSpin 24 plus	Peqlab
PeqMixplus	Peqlab
PeqStar Dual 48-well PCR Thermal cycler	Peqlab
PeqTwist vortex mixer	Peqlab
PerfectBlue Gel System Mini	Peqlab
PerfectSpin Mini	Peqlab
PGW 753M Precision balance	Adam Equipment Ltd
PowerPac Basic	Bio-Rad Laboratories
Sigma 1-14K Refrigerated Microfuge	SIGMA
Slide Scanner	NanoZoomerXR
Soniprep 150	MSE
Vacusafe comfort Aspiration System	Integra Biosciences
White Light Transilluminator	UVP
ZOE Fluorescent Cell Imager	Bio-Rad Laboratories

2. Reagents

Agarose NEEOULTRA	Sigma-Aldrich
40% Acrylamide/Bis solution 37,5:1	Bio-Rad Laboratories
Albumin Standard #23210	Thermo Scientific
Alkaline Phosphatase Calf Intestinal	New England BioLabs

Anza T4 PNK enzyme	Invitrogen
Brilliant Blue G-250 (BP100-25)	Fisher Scientific
BSA, Microbiological grade, Fraction V	Fisher Scientific
Cycloheximide ready-made solution C4859	Sigma-Aldrich
Fluoromount-G #0100-01	SouthernBiotech
Gel Loading Dye Purple (6x)	New England BioLabs
Geneticin (G418)	Sigma-Aldrich
GFP-Trap_A	Chromotek
GoTaq Hot Start DNA polymerase	Promega
HF Phusion Polymerase	Thermo Scientific
Hoechst 3342	Invitrogen
ImmPACT DAB SK-4105	Vector Laboratories
IPTG MB1008	Melford
Leupeptin A	Sigma Aldrich
Lipofectamine 2000 Transfection Reagent	Invitrogen
Mitotracker Red CMXRos 9082P	Cell Signaling
myc-Trap_A	Chromotek
NeutrAvidin Agarose resin #29200	Thermo Scientific
NP-40 (10%)	BioVision
PageRuler Plus Pre-stained protein ladder	Thermo Fisher Scientific
PageRuler Prestained Protein Ladder	Thermo Fisher Scientific
Ponceau S (P3504)	Sigma-Aldrich
Prestained Protein Marker High Range	Cell Signaling
Pro-long Gold antifade reagent	Invitrogen

Protease cocktail inhibitor EDTA free	Roche Diagnostics Deutschland
Proteinase K	Roche
Protino Glutathione Agarose 4B	Macherey-Nagel
Quick-Load Purple 100bp DNA Ladder	New England Biolabs
Quick-Load Purple 2-Log DNA Ladder	New England BioLabs
superFasLigand (soluble human recomb.)	Enzo Life Sciences
SYBR Safe DNA Gel Stain	Invitrogen
T4 DNA Ligase	Thermo Scientific
T7 Endonuclease I	New England BioLabs
Vectamount	Vector Laboratories
Vectashield with DAPI hard set mounting	Vector Laboratories
Whatman chromatography paper, 3 mm	GE Healthcare Life Sciences

3. Chemicals

All chemicals mentioned in this thesis were purchased from the following suppliers: Sigma-Aldrich, Thermo-Fisher Scientific, Roche and Roth.

4. Commercial kits

Amaxa Cell line Nucleofector kit T VACA-1002	Lonza
Amersham Protran 0.2 μm nitrocellulose	GE Healthcare Life Sciences
DC Protein Assay	Bio-Rad Laboratories
GeneJET Gel Extraction kit #	Thermo Scientific
GeneJET Plasmid Miniprep kit #	Thermo Scientific
NucleoBond Xtra Midi	Macherey-Nagel

Nucleospin Gel and PCR Clean-up	Macherey-Nagel
Quick change II XL Site directed mutagenesis	Agilent Technologies
Vectastain ABC Elite Kit (Universal)	Vector Laboratories

5. Antibodies

5.1 Primary Antibodies

Antibody	Host	Application	Supplier
β-catenin	Mouse	IF (1:250) WB (1:2000)	BD Transduction Labs
β-tubulin (monoclonal) T4026	Mouse	WB (1:5000)	Sigma-Aldrich
Alix (monoclonal) 1A12	Mouse	WB (1:500)	Santa Cruz
Anti c-Myc Monoclonal 9E10	Mouse	WB (1:1000)	Acro Biosystems
Anti-Human CD95 (Fas), clone DX2	Mouse	IHC (1:25)	BioLegend
Cleaved Caspase 3 (Asp175)	Rabbit	IF (1:400)	Cell Signaling
Dysbidin (ab124967)	Rabbit	WB (1:500)	Abcam
E-cadherin	Mouse	IF (1:250) WB (1:500)	BD Transduction Labs
EEA-1	Mouse	IF (1:300)	BD Transduction Labs
EEA-1	Rabbit	IF (1:100)	Cell Signaling
FAP-1 (PTPN13) H-300 sc-15356	Rabbit	IF (1:250) WB (1:500)	Santa Cruz Biotechnology
Fas C18C12	Rabbit	WB (1:500)	Cell Signaling

Fas (C-20) sc-715	Rabbit	WB (1:500)	Santa Cruz Biotechnology
Fas (human, activating) clone CH11 #05-201	Mouse	FC (1:500)	Millipore
GFP	Rabbit	WB (1:2000)	Peden lab
HRS1	Rabbit	WB (1:1000)	Cell Signaling
N-Cadherin Monoclonal	Mouse	WB (1:500)	Santa Cruz Biotechnology
Pallidin polyclonal AB169037	Mouse	WB (1:500)	Abcam
PTPN13 NB100-56139	Rabbit	IF (1:500) IHC (1:1000)	Novus Biologicals
SDCCAG3 PolyAb (ENTR1 antibody)	Rabbit	IF (1:300) WB (1:500) IHC (1:250)	Proteintech
Transferrin Receptor (CD71)	Rabbit	WB (1: 2000)	Cell Signaling
TSG101	Rabbit	WB (1:500)	Proteintech
VPS28 (monoclonal) Clone E7	Mouse	WB (1:500)	Santa Cruz
YAP sc-101199	Mouse	IF (1:200) WB (1:200)	Santa Cruz Biotechnology
ZO1 Monoclonal (ZO1-1A12)	Mouse	IF (1:100)	ThermoFisher Scientific

IF- Immunofluorescence; FC – Flow cytometry; IHC – Immunohistochemistry; WB- Western Blotting

5.2 Secondary Antibodies

Antibody	Application	Supplier
Alexa Fluor 680 rabbit IgG	WB (1:10000, LICOR)	Thermo Fisher Scientific
DyLight 800 mouse IgG	WB (1:10000, LICOR)	Thermo Fisher Scientific
Alexa Fluor 488 g/m IgG	IF (1:500)	Thermo Fisher Scientific
Alexa Fluor 488 g/r IgG	IF/FC (1:500)	Thermo Fisher Scientific
Alexa Fluor 594 d/r IgG	IF (1:500)	Thermo Fisher Scientific
Alexa Fluor 633 g/m IgG	IF/FC (1:500)	Thermo Fisher Scientific
Alexa Fluor 647 g/m IgG	IF/FC (1:500)	Thermo Fisher Scientific

6. Primers

Name / No	Sequence	Application
ENTR1 gRNA1 sense / 1	CACCGTGGCCGGATCCTCTTTCGAG	Cloning gRNA in Cas9 vectors
ENTR1 gRNA1 antisense / 2	AAACCTCGAAAGAGGATCCGGCCAC	Cloning gRNA in Cas9 vectors
ENTR1 gRNA1 primer PCR FW / 3	GCCACACTCATGCACGATTC	T7 assay, sequencing screening

ENTR1 gRNA1 primer PCR RV / 4	TCAGCCACCTTCACACTTCC	T7 assay, sequencing screening
ENTR1-GFP FW /17	TAATAGGTACCTCGGGCTACCAGCGCCG	Cloning
ENTR1-GFP RV /18	AATAGCGGCCGCTCAAGAGTCTTCCTCCTCGTCTT	Cloning
SDMAG3mutPFW / 19 (ENTR1)	GATGGCGGACGCCAGGTAGGCCC	Site directed mutagenesis
SDMAG3mutPRV / 20 (ENTR1)	GGGCCTACCTGGCGTCCGCCATC	Site directed mutagenesis
SDMAG3mutEFW / 21 (ENTR1)	GGGTGAGTCTGCGCGATGGCGGACG	Site directed mutagenesis
SDMAG3mutERV / 22 (ENTR1)	CGTCCGCCATCGCGCAGACTCACCC	Site directed mutagenesis
ENTR1 mutagenesis resist siRNA8 FW / 35	GAAAACCACGTAGTCAAGCTAAAACAGGAA	Site directed mutagenesis
ENTR1 mutagenesis resist siRNA8 RV / 36	GATTTCCTGTTTTAGCTTGACTACGTGGTT	Site directed mutagenesis
Human U6 promoter 5'	GACTATCATATGCTTACCGT	Sequencing
EBV RV	GTGGTTTGTCCAAACTCATC	Sequencing
CMV FW	CGCAAATGGGCGGTAGGCGTG	Sequencing

GFP (N-terminal)	GTCCGCCCTGAGCAAAGACCC	Sequencing
BGH reverse	TAGAAGGCACAGTCGAGG	Sequencing
T7 forward	TAATACGACTCACTATAGGG	Sequencing

** All primers were purchased from Sigma-Aldrich

7. DNA Constructs

Name	Description and source
pcDNA3-myc	pcDNA3 vector backbone, Erdmann lab
pcDNA3-GFP	pcDNA3 vector backbone, Erdmann lab
pEGFP-C1	peGFP vector with N-terminal GFP, Erdmann lab
GFP-PTPBL	pcDNA3 vector backbone, Erdmann lab
Myc-PTPBL	pcDNA3 vector backbone, Erdmann lab
GFP-FERM (PTPBL)	pcDNA3 vector backbone, Erdmann lab
GFP-PDZ 1-5 (PTPBL)	pcDNA3 vector backbone, Erdmann lab
pCIneoMyc-LATS1	Addgene #66851 from Yutaka Hata*
pCIneoMyc-LATS2	Addgene #66852 from Yutaka Hata
pGEX-6-P1-GST	GE Healthcare (München)
pGEX-GST-ENTR1	pGEX vector backbone, Erdmann lab
pGEX-GST-VAMP3	Kind gift from Andrew Peden

Myc-ENTR1 wt	Isoform 2, pcDNA3 vector backbone, Erdmann lab
GFP-ENTR1 wt	Isoform 2, pcDNA3 vector, siRNA resistance
GFP-ENTR1 P167A	Isoform 2, pcDNA3 vector, siRNA resistance (lacks PTPN13 interaction site), P167A mutation
GFP-ENTR E171A	Isoform 2, pcDNA3 vector, siRNA resistance (lacks PTPN13 interaction site), E171A mutation
GFP-ENTR1 Δ397-413	Isoform 2, pcDNA3 vector, siRNA resistance (lacks dysbindin interaction site), created by Agnieszka Skowronek
GFP-ENTR1 D213A	Isoform 2, pcDNA3 vector, siRNA resistance, resistant to caspase cleavage, created by Agnieszka Skowronek
GFP-Rab11 wt	Kind gift from Elizabeth Smythe
GFP-Rab11 DN (R28)	pEGFP vector backbone, Erdmann lab
GFP-RCP (RBD from RCP H13)	Kind gift from Andrew Peden
GFP-Rab4a wt	Kind gift from Elizabeth Smythe
GFP-Rab4a DN S22N	Kind gift from Elizabeth Smythe
px458 Cas9	pSpCas9(BB)-2A-GFP (Addgene #48138) from Zhang lab
px459 Cas9	pSpCas9(BB)-2A-Puro v2.0 (Addgene #62988) from Zhang lab

8. siRNA

Name	Sequence / Catalogue number	Supplier
AllStar Negative Control siRNA	n/a #1027281	Qiagen
PTPN13 siRNA1	AAGUAAGCCUAGCUGAUCCUGUU	Dharmacon
PTPN13 siRNA2	CAGAUCAGCUUUCCUGUAAUU	Dharmacon
Hs_SDCCAG3_6	CGACGCACUGAAAGAUGAA*TT* #SI04185888 (ENTR1)	Qiagen
Hs_SDCCAG3_7	ACUGAAUCUUGUUGCCGAATT #SI04216499 (ENTR1)	Qiagen
Silencer Select Pre-designed ENTR1 siRNA	CCACGUCGUGAAACUAAAA*TT* #s21238	Ambion by Life Technologies

9. Biological Material

9.1 Bacterial strains

Name	Application	Supplier
E. coli Nova Blue (XL1)	Plasmid DNA isolation, cloning and subcloning	Stratagene GmbH
E. coli BL-21 Rosetta2(DE3)	GST fusion protein expression	Novagene

XL1-Blue supercompetent bacteria	Site directed mutagenesis.	Agilent

9.2 Mammalian cell lines

Name	Description	Supplier
BJAB	Human Burkitt lymphoma B cell line	DSMZ
Caco2	Human colon colorectal adenocarcinoma epithelial cell line	ATCC
Caco2	Human colon colorectal adenocarcinoma epithelial cell line	Sigma
DLD-1	Colon colorectal adenocarcinoma (Dukes' type C) epithelial cell line	ECACC
HCT-116	Human colon colorectal carcinoma epithelial cell line	ATCC
HEK293	Human embryonic kidney cell line	ECACC
HeLa	Human cervical cancer cell line	ECACC
MCF-10	Breast mammary gland non-tumourigenic epithelial cell line	ATCC
MDCKII	Madin-Darby canine kidney epithelial cell line	ECACC

10. Culture media and plates

Mammalian cell lines

	Description	Supplier
DMEM	DMEM (1x) + GlutaMAX-I – Dulbecco's Modified Eagle Medium [+] 4.5 g/L D-glucose [+] Pyruvate	Gibco (Life Technologies)
MEM	MEM (1x) – Minimum Essential Medium [+] Earle's Salts [+] L-Glutamine	Gibco (Life Technologies)
DMEM/F12	DMEM/F12 (1:1) (1x) – Dulbecco's Modified Eagle Medium / F12 Nutrient Mixture (Ham)	Gibco (Life Technologies)
RPMI-1640	RPMI-1640 medium with L-glutamine and sodium bicarbonate	Sigma-Aldrich
Opti-MEM	Opti-MEM I (1x) – Reduced Serum Medium [+] L-Glutamine [+] HEPES [-] Phenol Red	Gibco (Life Technologies)

Bacteria plates

Luria-Bertani (LB) broth bacterial medium: 10 g/L peptone, 5 g/L yeast extract, 10 g/L NaCl and ddH_20.

LB bacterial plates: 10 g/L peptone, 5 g/L yeast extract, 10 g/L NaCl, 15 g/L agar and ddH_20. Supplemented with appropriate antibiotics.

II. Methods

1. Bacteria procedures

1.1 Competent E. coli preparation

E. coli strains mentioned above were thawed at RT and spread on LB agar plates without antibiotics overnight at 37°C. The following day, a single colony was inoculated in 50 mL of LB medium without antibiotics, incubated at 37°C and 220 rpm and bacterial growth was monitored by measuring OD_{595}. When the bacterial suspension reached OD_{595} = 0.5, suspension was chilled on ice for 10 minutes. Cells were then centrifuged at 5000 rpm for 10 minutes at 4°C and resuspended in 15 mL of ice-cold sterile transformation buffer. Cells were chilled on ice for additional 15 minutes, centrifuged again as before and resuspended in 4 mL of transformation buffer and 15% of glycerol (v/v). After aliquoting, cells were immediately stored at -80°C to prevent bacteria from losing competence.

Transformation buffer:

10 mM Tris-HCl pH 7.0

50 mM $CaCl_2$

Sterile H_2O

1.2 Bacterial transformation with DNA

Competent cells (50 or 100 µl) were thawed on ice for 5 minutes, mixed with (i) 1 µl of plasmid DNA (from 1000 ng/µl stock), (ii) 5 µl of ligation product or 10 µl of mutagenized plasmid and incubated on ice for 15 minutes. The mixture was then subjected to a heat shock treatment at 42°C for 45 seconds to induce DNA uptake by the cell and immediately cooled on ice for 2 minutes. Transformed bacteria was incubated with 450 µl or 900 µl (depending on the initial aliquot) of pre-warmed LB medium and incubated at 37°C for 1 hour and constant shaking at 220 rpm. Afterwards, (i) 50 µl or 100 µl (depending on the initial aliquot) of the transformed bacteria suspension was spread on LB agar plate with the appropriate antibiotic (Ampicilin 100 µg/mL or Kanamycin 50 µg/mL), (ii) transformed bacteria suspension was centrifuged for 2 minutes at 7000 rpm and removed 450 µl or 900 µl of supernatant. Cell pellet was resuspending in the remaining LB medium and plated on LB agar plate with the appropriate antibiotic. Finally, plates were incubated overnight at 37°C and checked the following day for the presence or absence of bacterial colonies.

2. Mammalian Cell Culture

HeLa, HEK293, HCT116, MDCKII and Caco2 cells from Sigma were maintained in DMEM-Glutamax supplemented with 10% Foetal Bovine Serum (FBS) and 1% Penicillin/Streptomycin. Caco2 cells from ATCC were maintained in MEM supplemented with 10% FBS, 1% Penicillin/Streptomycin and 1% of Non-Essential Aminoacids. DLD-1 and BJAB cells were cultured in RPMI-1640 medium

supplemented with 10% of FBS (DLD-1) or 20% of FBS (BJAB) and 1% Penicillin/Streptomycin. MCF-10A cells were maintained in DMEM-F12 medium supplemented with 5% horse serum, 1% Penincilin/Streptomycin, 20 ng/mL EGF, 10 μg/μL insulin and 0.5 μg/ml hydrocortisone. All cell lines were kept at 37°C in a 5% CO_2 atmosphere.

2.1 Cell subculturing and seeding

Cells were cultured in the appropriate format (T75, T25 flask or 10 cm dish) and generally subcultured when reached 80-100% confluence. Cells were washed once with PBS1x and trypsin was added and spread all over the flask in order to detach cells. Flask was incubated at 37°C for 5-15 minutes (depending on the cell line) and checked every 5 minutes until complete detachment was observed. Next, 5 mL of full medium was added to the flask to stop trypsinization and cells were pipetted repeatedly to homogenize cell suspension. Cells were centrifuged 2000 rpm for 2 minutes or 1000 rpm for 5 minutes and the resulting supernatant aspirated. Cell pellet was resuspended in 5 mL of full medium and splitted in fresh flasks in ratios ranging from 1:3 to 1:10 depending on the specific growth rate of the cell line. Cell concentration can be determined after the centrifugation step by using Neubauer counting chamber. Cells were seeded accordingly depending on the purpose of the experiment and the plate format.

2.2 Cell transfection

Cells were seeded 24 hours prior to transfection as described above to reach a 50-70% confluency for DNA transfection or 30-50% confluency for siRNA transfection. In a 6-well plate format, 2 µg of DNA or 20 µM to a final concentration of 100 pmol of siRNA were diluted in 250 µl of Opti-MEM (according to the manufacturer's protocol). In a separate tube, 2.5-5 µl of Lipofectamine 2000 was also diluted in 250 µl of Opti-MEM. Mixtures were incubated for 5 minutes at RT and combined to a total volume of 500 µl containing DNA/siRNA + lipid complexes. After 20 minutes incubation, the mixture was added to the 6-well plate containing cells in 1.5 mL of medium without antibiotics. Medium without antibiotics was replaced 6 hours after transfection and full medium was added to the cells.

Transfection with DNA requires 48 hours incubation before harvesting cells, whereas siRNA transfection requires 72 hours. In cell lines exhibiting low transfection efficiency (such as Caco2 or MDCKII cells), two consecutive transfections were performed.

3. DNA techniques

3.1 Standard PCR

Primers were designed with an approximate length of 25 nucleotides and palindromic sequences recognized by specific restriction enzymes were also included with the aim of using the resulting PCR products for cloning purposes.

PCR was performed with *Phusion High Fidelity DNA Polymerase* following manufacturer's indications and adapted to each PCR reaction.

PCR reaction component	Volume added
Phusion Green buffer 5x	10 µl
DNA template	20-40 ng
Forward primer (10 µM)	2.5 µl
Reverse primer (10 µM)	2.5 µl
dNTPs (10 mM)	1 µl
Phusion HF DNA polymerase	0.5 µl
ddH_2O	Up to 50 µl (total reaction)

Cycling parameters and such as melting temperature or extension time were optimized for each of the PCR reactions. Amplification was carried out in the thermocycler and obtained PCR products were analysed in an agarose gel (as described in section 3.2.1).

Cycle stage	Temperature and time	Cycles
Initial denaturation	98°C, 30”	1
Denaturation	98°C, 10”	35
Annealing	Depending on primers T_m, 30”	
Extension	72°C, 30” per kb of plasmid length	
Final extension	72°C, 10’	1

3.2 DNA Cloning

3.2.1 Agarose gel electrophoresis

Agarose gel electrophoresis was used to separate and visualize DNA fragments of different size. For preparation, the appropriate percentage of agarose was diluted in TAE buffer 1x and heated in microwave for 2 minutes. 1% agarose gels were prepared as standard procedure for DNA fragments ranging from 300 bp to 10 Kb, whereas 2% agarose gels were used to detect DNA fragments under 300 bp (such as for T7 assay). SYBR Safe DNA stain was added to the solution at 1:10000 dilution, allowing the visualization of DNA under Blue Led Illuminator or Gel Doc EZ System.

DNA samples were diluted in NEB Purple DNA loading dye upon gel casting and loaded in the wells. Agarose gels were run at 100 V and results visualized in the abovementioned devices. For further purification, DNA bands of interest were

excised from the gel and purified by using GeneJET Extraction kit according to the manufacturer's protocol.

50X TAE buffer:

40 mM Tris Base pH 7.0

20 mM Glacial Acetic Acid

1 mM EDTA pH 8.0

Sterile H_2O

3.2.2 Digestion with restriction enzymes

Restriction enzymes used in molecular cloning and sub-cloning of PCR products into DNA vectors were selected from the New England Biolabs NEBcutter online tool. Specific digestion protocols were provided by NEBcutter and DNA was incubated with the restriction enzymes for the indicated time and temperature. For double digestion, reaction was prepared as follows:

Digestion component	Volume added
DNA (vector or PCR product)	1-2 µg
CutSmart buffer 10x	5 µl
Restriction enzyme 1 (1-2 U) *	1-2 µl
Restriction enzyme 2 (1-2 U) *	1-2 µl
ddH_2O	Up to 50 µl (total reaction)

*1-2 units/µl and 1 unit = 1 µg of DNA – Add as many µl as µg of DNA

Standard double digestion protocol consisted of 1 hour incubation at 37°C. After double digestion DNA was diluted in 6x loading dye and run in agarose gel for subsequent purification with GeneJET Extraction kit.

3.2.3 Ligation

After double digestion vectors were dephosphorylated by incubating with 2 units of Calf Intestinal Alkaline Phosphatase (CIP) at 37°C for 30 minutes (1 U = 1 µg of digested DNA). Dephosphorylation of 5' ends of DNA in the vectors prevent self-circularization during subsequent ligation.

Digested vector and insert DNA were ligated by using T4 ligase in a reaction consisting of:

- Digested and dephosphorylated vector: 50 ng
- Digested DNA Insert:

$$Insert = \ ng\ vector \cdot \frac{length\ kb\ insert}{length\ kb\ vector} = ng\ insert\ 1{:}1\ ratio\ x\ 5\ (for\ 1{:}5\ ratio)$$

- T4 DNA ligase buffer 10x: 2 µl
- T4 DNA ligase: 1 µl
- ddH_2O: up to 20 µl

Ligation reaction was incubated for 5 hours or overnight at room temperature. A control for self-ligation of vector was always included, consisting of the previous ligation reaction but without adding DNA insert, expecting no colonies in the control agar plate when transformed into bacteria.

3.3 Plasmid DNA isolation and purification

Single colonies were picked from LB agar plate after transformation and inoculated into 5 mL of LB medium in a bacterial culture tube (Miniprep) or 100 mL of LB medium in a sterile Erlenmeyer flask (Midiprep) containing the adequate antibiotic. Liquid culture was incubated overnight at 220 rpm and 37°C and the following day bacteria were pelleted. Plasmid DNA was isolated and purified from bacteria using GeneJet Plasmid Miniprep Kit or NucleoBond Xtra Midi Kit, following the manufacturer's protocol.

3.4 Site directed mutagenesis

Single point mutations for specific siRNA resistance were introduced by using Quick change II XL Site directed mutagenesis kit, according to manufacturer's protocol. In order to generate siRNA resistance but not a change in the amino acid sequence of the protein, three silent mutations were introduced and mutagenic primers were designed accordingly, adding 10 nucleotides of DNA sequence flanking both sides of the mutation site (primer sequences can be found in Material's section 6). PCR reaction for site directed mutagenesis was prepared as follows:

PCR reaction component	Volume added
Pfu Ultra buffer 10x	5 µl
Forward primer mutagenesis	125 ng
Reverse primer mutagenesis	125 ng
DNA template	50 ng
dNTPs (10 mM)	1 µl
Pfu Ultra HF DNA polymerase (2.5 U/µl)	1 µl
ddH_2O	Up to 50 µl (total reaction)

The cycling program used to amplify the target plasmid DNA was adapted from manufacturer's protocol as follows:

Cycle stage	Temperature and time	Cycles
Initial denaturation	98°C, 30"	1
Denaturation	98°C, 10"	35
Annealing	Depending on primers T_m, 30"	
Extension	72°C, 30" per kb of plasmid length	
Final extension	72°C, 10'	1

Upon PCR reaction, 1 µl of DpnI restriction enzyme (10 U/µl) was added directly to the PCR reaction and incubated at 37°C for 3 hours in order to digest parental supercoiled double stranded DNA. A control reaction consisting of all

PCR reaction components except Pfu DNA polymerase was also included to assess digestion efficiency.

Digested DNA was then precipitated by adding 1/10 volume of 3M Sodium Acetate (pH 5.2), mixing thoroughly. Afterwards, 2.5 volume of cold 100% Ethanol was added and DNA was incubated at -80°C for 20 minutes. DNA was then centrifuged at 15.000 rpm for 15 minutes and a transparent pellet was obtained and washed with 70% of Ethanol. Samples were centrifuged again at 15.000 rpm for 5 minutes and supernatant was discarded, leaving pelleted DNA for drying and finally re-suspended in 10 µl of ddH_2O. Purified DNA plasmid with introduced mutations was transformed into XL-1 Blue Supercompetent bacteria as described in Methods section 1.2. After transformation, the absence of colonies in the agar plate with bacteria transformed with the DNA from –Pfu control confirmed that the digestion of parental DNA used as a template was complete.

3.5 Genomic DNA extraction

Genomic DNA from mammalian cells was extracted based on a protocol consisting of phenol-chloroform liquid-liquid extraction followed by DNA precipitation. Confluent cells were washed once with PBS1x and scrapped from the 6-well plate, transferring cell suspension to a fresh tube. Cells were centrifuged at 500xg for 5 minutes and the remaining cell pellet was lysed with 250 µl of lysis buffer supplemented with Proteinase K, which digests proteins and remove contamination from the DNA preparation. Mixture was incubated 1 hour

at 37°C, followed by an incubation at 95°C for 5 minutes to inactivate Proteinase K.

Lysed cells were centrifuged 5 minutes at 13.000 xg RT and the viscous supernatant was transferred to a fresh tube. Equal volume of the lower phase of phenol-chloroform was added to a ratio of 50:50 and spun in the microfuge at top speed for 2 minutes. Resulting top phase, consisting of water and DNA was transferred to a new tube and previous steps were repeated again.

Finally, 1:10 volume of 3M Sodium Acetate (pH 5.2) and same volume of isopropanol was added to the aqueous phase to precipitate DNA, vortexed briefly and incubated 2 hours at -80°C. Upon thawing, mixture was centrifuged at 13.000 xg for 30 minutes at 4°C, supernatant was discarded and remaining pellet washed with 1 mL of 70% ethanol. Precipitated DNA was spun one more time at top speed for 5 minutes, supernatant was discarded and DNA pellet was dried before re-suspending it in 30-50 µl of ddH_2O

Lysis buffer:

20 mM EDTA

10 mM Tris 8.0

200 mM NaCl

0.2% Triton X-100

Supplement with Proteinase K (final concentration 100 µg/ml from a 20 mg/ml stock) just before lysing cells.

3.6 CRISPR-Cas9: gRNA design, cloning and efficiency testing by T7 assay.

3.6.1 Design of sgRNA for ENTR1 gene

Guide RNAs were designed with CRISPOR online tool providing the target sequence of ENTR1. As a general rule, introns were never targeted and exons 1 or 2 are usually the most suitable target candidates. However, for ENTR1 gRNA design exon 4 was targeted as targeting exons 1 and 2 would not affect ENTR1 isoform 3 (information obtained from UNIPROT).

CRISPOR online tool designed a pair of gRNA to be cloned in px458 and px459 vectors. gRNA sequence included 4 nucleotides overhangs compatible with desired vectors and a PAM motif. CRISPOR also provided primers forward and reverse to amplify on-target sites from genomic DNA for sequencing or T7 assay.

3.6.2 Cloning sgRNA annealed oligos in BbsI site of px458 and px459 vectors.

Previously designed gRNAs were cloned in px458-GFP and px459-Puromycin vectors following Zhang lab protocol. Cloning of gRNAs was achieved by synthesizing the two partially complementary oligos. When annealed, the oligos form double stranded DNA with overhangs, which are easy to clone into BbsI site in the px458/px459 vectors.

First, gRNA oligos were phosphorylated and annealed according to the following reaction:

	Volume added
sgRNA (sense) 100 μM stock	1 μl
sgRNA (antisense) 100 μM stock	1 μl
T4 ligation buffer	1 μl
T4 PNK (poly kinase)	1 μl
ddH_2O (total reaction 10μl)	6 μl

Mixture was incubated 30 minutes at 37°C, followed by incubation at 95°C for 5 minutes. Tubes were cooled down at room temperature for 1-2 hours. Simultaneously, px458 and px459 vectors were digested with BbsI restriction enzyme as follows:

Digestion reaction component	**Volume added**
px458/px459 vector	2 μg
CutSmart buffer	5 μl
BbsI HF restriction enzyme	1 μl
ddH_2O	Up to 50 μl

Digestion reaction was incubated at 37°C for at least 3 hours, followed by addition of 2 μl of CIP and additional incubation for 30 minutes at 37°C. Samples were run in 1% Agarose gel and the corresponding bands were extracted with GeneJET Extraction kit.

Finally, ligation reaction was set up as follows (also including control ligation) and incubated for 1 hour on the bench.

Ligation reaction component	Volume added
px vector digested with BbsI	100 ng
Annealed oligos (1:2000 dilution)	1 µl
10x DNA ligase buffer	1 µl
T4 DNA ligase	0.5 µl
ddH_2O	Up to 10 µl

E. coli Nova blue bacteria were transformed with 5 µl of the ligation product for subsequent Miniprep plasmid DNA purification and sequencing in order to confirm that gRNA sequences were correctly inserted in the vectors.

3.6.3 Amplification of gRNA target genomic region by PCR

In order to amplify the specific gRNA target region from the whole genomic DNA for screening purposes, GoTaq polymerase PCR was performed using specific primers designed by CRISPOR.

PCR reaction component	Volume added
GoTaq Flexi uncoloured buffer 5x	10 µl
Forward primer gRNA (10 µM)	2.5 µl
Reverse primer gRNA (10 µM)	2.5 µl
DNA template (genomic DNA from extraction)	100-500 ng
dNTPs (10 mM)	1 µl
$MgCl_2$ GoTaq	4 µl
GoTaq polymerase	0.25 µl
ddH_2O	Up to 50 µl (total reaction)

The cycling program used to amplify the gRNA target genomic region was adapted from GoTaq manufacturer's protocol as follows:

Cycle stage	Temperature and time	Cycles
Initial denaturation	95°C, 3'	1
Denaturation	95°C, 30"	30
Annealing	Lowest T_m of the pair of primers – 3°C, 30"	
Extension	72°C, 30"	
Final extension	72°C, 5'	1

A 5 µl aliquot of the PCR product was run in 1% agarose gel to check that the target region was amplified correctly (band should correspond with the expected size of the specific amplified region). Once confirmed, the rest of PCR product was purified with Nucleospin Gel and PCR Clean-up kit as manufacturer's protocol and subsequently sent for sequencing or used for T7 assay.

3.6.4 T7 Endonuclease I assay: determining genome targeting efficiency

As CRISPR-Cas9 based genome editing does not target all loci with the same efficiency, it is necessary to assess the efficiency of gRNA in generating mutations in the target site. T7 Endonuclease I assay was performed to detect on-target editing events in genomic DNA from cells (for example knockout clones or bulk population of gRNA transfected cells) (Figure 16). PCR products are

denatured and reannealed to produce heteroduplex mismatches where gRNAs generated double-strand breaks, leading to in/del introduction. T7 enzyme is able to recognize these mismatches and, when detected, cleave the DNA in that specific site.

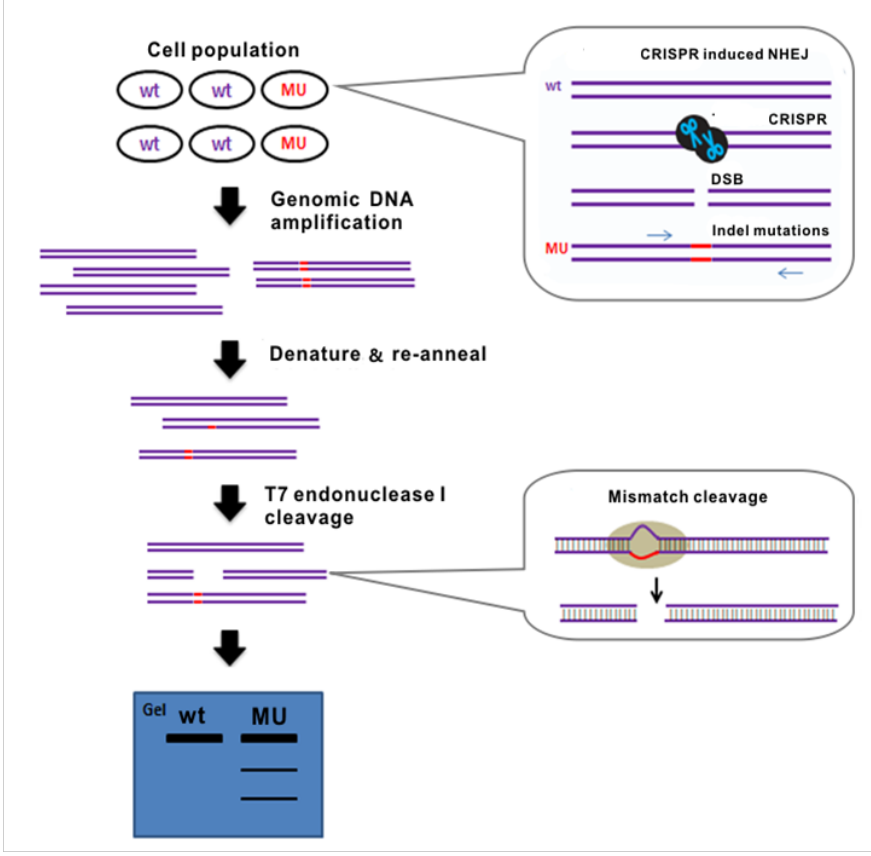

Figure 16. How T7 endonuclease I assay works. Upon gRNA transfection a mixed population is obtained (wild-type and mutant cells). The specific genomic region that the gRNA is targeting is amplified by PCR. The resulting PCR products are denatured and subsequently reannealed to produce an heterogenous population of DNA fragments. T7 enzyme identifies heteroduplex mismatches where gRNAs generated double-strand breaks and, when detected, cleave the DNA in that specific site. As a result, it is possible to observe the efficiency of the cleavage by agarose gel electrophoresis. Adopted from https://www.genecopoeia.com

First, PCR products from the previous GoTaq amplification were annealed by preparing the following reaction and using the appropriate hybridization conditions:

Component	Volume added
DNA (clean-up PCR product)	200 to 600 ng
10X NEBuffer 2	2 µl
Nuclease-free Water	To 19 µl

Step	Temperature	Ramp Rate	Time
Initial Denaturation	95°C		5 minutes
Annealing	95-85°C	-2°C/second	
	85-25°C	-0.1°C/second	
Hold	4°C		Hold

Finally, 1 µl of T7 Endonuclease I was added to the annealed PCR products and incubated for 1 hour at 37 °C. Control reaction with no addition of T7 was also included. Samples were loaded in 2% agarose gel and the DNA fragments resulting from T7 cleavage were analysed.

3.7 Generation of stable HeLa cell line

Stable cell lines were generated by transfecting cells with plasmids carrying geneticin (G418) resistance gene:

- pcDNA 3.1 GFP

- pcDNA 3.1 GFP-ENTR1 wt
- pcDNA 3.1 GFP-ENTR1 D213A (caspase cleavage resistant)

The optimal concentration of G418 was previously determined by treating cells with a concentration range of antibiotic (from 0 mg/ml to 2 mg/ml) for a week and calculating a kill curve. For HeLa ENTR1 knockout cells the optimal concentration of G418 (minimum concentration in which all cells were dead after one week) was 0.75 mg/ml.

HeLa ENTR1 knockout cells were seeded on 10 cm dish and transfected with 10 µg of the corresponding DNA constructs. Untransfected cells were seeded as well as a control to monitor cell death after G418 treatment. After 48 h cells were treated with 0.75 mg/ml of G418 in DMEM supplemented with 10% FBS. The selection medium was refreshed every 2-3 days depending on cells death rate. After 10-14 days cell suspensions were prepared for FACS sorting. First, cells were trypsinized, re-suspended in 1 mL of full medium and centrifuged at 1000 rpm for 5 minutes. Supernatant was then removed and pellet was re-suspended in 1 ml of Opti-MEM. Cell suspension was transferred to flow cytometry tubes and kept on ice. Index sorting of GFP positive single cells into 96-well plates, as well as a GFP positive bulk cell population was performed with BD FASC Aria IIu (Flow cytometry Core Facility, The University of Sheffield).

After 2-3 weeks 10 viable colonies from the 96-well plates were expanded into 60 mm dishes and expression of the appropriate proteins was verified by

Western Blot. Expression of GFP in the colonies during expansion was assessed regularly by using ZOE Fluorescent Cell Imager.

4. Protein methods

4.1 Assessment of protein concentration

Protein concentration was measured with Bio-Rad DC Assay Kit according to manufacturer's protocol. On a 96-well plate 5 µl of lysate (per triplicate) was mixed with 25 µl of reagent A and 200 µl of reagent B. Plate was incubated for 15 minutes in the dark and 750 nm wavelength absorbance was measured in FLUOStar OPTIMA Absorbance Reader. Protein concentration of each sample was estimated using the A_{750} values and a linear regression equation calculated from Albumin standard curve. For experiments requiring same protein concentration such as knockdown, degradation or cell fractionation analysis, protein concentration in all set of samples was equalized as follows:

$$\mu\text{l sample} = \frac{Lowest\ protein\ concentration\ in\ set\ of\ samples}{Concentration\ of\ sample} \cdot Final\ volume\ sample\ (\mu\text{l})$$

Samples were finally adjusted to the same final volume with the appropriate buffer.

4.2 Western Blotting

4.2.1 Cell lysis

Confluent cells on 6-well plates or 60 mm dishes were kept on ice and washed once with ice-cold PBS. Proteins were extracted from the cells by adding the appropriate volume of lysis buffer (supplemented with protease inhibitors) and incubating in the plates for 15 minutes on ice. Then, cells were scrapped from the plate, transferred to a pre-chilled tube and incubated for 30-45 minutes on ice, vortexing thoroughly every 10 minutes. Cell lysate was finally cleared by centrifugation at 15.000 rpm for 15 minutes at 4ºC and supernatant containing protein extract was transferred to a new tube. If necessary, protein concentration was measured after this step.

Samples for Western Blot were preparing by diluting the lysate with 4x Laemmli buffer (to a final concentration of 1x Laemmli buffer) and boiling the samples for 5 minutes and 98ºC with the aim of denaturing proteins. Prior to be loaded in acrylamide gels, samples were cooled down to room temperature, vortexed and shortly spun down.

4.2.2 Western blotting

Polyacrylamide gels for SDS-PAGE electrophoresis were prepared in order to separate proteins contained in the cell lysate by their specific molecular weight. Gels were composed of a 5% acrylamide (pH 6.8) stacking part and a resolving gel (pH 8.8) ranging from 6% to 12% acrylamide, depending on the

molecular weight of the protein/s of interest. Stacking gel allowed samples to pack prior to enter resolving gel, and the percentage of the resolving gel was inversely co-related to the molecular size of the protein to analyse (6% gels were used for high molecular weight proteins, whereas 10-12% gels were used to visualize smaller proteins).

Protein extracts diluted in Laemmli buffer were loaded into the gel in the appropriate volumes, including the correct prestained protein ladder as a marker for molecular weight of the analysed proteins. Gels were mounted in the tank and immersed in running buffer 1x. First, voltage was set at 50V and when the samples were out of the stacking gel, gradually increased to 100-120V. Running was stopped when Laemmli buffer was out of the gel and samples properly resolved.

Transfer of the proteins in the gel to nitrocellulose membrane was performed in transfer buffer 1x and settings were adjusted depending on the molecular weight of the analysed protein:

- As standard procedure, proteins were transferred at 250 mA for 90 minutes at room temperature.
- For high molecular weight proteins such as PTPN13 (> 200 KDa), proteins were transferred overnight at 25 V and 4°C.

In order to test the efficiency of transfer, resulting nitrocellulose membranes were stained with Ponceau S red and washed thrice with PBS-T 1x to

remove stain completely. Membranes were subsequently blocked in 5% milk PBS-T for 1 hour at room temperature with gentle agitation.

After blocking, membranes were incubated with primary antibodies at the specific dilution in 5% milk PBS-T for 2 hours at room temperature or 4°C overnight, depending on the manufacturer's recommendation. Again, membranes were washed thrice with PBS-T 1x. Finally, membrane was incubated for 1 hour at room temperature with fluorescently conjugated secondary antibodies for *Odyssey LICOR* detection (680 nm Alexa Fluor for rabbit primary antibodies and 800 nm Alexa Fluor for mouse primary antibodies) diluted in in 5% milk PBS-T. Membranes were washed three times with PBS-T 1x and dried at room temperature. Odyssey Sa imaging system from LICOR was used to scan, visualize and quantify the proteins of interest in the membrane. Image Studio Lite software was used to analyse and edit the images obtained.

4.2.3 Buffers and solutions

PBS 20x:

160,0 g NaCl

4,0 g KCl

4,8 g KH_2PO_4

71,6 g Na_2HPO_4 x $12H_2O$

Top up to 1 L with ddH_2O

Basic lysis buffer

1% Triton in PBS 1x

Add fresh protease cocktail inhibitor 25x

HEPES lysis buffer

50mM HEPES, pH 7.5 = 2.5 ml

10% glycerol = 5 ml

150mM NaCl = 7.5 ml

1% Triton X-100 = 0.5 ml

1,5mM $MgCl_2$ = 75 µl

1mM EDTA = 100 µl

Top up with ddH_2O to 50 ml

Add fresh protease cocktail inhibitor

25x

NP-40 Lysis buffer

50mM HEPES-KOH pH 8 = 2.5 ml

10% glycerol = 5 ml

100mM KCl = 5 ml

0.1% NP-40 = 0.5 ml

2mM EDTA = 200 µl

Top up with water to 50 ml = 36,8 ml

mQ water

Add fresh protease cocktail inhibitor

25x

Stacking acrylamide gel (5%)

ddH_2O

0.5M Tris HCl pH 6.8

40% Acrylamide/Bis solution 37:5:1

10% SDS

10% APS

TEMED

Resolving acrylamide gel (6% to 12%)

ddH_2O

1.5M Tris HCl pH 8.8

40% Acrylamide/Bis solution 37:5:1

10% SDS

10% APS

TEMED

Running buffer 10x

30,3 g Tris

144,0 g glycine

10,0 g SDS

Top up with ddH_2O to 1 L

Transfer buffer 10x

30,3g Tris

144,0g glycine

Top up with ddH_2O to 1 L

Transfer buffer 1x

10% of Transfer buffer 10x

20% methanol

Top up with ddH_2O to final volume

PBS-T 0.05%

0.05% Tween20 in PBS 1x

Blocking/antibodies solution

5% non-fat dry skimmed milk in PBS-Tween 0.05%

SDS-Sample buffer (Laemmli buffer 4X)

40% glycerine = 20 ml

1% bromophenol blue = 0.5 g

8% SDS = 4 g

250 mM Tris-HCl pH 6.8 = 12.5 ml

20% β-mercaptoethanol = 10 ml

ddH_2O = 7.5

4.3 Co-immunoprecipitation (GFP and myc trap pull-down)

Pull-down experiments are commonly used for analysis of protein to protein interactions. This technique is based on the co-immunoprecipitation of agarose beads coupled to a GFP or myc tagged protein with its interacting partners, allowing subsequent detection of the immunoprecipitated proteins by Western Blotting. Interactions between two overexpressed tagged proteins or between an overexpressed tagged protein and endogenous protein were analysed by GFP trap_A or myc trap_A co-immunoprecipitation.

48 hours upon transfection lysates were obtained from confluent cells seeded in 6-well plates or 60 mm dishes, as described in section *4.2.1.* 10% of the cleared protein extract was used as input sample representing the total protein levels.

Either GFP trap_A or myc trap_A beads were equilibrated in the same lysis buffer as before. 15 µl of the bead slurry was re-suspended in 200 µl of ice cold lysis buffer and centrifuged at 7000 rpm for 2 minutes and 4°C. Supernatant was removed and beads were washed twice more by the same procedure. Next, cell lysate was mixed with the equilibrated beads and incubated under continuous rotation for 3-4 hours at 4°C.

Finally, beads were washed thrice with 500 µl of lysis buffer as previously indicated and re-suspended in 60 µl of Laemmli buffer 2x. Beads were boiled at

95°C for 5 minutes and samples to dissolve the protein immuno-complexes from the beads and centrifuged at 15.000 rpm for 2 minutes to precipitate the beads. Input and pull-down samples were loaded in acrylamide gels and blotted with antibodies for either GFP/myc tags or for the specific protein of interest. Western Blotting was performed as described in section *4.2.2*

4.4 Fusion GST-tag protein expression and GST-pull down

4.4.1 GST-fusion protein purification

Gluthatione S-transferase (GST) gene fusion is the standard system for expression and production of recombinant proteins in bacteria. Protocol described represents volumes of LB medium, buffers and beads required per 1 L of bacteria culture. pGEX expression vectors containing ENTR1 and VAMP3 or empty pGEX vector were transformed into BL21 (DE3) bacteria and a single colony was inoculated into 100 mL of LB medium supplemented with ampicillin (100 μg/mL), incubated for overnight at 37°C and 220 rpm. Following day, liquid culture was divided in two 50 mL cultures and each diluted in 450 mL of LB medium supplemented with ampicillin for further incubation at 37°C until the optical density (OD_{595}) of the culture reached 0.6-0.8 units.

Liquid cultures were then chilled on ice. With the aim of achieving induction and subsequent expression of the GST-recombinant protein, culture was incubated with 0.5 mM of Isopropyl β–D-1-thiogalactopyranoside (IPTG) for 5-6 hours at 18°C and 220 rpm. Bacteria were pelleted by centrifuging for 20

minutes at 6000 rpm, supernatant was removed and pellet was re-suspended in 0.5% Triton-X100 in PBS 1x supplemented with protease inhibitors. After gentle re-suspension, bacteria were incubated on ice for 30 minutes and sonicated for 5 minutes (15 seconds ON/OFF cycles) to improve cell lysis. Lysate was finally cleared by centrifugation at 10.000 rpm for 30 minutes and 4°C.

Supernatant was collected and incubated with 400 µl of Protino Glutathione Agarose 4B beads per 500 mL of initial culture. Glutathione beads were previously equilibrated by re-suspending in 10 mL of 0.5% Triton in PBS 1x buffer and centrifuging at 1800 rpm for 4 minutes and 4°C, repeating the wash three times. Clarified bacteria lysate was mixed with equilibrated beads and kept in continuous rotation for 4-5 hours at 4°C. Upon incubation, beads were washed three times with 10 mL of 0.5% Triton in PBS 1x as before. Beads were finally re-suspended in 800 µl of 0.5% Triton in PBS (50% suspension) and either stored at -20°C or subjected to GST-pull down.

4.4.2 GST pull-down

Lysates were obtained from 60 mm confluent dishes of HeLa cells as described in section *4.2.1* and 10% of the cleared protein extract was used as input sample representing the total protein levels. The remaining cell lysate was added to 50 µl of GST fusion protein or 10 µl of GST control beads slurry and incubated for 4 hours at 4°C and constant mixing. After incubation, samples were spun at 8000 rpm for 2 minutes at 4°C and 10% of resulting supernatant used as non-

bound sample. Wash beads five times with 500 µl of cold 0.5% Triton X-100 in PBS by centrifuging at 8000 rpm for 2 minutes in between each of the washing steps. Finally re-suspend the beads in 60 µl of Laemmli buffer 2x and boil samples for 5 minutes at 95°C to dissociate the immunocomplexes from the beads.

Two SDS-PAGE gels were run side by side, loading input and pull-down samples with corresponding controls. 10% acrylamide gel was used for Coomassie staining (to visualize GST fusion proteins abundance) and a second gel of variable acrylamide percentage (depending on proteins to detect) was used for Western Blotting as described in section *4.2.2*

5. Flow Cytometry: measuring levels of Fas in the cell surface

HeLa cells were cultured in 6-well plates at a density of $3 \cdot 10^5$ cells and co-transfected the following day with ENTR1 siRNA and the corresponding GFP-labelled DNA plasmid. Controls included in the experiments were: unstained, secondary antibody only, GFP positive only, primary + secondary antibody GFP negative cells and GFP positive + secondary antibody cells. After 72 hours, cells were collected by adding 250 µl of Trypsin/EDTA per well and transferred to fresh tube. Cells were centrifuged at 180 xg for 5 minutes and pellet re-suspended in 1 ml of pre-cooled 1% BSA in PBS 1x. Keeping the tubes on ice during the whole process, cells were aliquoted for each of the mentioned controls and experimental samples.

Cells were incubated with CH11 Anti-Human Fas antibody in 1% BSA PBS solution and incubated for 1 hour at 4°C in constant rotation. Followed incubation, samples were washed three times with 1% BSA in PBS, centrifuging at 180 xg for 2 minutes. Subsequently, samples were incubated with either Alexa Fluor 633 nm or 488 nm secondary antibodies in 1% BSA PBS for 1 hour at 4°C and constant rotation. Cells were again washed thrice in 1% BSA PBS, re-suspended in 1 ml of PBS and transferred to a flow cytometry glass tube.

Fas levels in the cell surface were analysed in the BD LSRII flow cytometer (Flow cytometry Core Facility, The University of Sheffield) and the following gating hierarchy was established (Figure 17). First, the subpopulation of viable HeLa cells and the cells negative for Fas staining are selected by plotting Side Scatter against Forward Scatter in Unstained cells control. Then, subpopulation of GFP positive cells is gated by plotting the Side Scatter against the 488 nm channel in the GFP positive control. Finally, we can analyse the median intensity of Fas in the cell surface (median intensity of 633 nm) in the GFP positive cells by plotting 633 nm channel against the 488 nm channel. Data files exported in FCS format were analysed with FlowJo software.

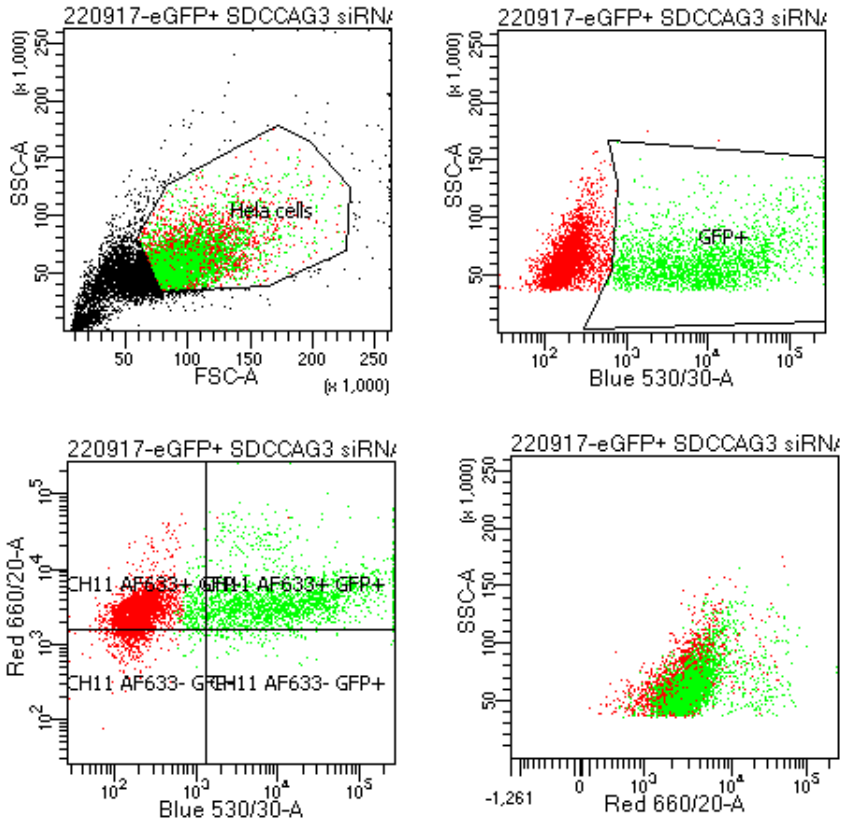

Figure 17. Example of analysis of Fas cell surface levels by flow cytometry. (1) Gating of viable HeLa cells (SSC vs. FSC) (2) Defined subpopulation of GFP positive cells (SSC vs. Blue 530/30A laser) (3) Defining quadrants (Red 660/20A laser vs. Blue 530/30A laser): upper left quadrant represents Fas positive but GFP negative cells, upper right Fas positive and GFP positive cells (our subpopulation of interest), lower left Fas negative and GFP negative cells and finally lower right Fas negative and GFP positive cells. (4) Only the median intensity of Fas in the cell surface (median intensity of 633 nm) in the GFP positive cells is considered for analysis.

6. Immunofluorescence

6.1 Standard protocol

Cells were seeded in coverslips in the appropriate cell density depending on the plate format (usually one coverslip per well in 12-well plates or two coverslips per well in 6-well plate) and transfected with DNA constructs or siRNA if necessary. 48/72 hours post-transfection, medium was removed and cells were washed once with PBS 1x, followed by fixation with (1) 4% PFA for 20 minutes at room temperature (2) 100% Methanol for 20 minutes at -20°C. Coverslips were washed five times with PBS 1x to remove PFA traces.

Cells were permeabilized by incubating 10 minutes with 0.5% Triton in PBS 1x at room temperature. Next, coverslips were washed twice with PBS 1x and incubated with blocking buffer for 1 hour at room temperature to block potential non-specific binding sites. Primary antibodies were diluted in 1% BSA in PBS 1x at the appropriate dilutions and cells were incubated for 1 hour and room temperature with 40 µl of antibody solution per coverslip placed on a parafilm strip in a humidified chamber.

After incubation cells were washed thrice with PBS 1x, and secondary antibody staining was carried out as with primary antibodies. Alexa Fluor conjugated antibodies were used as secondary antibodies at a 1:500 dilution, and coverslips incubated for 1 hour at room temperature in a humidified chamber.

Hoechst 3342 nuclear dye was also added to the antibody solution in a 1:1000 dilution. Finally, coverslips were mounted in 6 µl of either Pro-Long Gold anti fading or Fluoromount-G mounting medium and left to dry in the dark for overnight at room temperature.

Fixation buffer

(1) 4% PFA in PBS 1x (pH 7.2-7.4)

(2) 100% Methanol at -20°C

Permeabilization buffer

0.5% Triton in PBS 1x

Blocking buffer

1% BSA in PBS 1x

6.2 YAP Immunofluorescence protocol

This protocol is adapted from Mohseni et al.[174] and follows the same steps as the standard protocol but using different buffer composition (described below). Coverslips are incubated with YAP primary antibody for overnight and 4°C instead of 1 hour at room temperature.

Washing buffer

0.01% Tween in PBS 1x

Permeabilization buffer

0.1% Triton in PBS1X

Blocking buffer

0.5% FBS

0.01% Tween

Diluted in PBS 1x

6.3 Microscopy

Slides were visualized in the Olympus epifluorescence microscope or the Nikon A1 Confocal microscope (Wolfson Light Ficroscopy Facility, The University of Sheffield) in a range of 10x to 60x magnification. Images in tiff format were exported from Volocity software (epifluorescence microscope) or Nikon imaging software (confocal microscope) and edited with FIJI (FIJI is just Image J) software.

7. Immunohistochemistry for colon cancer tissue microarrays

7.1 Staining protocol using Vectastain ABC Elite kit

Expression of ENTR1, PTPN13 and Fas proteins was analysed on colon cancer tissue microarrays consisting of multiple colon adenocarcinoma samples together with normal adjacent tissue. Paraffin-embedded tissue arrays were

acquired from US Biomax and immunohistochemistry protocol was performed with Vectastain ABC Elite Universal kit (Figure 18).

First, tissue array was deparaffinised by immersing slides twice in xylene for 10 minutes, followed by immersions in 100%, 95% and 70% of ethanol 5 minutes each. Slide was immersed in tap water and rinsed twice in PBS 1x for 5 minutes. In order to inactivate endogenous peroxidase activity, slides were incubated for 20 minutes with 3% H_2O_2. After a 5 minutes wash in PBS 1x, antigen retrieval was carried out by cooking slides for 10 minutes in the microwave, immersed in Na-Citrate buffer. This step unmasks antigens that might be covered after paraffin treatment.

Next, tissue array was incubated with normal blocking serum in humidified chamber for 40 minutes at room temperature. Blocking buffer was added directly on top of the samples and sealed with PAP pen to prevent spilling of the solution. Upon incubation, residual excess fluid was thrown off and washed 5 minutes in PBS 1x. 500 µl of the primary antibody solution containing the appropriate antibody dilution was added on the slides and incubated overnight at 4°C.

The following day, array slides were rinsed twice in PBS 1x for 5 minutes and incubated with biotin-conjugated secondary antibody at RT for 30 minutes in a humidified chamber, followed by addition of the Vectastain ABC reagent at RT for 30 minutes. After 4 final washes in PBS 1x, slide was incubated in peroxidase substrate (ImmPACT DAB chromogen) until the desired stain intensity was

developed. Reaction was stopped by removing the remaining DAB and immersing the slides in cold tap water for 10 minutes. Finally, slides were transferred into 95% ethanol (2 changes for 2 minutes each), 100% ethanol (2 changes for 2 minutes each) and xylene (3 changes for 5 minutes each) to dehydrate and clear slides. Excess of solutions was drained from slides and dried for 10 minutes. Coverslips were mounted in Vectamount (non-aqueous mounting medium) and dried for at least 24 hours.

Antigen retrieval buffer

10 mM Na-Citrate in water (pH 6.5). Pre-heat in the microwave prior to use

Blocking buffer

3 drops (150 μl) of serum stock (kit) in 10 ml of PBS 1x.

Primary antibody solution

2.5% of normal blocking serum (kit) in PBS1x

Biotinylated secondary antibody buffer

3 drops (150 μl) of normal blocking serum stock (kit) and 1 drop (50 μl) of biotinylated antibody stock (kit) in 10 ml of PBS 1x.

ABC reagent

2 drops (100 μl) of Reagent A (Avidin DH solution, kit) and 2 drops (100 μl) of Reagent B (biotinylated enzyme, kit) in 5 ml of PBS 1x.

DAB substrate

1 drop (30 μl) of ImmPACT DAB Chromogen concentrate in 1 ml of ImmPACT DAB diluent.

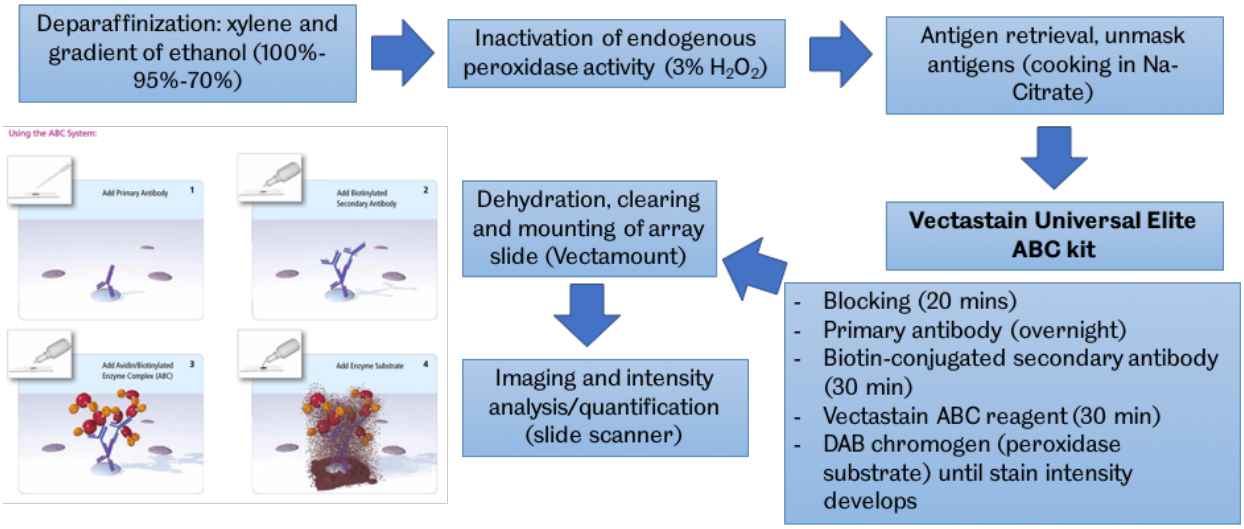

Figure 18: General scheme for Immunohistochemistry protocol on tissue array for Vectastain ABC Elite Kit. Image adapted from: https://vectorlabs.com/uk/vectastain-elite-abc-kit-universal.html

7.2 Imaging and intensity analysis

The imaging and analysis of the tissue microarrays was performed at the Sheffield Institute for Translational Neuroscience (SITraN) with the great help of Daniel Fillingham and Claire Devlin. Slide scanner NanoZoomerXR was used for the imaging and the software used to analyse the cores was Visiopharm. The parameters measured were the total area of the core and the mean intensity of the histocore (measuring 4 regions of interest per core) in a scale from 0 to 255.

8. CRISPR-Cas9: generating knockout cell lines.

8.1 FACS sorting of GFP+ single cells transfected with gRNA px458

In order to isolate the knockout clones containing a deleterious mutation generated upon transfection of gRNA, FACS sorting of GFP positive single cells

was performed (Figure 19). Cells were seeded in 6-well plate at the appropriate cell density to reach 50-70% confluence in 24 hours. 2 μg of px458-GFP plasmid containing gRNA for ENTR1 were transfected to the cells.

After 48 hours, cells were trypsinized, re-suspended in 1 mL of full medium and centrifuged at 1000 rpm for 5 minutes. Supernatant was removed and cells were re-suspended in 500 μl of Opti-MEM. Cell suspension was transferred to flow cytometry tubes and kept on ice. Sorting of GFP positive single cells into 96-well plates, as well as a GFP positive bulk cell population was performed with BD FASC Aria IIu (Flow cytometry Core Facility, The University of Sheffield).

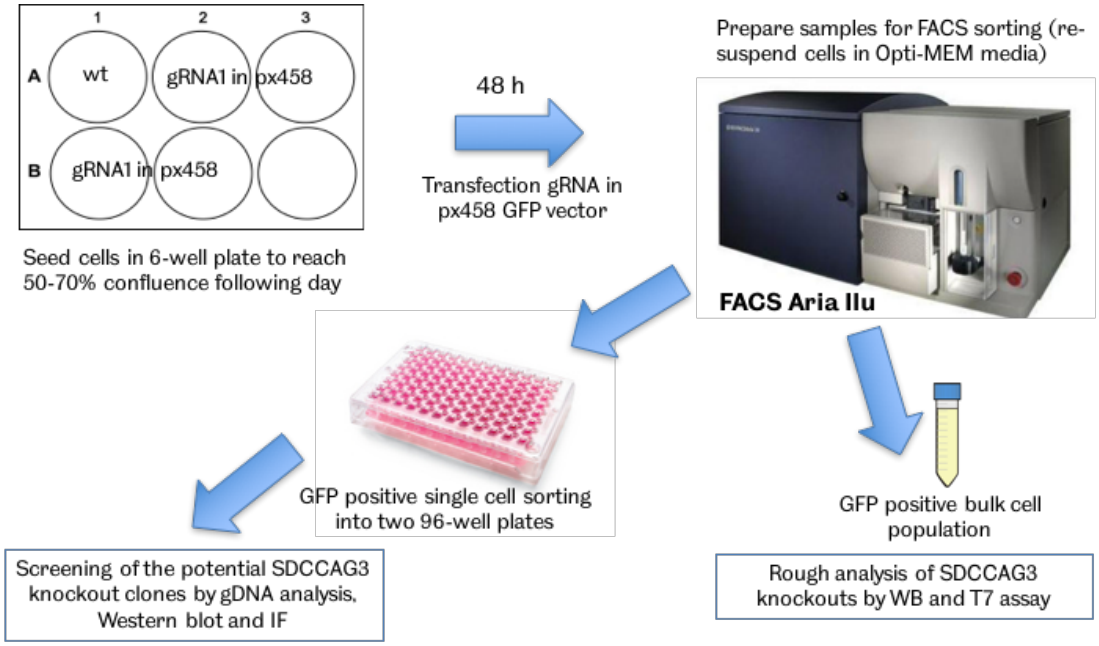

Figure 19. General scheme of ENTR1 knockout clone selection by FACS sorting after transfection with ENTR1 gRNA in px458 vector.

8.2 ENTR1 knockout clones expansion and screening

On one hand, GFP positive bulk cell population was analysed as follows:

(i) Genomic DNA extraction and T7 assay was carried out as described in section *3.6.3* and *3.6.4* to assess the efficiency of gRNAs in introducing mutations.

(ii) ENTR1 expression at the protein level was determined by Western blot (the effect on protein levels were expected to be similar to a knockdown).

On the other hand, sorted single cells were incubated in 96-well plates and screened for colonies after 2-3 weeks. Colonies generated after proliferation of one single clone were sequentially expanded into 24-well and 6-well plates. At this point, genomic DNA extraction followed by sequencing analysis and determination of protein levels by Western blotting were used to screen for positive knockout clones. Positive ENTR1 knockout clones were subsequently expanded into 10 cm dishes and used in further experiments.

9. Assays

9.1 Rescue of Fas levels in cell surface analysis by flow cytometry

First, siRNA-resistant ENTR1-GFP constructs bearing point mutations that abolish the interaction with either PTPN13 or dysbindin were generated by site directed mutagenesis as described in section *3.4*. Next, HeLa cells were co-transfected with ENTR1 siRNA and 500 ng of ENTR1-GFP constructs (wild-type

and mutant) and incubated for 72 hours. Finally, Fas levels in the cell surface were measured by flow cytometry as described in section 5.

9.2 Apoptosis assay with Cleaved Caspase 3

HeLa cells were seeded on coverslips in 12-well plates at the appropriate cell density and 24 hours later transfected with either control or ENTR1 siRNA. Upon 72-hour incubation cells were treated with CH11 (500 ng/mL) or SuperFas soluble ligand (0.5 μg/mL) and cycloheximide (50 μg/mL) in full DMEM medium for 2 hours. Untreated cells were incubated with just full DMEM medium. Cells were subsequently fixed with 4% PFA and standard immunofluorescence protocol was performed as in section *6.1*. Cells were stained for Cleaved Caspase 3 in a 1:400 dilution to allow the detection of apoptotic cells. Finally, coverslips were imaged in Olympus Epifluorescence microscope by taking ten random pictures of 20x magnification from every condition. Quantification was based on the percentage of positive cells for Cleaved Caspase 3 (representing apoptotic cells) with respect to the total number of cells.

9.3 Endogenous Fas degradation assay

(i) HCT-116 wild type cells were seeded at the appropriate cell density in 6-well plates, transfected with either control or ENTR1 siRNA and incubated for 72 hours. (ii) HCT-116 wild type and HCT-116 ENTR1 knockout (clone 4) cells were seeded in 6-well plates and incubated until confluence was reached.

Cells were treated with Fas CH11 agonistic antibody (500 ng/mL) and cycloheximide (150 μg/mL) diluted in full DMEM medium at different time points ranging from 0 to 2 hours. After induction of Fas-mediated apoptosis, cells were lysed with 1% Triton in PBS 1x lysis buffer as described in section *4.2.1*. Protein concentration was measured with DC assay and equalized in all the samples. Protein extracts were diluted in 4x Laemmli buffer, boiled at 95°C for 5 minutes and subsequently used for Western blotting as in section *4.2.2*. Immunoblotting of β-tubulin was used as a loading control and transferrin receptor as a control receptor which is not affected for Fas apoptotic stimulation.

10. Statistical Analysis

All statistical analyses were performed using Graph Pad Prism software with data obtained from three independent experiments (biological replicates) as specified in the figure legends. The statistical significance was calculated using either Student t-test analysis or ANOVA analysis of variance (multiple comparisons by Tukey's test). Data is showing error bars (Mean ± SEM). Detailed statistical test and conditions used in each set of experiments are specified through the thesis in the corresponding figure legends.

4. Chapter I: PTPN13/ENTR-1 complex regulates post-endocytic sorting of the death receptor Fas

1. Introduction

Fas plays a cardinal role in the regulation of ligand-induced apoptosis in normal as well as tumour cells. This chapter will focus on ENTR1 as a regulator of the cell surface levels of Fas and Fas-mediated apoptotic signaling. Moreover, we describe a novel endocytic complex formed by ENTR1 and PTPN13 that controls the delivery of Fas from endosomes to lysosomes thereby regulating Fas cell surface levels and termination of Fas signal transduction.

2. Depletion of ENTR1 expression levels correlates with increased Fas cell surface levels, sensitizing cells to Fas-mediated apoptosis.

ENTR1 was identified as a novel binding partner for the protein tyrosine phosphatase PTPN13 by Erdmann and collaborators[152]. As described in the introduction, PTPN13 is a known inhibitor of Fas induced apoptosis and negatively regulates Fas cell surface levels by an unknown mechanism. Given the tight interaction of ENTR1 with PTPN13, Sharma tested whether ENTR1 expression levels also affect Fas cell surface levels[175]. Interestingly, a significant increase in cell surface Fas upon ENTR1 siRNA transfection was observed by immunofluorescence and flow cytometry (Figure 20 b and c). Furthermore,

increased Fas surface levels upon ENTR1 depletion were confirmed by a biochemical approach using surface biotinylation followed by anti-Fas Western-blotting[175, 176]. Lastly, the increase in surface Fas upon ENTR1 depletion was also reflected in a trend towards increased levels of total Fas, which was found to be only significant for ENTR1 siRNA 3[176].

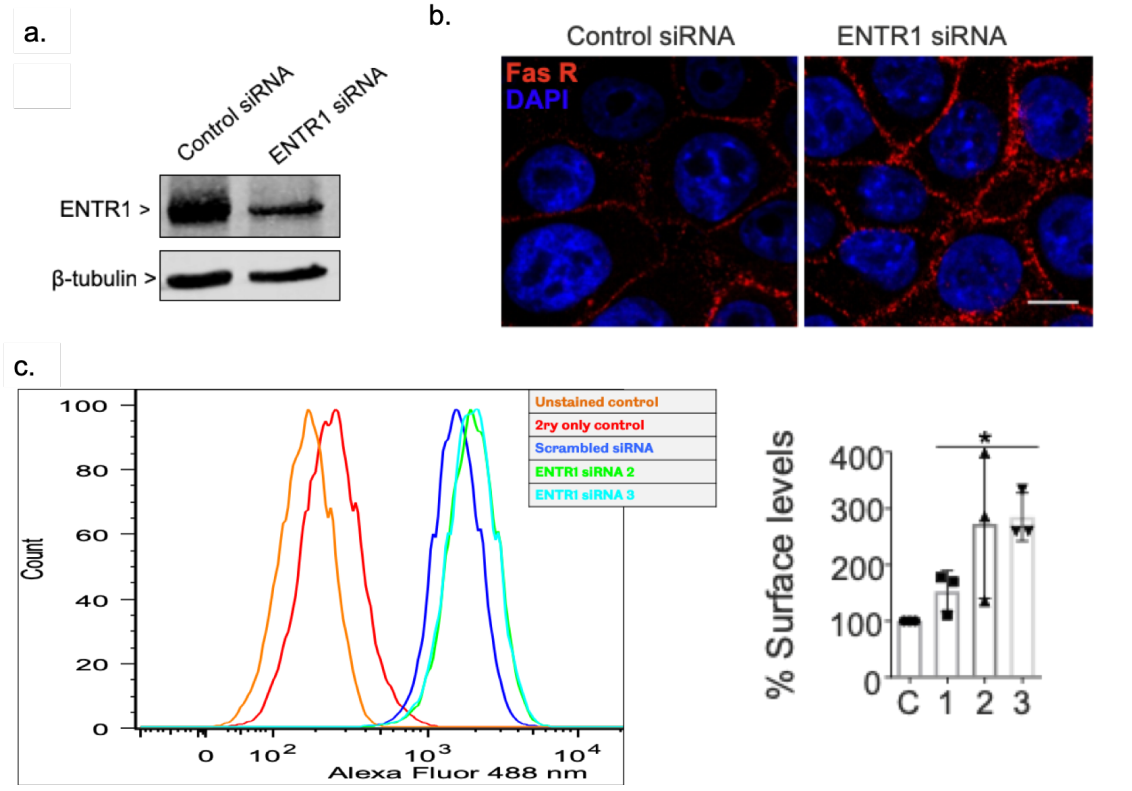

Figure 20: Surface levels of Fas receptors are increased upon silencing ENTR1. (**a**) Validation of ENTR1 siRNA by Western blotting in HeLa cells. β-tubulin used as a loading control. (**b**) Immunofluorescence analysis of cell surface levels of Fas receptors upon ENTR1 no.2 and control knock-down in HeLa cells. Non permeabilized HeLa cells were stained with Anti-Fas (CH-11) followed by Alexa 594 conjugated secondary antibody staining. Images were obtained using a confocal microscope. Scale bar represents 5µm. *(data from Shruti Sharma[175, 176])* (**c**) Quantitative analysis of Fas cell surface levels in HeLa cells represented as bar graphs. The quantification shows mean of three independent experiments (n=3), error bars represent ± SEM; one-way ANOVA test, p-value; **<0.05; p=0.0340 for Fas receptors *(combined data from Shruti Sharma[175] and my own data).*

Conversely, the increase of ENTR1 expression levels by transfecting a GFP-ENTR1 expression construct correlated with reduced presentation of Fas at the cell surface in HeLa cells (Figure 21).

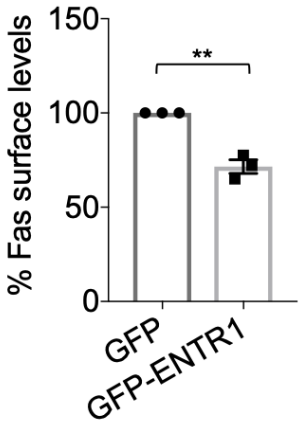

Figure 21: Surface levels of Fas receptors are decreased upon ENTR1 over-expression. Flow cytometry analysis of surface abundance of Fas in HeLa cells upon GFP-ENTR1 overexpression. Quantification of the flow cytometry analysis of Fas receptor levels expressed as a percentage where GFP-transfected HeLa cells control is 100%. Bar graphs represent the mean of the Alexa Fluor 488 nm median intensities (n=3). Error bars represent ± SEM.

As downregulation of ENTR1 by siRNA is transient and with the aim of improving the efficiency of ENTR1 depletion to observe clearer and permanent phenotypes, we generated ENTR1 knockout cell lines by using CRISPR-Cas9 technology. We first designed gRNA targeting exon 4 of ENTR1 gene by using CRISPOR software (Figure 22). Next, designed ENTR1 gRNAs were cloned into a px458-Cas9-GFP vector as described by Zhang lab[177] *(detailed in the Materials and Methods section)*. HeLa and HCT-116 cells were transfected with the ENTR1 gRNA-px458 and GFP positive cells were FACS sorted and cultured in 96-well plates. Bulk population of FACS-sorted HeLa cells was analysed by T7 Endonuclease assay and we confirmed that the generation of mismatches by ENTR1 gRNA was considerably efficient (Figure 22).

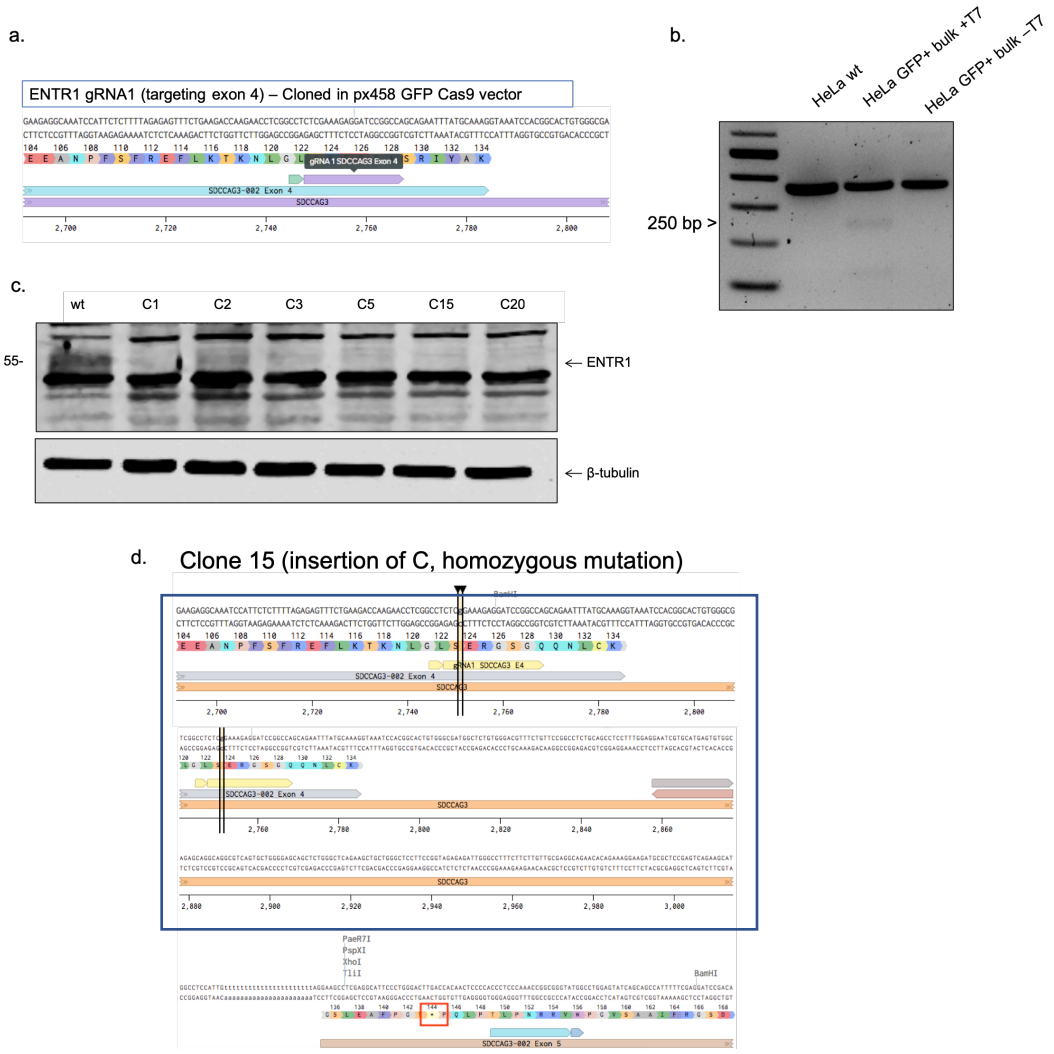

Figure 22. Generating ENTR1 knockout cell lines with CRISPR-Cas9 technology. (a) Snapshot from Benchling™ displaying ENTR1 gRNA targeting exon 4 of ENTR1 gene. ENTR1 gRNA was designed by using CRISPOR online tool. (b) Bulk population of FACS-sorted HeLa cells was analysed by T7 Endonuclease assay to assess the efficiency of ENTR1 gRNA in generating mismatches in ENTR1 exon 4 (c) Example of the Western blot screening for ENTR1 knockout clones in HeLa cells (d) Example of one of the mutations found in ENTR1 knockout clone 15 (HeLa cells), which consists on an insertion of C (homozygous) that generates a premature stop codon and a truncated ENTR1 protein.

A total of 30 and 14 potential knockout clones were generated in HeLa and HCT-116 cells respectively. We screened all the potential knockout clones for each

cell line by sequence analysis of ENTR1 exon 4 and Western blotting (Figure 22). Finally, we validated two ENTR1 knockout clones for both HeLa and HCT-116 cells (Figure 23).

Genomic analysis of the ENTR1 exon 4 in the knockout clones revealed the following homozygous mutations (Figure 23):

- In HeLa cells: clone 15 exhibited an insertion of C and clone 20 a 14 bp deletion, both in the target site for ENTR1 gRNA.
- In HCT116 cells: clone 1 exhibited an insertion of G and clone 4 an insertion of C (exactly the same on as HeLa Clone 15), both in the target site for ENTR1 gRNA.

a. HeLa cells

Clone 15 (insertion of C, homozygous mutation)

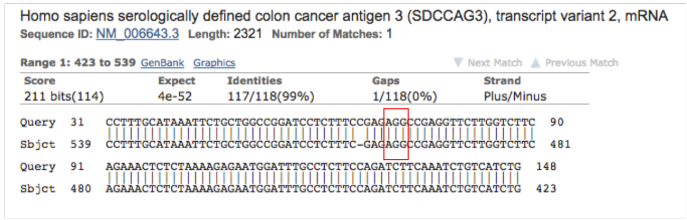

Clone 20 (homozygous 14 bp deletion)

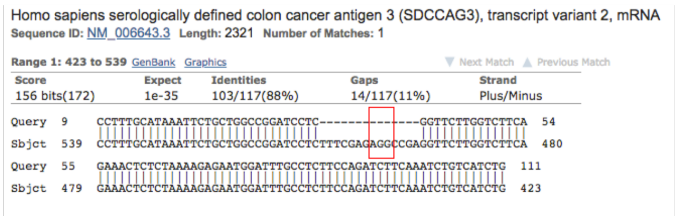

b.

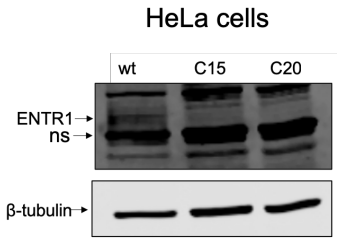

PAM sequences

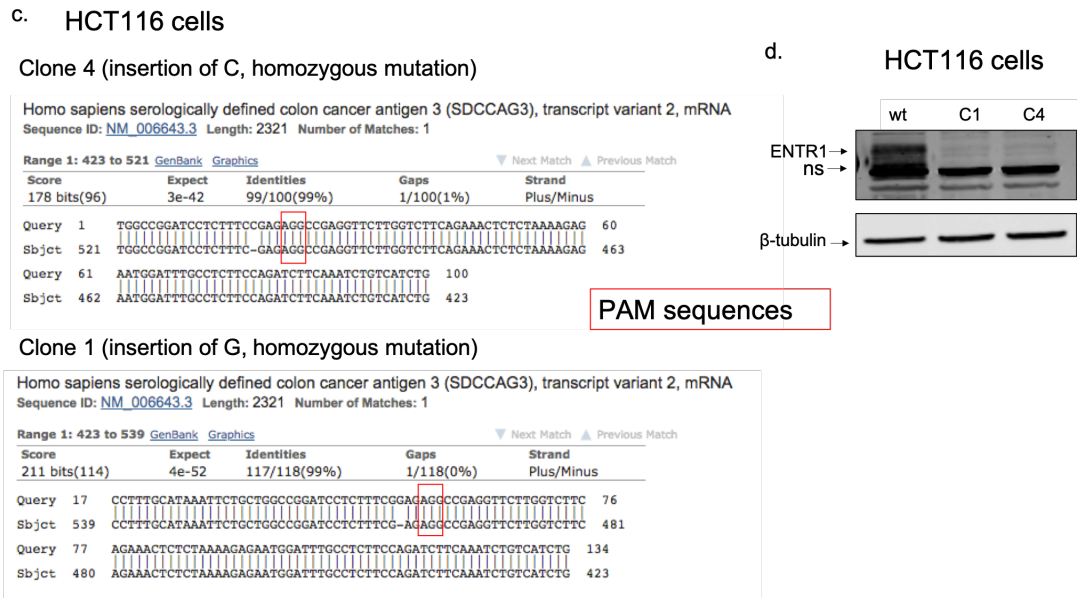

Figure 23. Validation of ENTR1 knockout cell lines generated by CRISPR-Cas9. Analysis of the ENTR1 knock-outs in HeLa cell line (clones 15 and 20) by sequence analysis of the gRNA target region (a) and Western Blotting (b). Analysis of the ENTR1 knockout in HCT-116 cell line (clones 1 and 4) by sequence analysis of the gRNA target region (c) and Western Blotting (d). *PAM sequences are indicated in red. ß-tubulin shown as a loading control.*

To complement the data obtained by transiently downregulating ENTR1 with siRNA, Fas cell surface levels were also examined in the ENTR1 knock-out cells. In line with the results observed upon ENTR1 siRNA transfection, we also observe a significant increase in the abundance of Fas at the cell surface in the ENTR1 knock-out clones 15 (HeLa cells) and 4 (HCT-116 cells) compared to wild type cells (Figure 24). These data further support that ENTR1 regulates Fas receptor presentation in the cell surface.

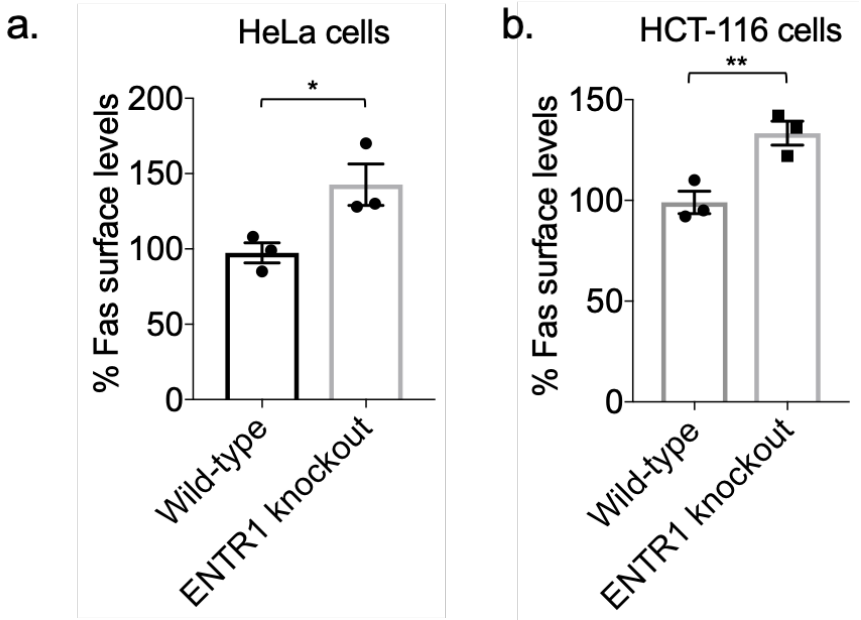

Figure 24. ENTR1 knockout cell lines generated by CRISPR-Cas9 show increased surface Fas expression. Flow cytometry analysis of surface levels of the Fas receptor in ENTR1 knockout compared to wild-type HeLa cells (a) or wild-type HCT-116 cells (b). ENTR1 knockout clone 15 was used for HeLa cells, while ENTR1 knockout 4 was used for HCT-116 cells Live cells were stained with anti-Fas CH11 primary antibody followed by Alexa 488 conjugated secondary antibody and analysed in the BD LSRII flow cytometer. Bar graphs represent the mean of the Alexa Fluor 488 nm median intensities (n=3). Error bars represent ± SEM.

Interestingly, we also observed enlarged endosomes in ENTR1 knockout HeLa cells compared to wild-type (Figure 25). This could mean that ENTR1 is essential not only for Fas sorting from the early endosomes to the lysosomes, but also for other cargoes that get stuck in the early endosomes causing the increase in endosomal size.

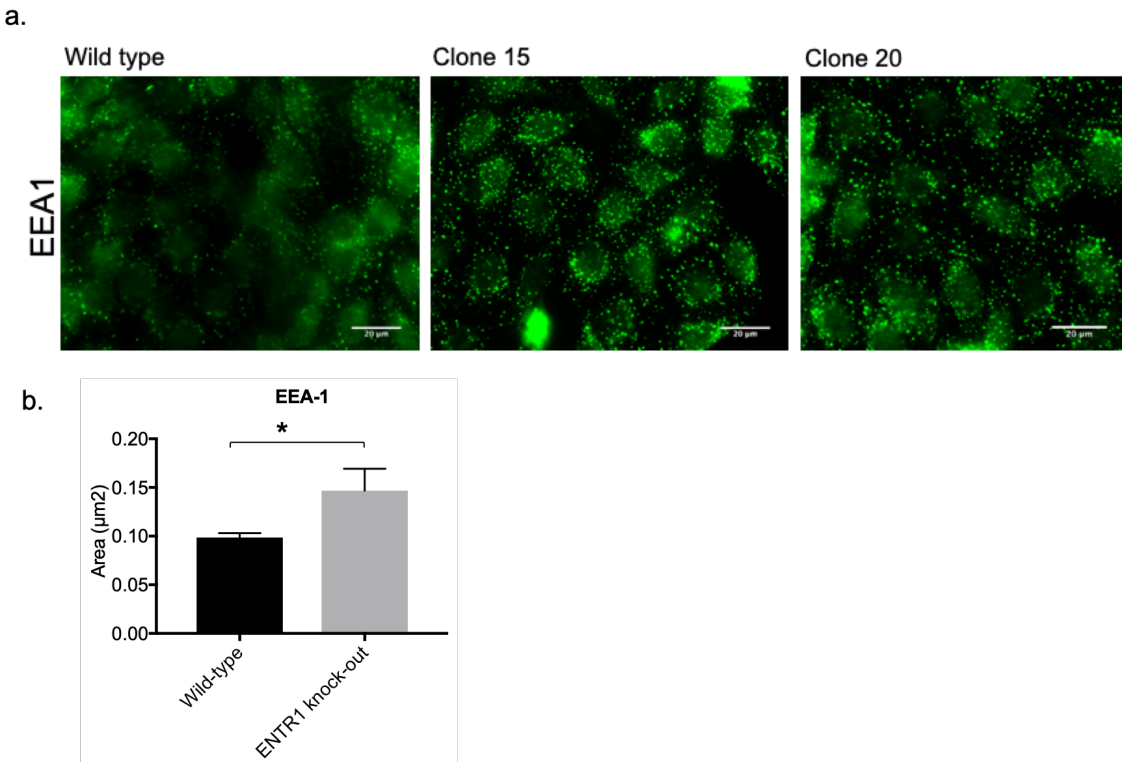

Figure 25. Early endosome morphology is altered in ENTR1 knockout HeLa cells. (a) Immunofluorescence analysis of early endosomes (EEA1 endosomal marker) in HeLa wild-type and ENTR1 knockout cells. (b) Quantification of the average area of early endosomes (determined by EEA1 staining) by Image J particle analysis. Early endosomes are significantly increased in HeLa ENTR1 knockout clone 15 cells when compared to HeLa wild type cells. Significance was analysed by Student's t-test ($p<0,05$), n=1.

Higher levels of Fas in the cell surface should increase the sensitivity of these cells to Fas-mediated apoptosis. To test whether the increase of Fas in the cell surface also correlates with enhanced Fas-mediated apoptosis we incubated HeLa cells, transfected with siRNA targeting ENTR1 or control siRNA, with anti-human Fas agonistic antibody CH11 and cycloheximide (Fas-mediated apoptosis triggers) and monitored the extent of apoptosis. Fas is known to activate a signaling cascade which leads to proteolytic activation of procaspase 8 and 3. To

test whether depletion of ENTR1 affects the activation of procaspase 3, we performed a cleaved Caspase 3 apoptosis assay.

We observed a significant increase of apoptotic cells (positive for Cleaved Caspase 3 staining) upon ENTR1 siRNA knock-down when inducing Fas-mediated apoptosis with CH11 and CHX (Figure 26 a). HCT-116 cells were also tested with similar results (Figure 27). However, to demonstrate that this is not only specific for CH11 as an agonistic trigger, we also analysed apoptosis in HeLa cells treated with a soluble version of Fas-ligand (SuperFas-ligand), a more physiologically relevant mode of stimulating Fas apoptosis (Figure 26 b).

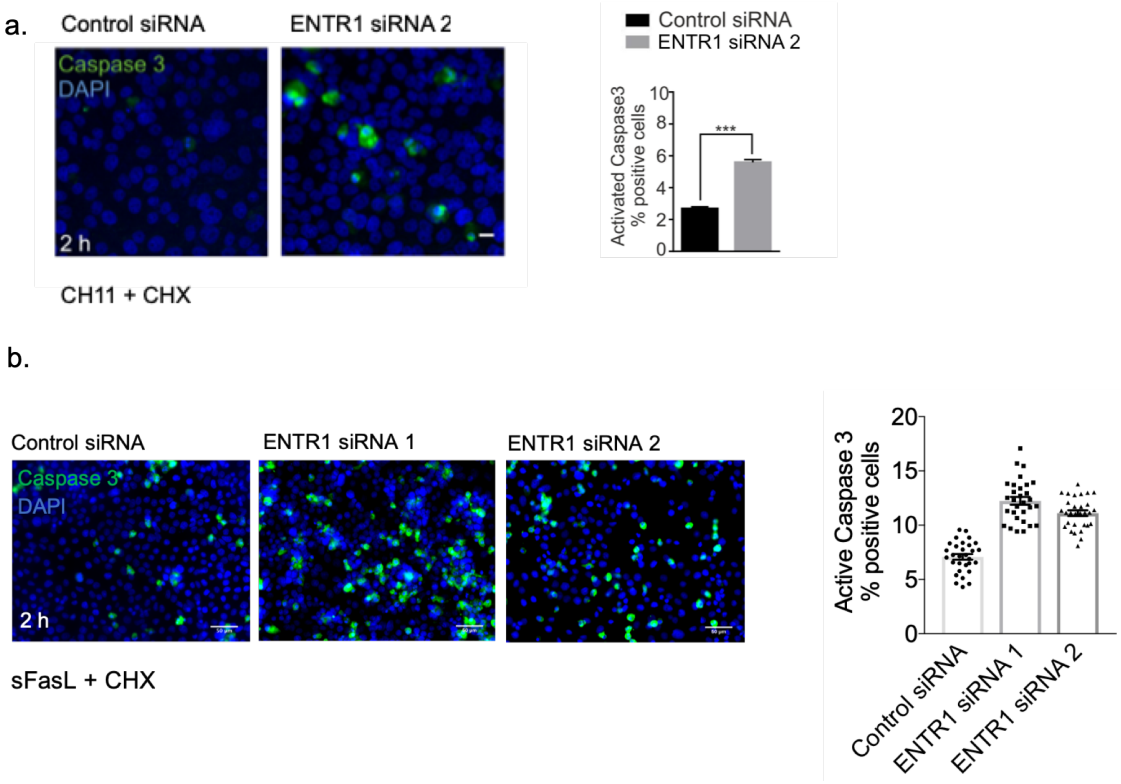

Figure 26. Downregulation of ENTR1 increases cell sensitivity to Fas-mediated apoptosis. Immunofluorescence analysis of activated caspase 3 in HeLa cells transfected with control or the indicated ENTR1 siRNAs after 2 hours of treatment with (a) CH11 (500 ng/ml) and CHX (50 ug/ml) or (b) sFasL (0.5 ug/ml) and CHX (50 ug/ml).

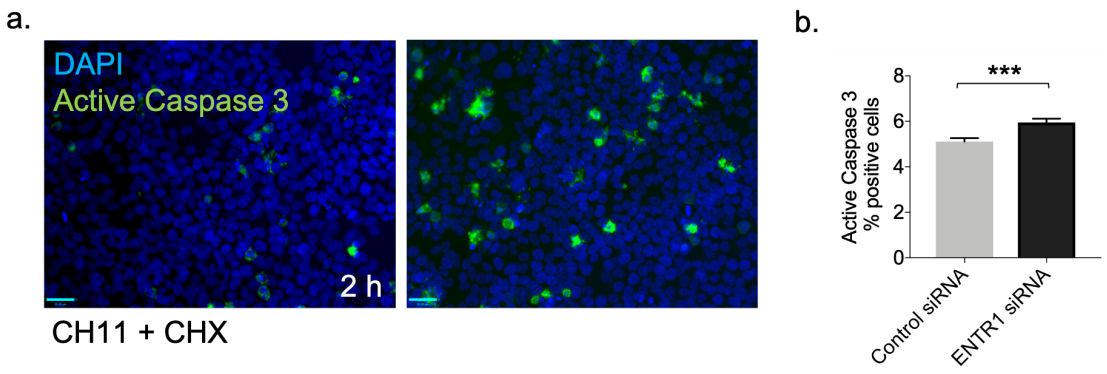

Figure 27. Downregulation of ENTR1 increases the sensitivity of HCT-116 cells to Fas-mediated apoptosis. (a) Immunofluorescence analysis of activated caspase 3 in HCT-116 cells transfected with control or ENTR1 siRNA 3 after 2 hours of treatment with CH11 (500 ng/ml) and CHX (50 ug/ml). (b) Quantification of the cells positive for activated caspase 3 in each condition. Data was collected from three independent experiments (n=3), student t-test was performed, ***p<0.01, error bars represent ± SEM.

HCT116 cells are particularly sensitive to Fas mediated apoptosis and do not require blocking anti-apoptotic molecules synthesis with CHX. Thus, we performed the apoptosis assay with sFasL but without CHX and also observed a significant increase in the number of apoptotic cells in the ENTR1 knockout cells compared to wild-type (Figure 28). These data strongly supported that downregulation or depletion of ENTR1 increases the sensitivity of HeLa and HCT116 cells to Fas-mediated apoptosis.

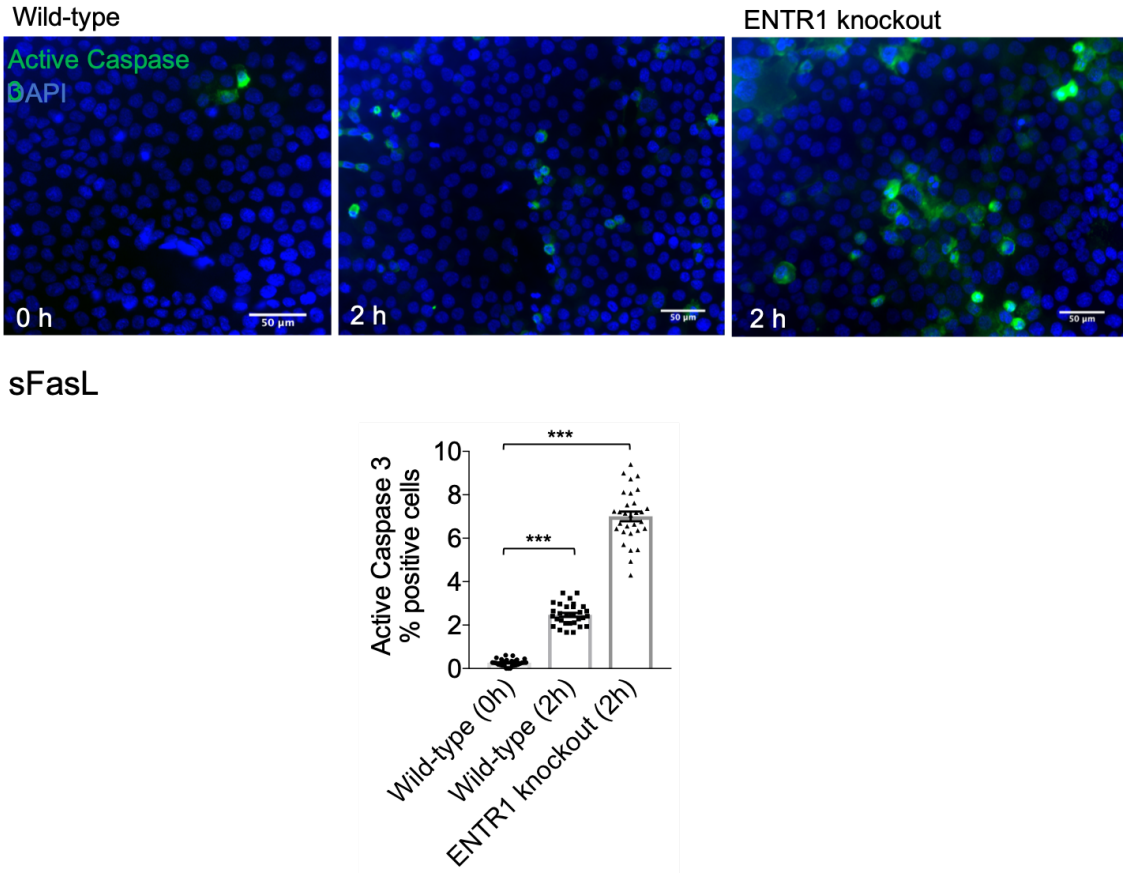

Figure 28. ENTR1 knockout increases cell sensitivity to Fas-mediated apoptosis. Immunofluorescence analysis of activated caspase 3 in HCT116 wild-type or ENTR1 knockout (Clone 4) cells after 2 hours of treatment with sFasL (0.5 ug/ml). Quantification of the cells positive for activated caspase 3 in each condition. Data was collected from three independent experiments (n=3), One-way ANOVA was performed, **p<0.01, error bars represent ± SEM.

3. PTPN13 forms a novel endocytic complex with ENTR1 and regulates Fas cell surface levels

ENTR1 has been previously shown to co-localise with Fas at the early endosomes, where it is potentially regulating its trafficking and abundance in the cell surface[175]. However, as ENTR1 and Fas are not directly interacting, it was not known how ENTR1 accessed Fas receptors at the early endosomes. Potentially,

there was another protein acting as a link between them. PTPN13 directly interacts with both Fas (via its PDZ2 domain)[142] and ENTR1 (via its FERM domain)[152] and what is more previous literature has reported the role of PTPN13 as a negative regulator of Fas cell surface expression[56, 57]. Altogether supported the candidacy of PTPN13 as the molecular bridge between ENTR1 and Fas at the endosomes.

As low surface levels of Fas have been previously correlated with increased levels of PTPN13 in a wide variety of tumour cell lines, we were expecting that downregulation of PTPN13 expression would correlate with increased Fas cell surface levels. As shown in Figure 29, flow cytometry analysis of Fas cell surface levels in HeLa cells revealed that knocking down PTPN13 with two different siRNAs increased the expression of Fas in the cell surface (validation of PTPN13 siRNA knockdown efficiency by Western blotting in Figure 29 a.).

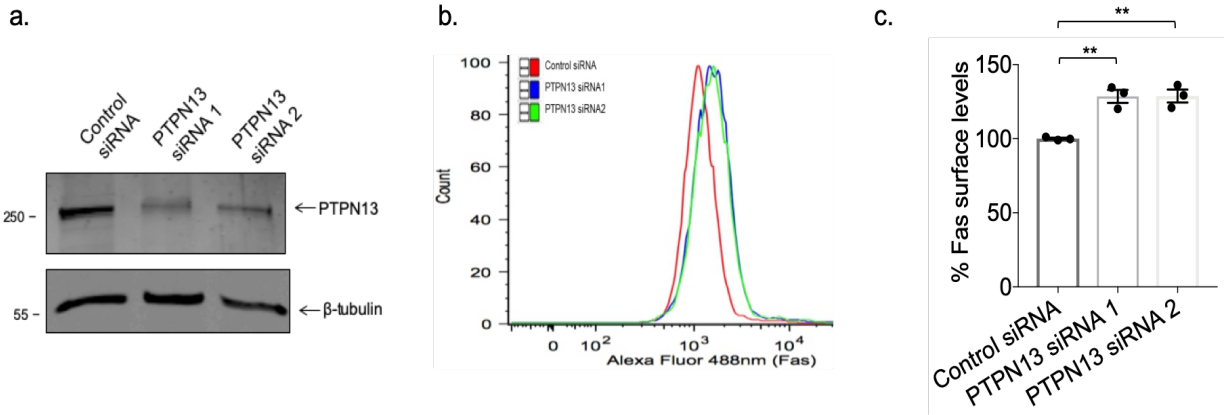

Figure 29. Downregulation of PTPN13 is correlated with an increase in cell surface Fas (a) Western blot validation of PTPN13 siRNA 1 and 2 knockdown efficiency in HeLa cells. β-tubulin as loading control. (b) Flow cytometry analysis of surface abundance of Fas in HeLa cells upon PTPN13 knock-down. Shift of the peaks towards the right in all the samples as compared to the control indicates increased Alexa 488 intensity. (c) Quantification of the flow cytometry analysis

of Fas receptor levels expressed as a percentage relative control siRNA transfected cells. Bar graphs represent the mean of the Alexa Fluor 488 nm median intensities (n=3).

In order to test whether interaction with PTPN13 is important for ENTR1 to regulate Fas cell surface levels we tested two ENTR1 point mutations, P167A and E171A, which were previously identified to abolish interaction with the FERM domain of PTPN13[152]. ENTR1 wild-type and mutants were created by site-directed mutagenesis, so they were resistant to ENTR1 siRNA and also have the corresponding point mutations in the PTPN13 binding site (in the case of the mutants). Mutants were validated by pull-down assay and were not able to interact with endogenous PTPN13, whereas the wild type ENTR1 was (Figure 30). It was important to validate the interactions with the full-length PTPN13, as previous studies only focused on the interaction of ENTR1 with PTPN13 FERM domain[152] and we could not rule out the possibility of a second binding site.

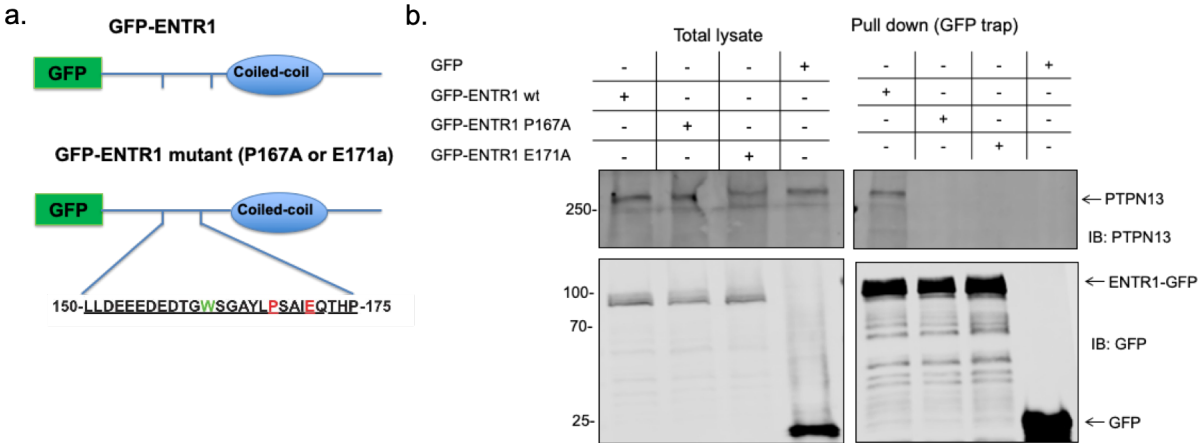

Figure 30. ENTR1 point mutants for PTPN13 binding site are not able to interact with endogenous PTPN13 (a) ENTR1 constructs used in the experiment. Site directed mutagenesis was used to generate ENTR1 siRNA resistant constructs by introducing 3 silent mutations in the ENTR1 siRNA target site. Point mutations P167A and E171A were also introduced in ENTR1 constructs by site-directed mutagenesis. (b) Co-immunoprecipitation analysis of the interaction

of wild-type and mutant ENTR1 with endogenous PTPN13. HEK293 cells were transfected with the indicated GFP-tagged ENTR1 constructs followed by GFP-trap and Western Blotting.

Subsequently, we determined whether interaction with PTPN13 is important for ENTR1 function in Fas receptor trafficking by performing a rescue experiment measuring Fas cell surface levels. HeLa cells were co-transfected with ENTR1 siRNA and either GFP, GFP-ENTR1 wt or GFP-ENTR1 mutant P167A and E171A constructs. After 72 hours cells were collected, stained with CH11 Fas antibody and analysed in BD LSRII flow cytometer. Transfection of wild-type ENTR1 rescued the Fas levels in the cell surface to control levels, whereas transfection of ENTR1 mutants lacking interaction with PTPN13 was not able to rescue the phenotype (Figure 31). This result strongly suggests that the formation of a PTPN13/ENTR1 endocytic complex is required to regulate Fas surface expression levels.

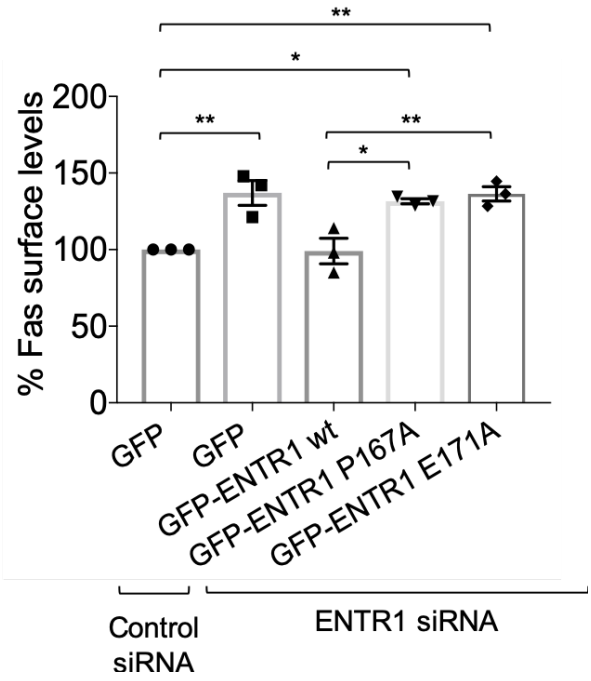

Figure 31. ENTR1 requires binding to PTPN13 to regulate Fas cell surface levels. Flow cytometry analysis of Fas surface levels in HeLa cells upon ENTR1 knock-down and rescue with aforementioned ENTR1 constructs. Bar graphs represent the mean of the Alexa Fluor 633 nm

median intensities. Data was collected from three independent experiments (n=3), One-way ANOVA was performed, **p<0.01, error bars represent ± SEM.

4. Depletion of ENTR1 expression levels correlates with delayed degradation of Fas

At this point, it is clear that ENTR1 depletion increases cell surface levels of Fas. However, what is the precise mechanism behind it? First, elevated expression of cell surface Fas could be due to impaired endocytosis upon ENTR1 depletion. Second, ENTR1 could be involved in the sorting of Fas from the early endosomes towards the degradation pathways. Consequently, upon ENTR1 depletion, the accumulation of Fas in the early endosomes might lead to an enhanced recycling of Fas back to the plasma membrane.

Previous work by Sharma ruled out that Fas endocytosis was affected by ENTR1 downregulation[175, 176]. HeLa cells were transfected with ENTR1 siRNA or control siRNA and rate of cell surface Fas endocytosis was monitored by flow cytometry upon stimulation with CH11 agonistic antibody. No difference was observed in the kinetics of Fas endocytosis in ENTR1 depleted cells compared to control suggesting that impaired endocytosis does not account for the increase in Fas cell surface levels upon ENTR1 knock-down[175].

Therefore, downregulation of ENTR1 could impair sorting of Fas receptors from the early endosomes to the lysosomes. Accordingly, we would expect to observe an effect on the degradation kinetics of Fas receptor upon ENTR1

downregulation, so we determined the rate of turnover of endogenous Fas receptor in HCT-116 cells treated with control or ENTR1 siRNA after CH11 stimulation. After 2 hours, only 60% receptors were remaining in control siRNA samples but in case of ENTR1 knock-down, at least 90% receptors were remaining (Figure 32). Transferrin receptor was used as a control and it was not affected by the stimulation with CH11 antibody. The delay in the rate of Fas degradation that is observed in ENTR1 knock-down samples compared to control is significant from 1 hour onwards.

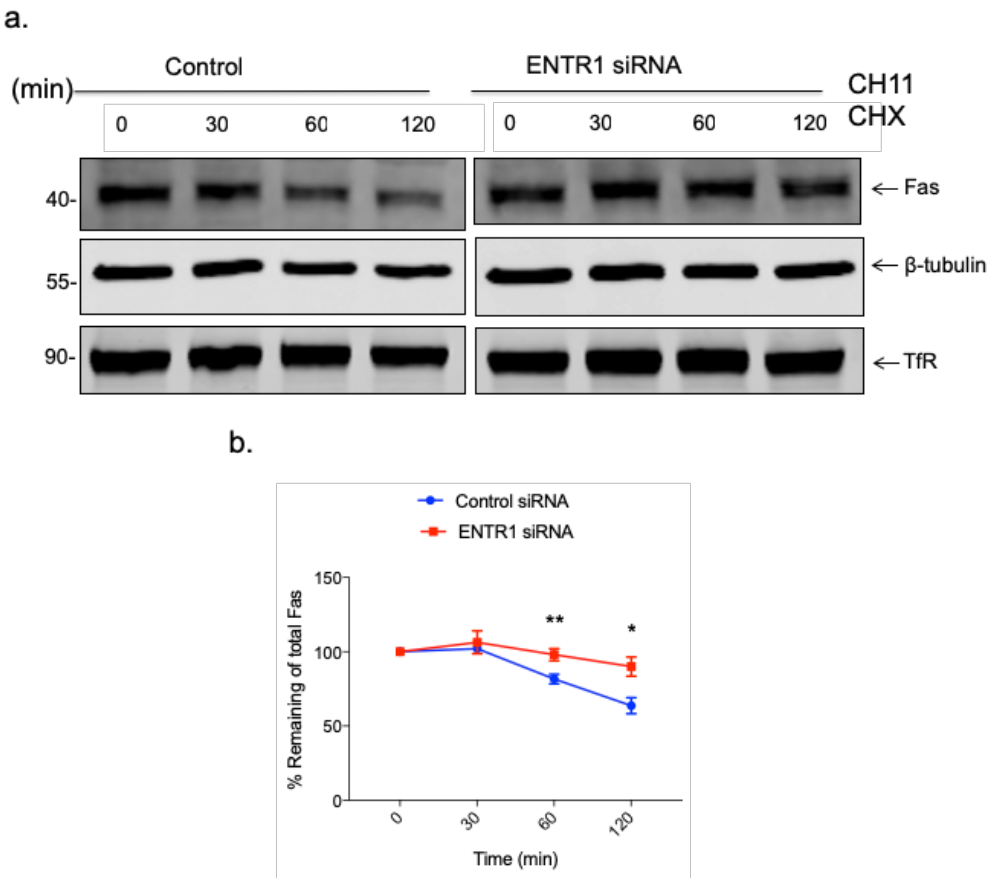

Figure 32. Degradation kinetics of endogenous Fas in ENTR1 siRNA knock-down (a) Immunoblot analysis of the kinetics of degradation of endogenous Fas in control or ENTR-1 siRNA transfected HCT-116 cells treated with agonistic anti-Fas (CH-11) antibody (500 ng/ml) and cycloheximide (150µg/ml) for the indicated time points. (b) Relative receptor abundance expressed as a percentage where 0 min is 100% in control or ENTR1 siRNA treated HCT-116 cells,

respectively, normalized to ß-tubulin expression. Data were collected from three independent experiments (n=3) and analysed by multiple comparisons test, *p<0.05, error bars represent ± SEM.

To complement this experiment, Fas degradation kinetics were also examined in our ENTR1 knockout HCT-116 cell line. Wild-type and ENTR1 knock-out cells were stimulated with CH11 for different times and the amount of Fas was measured by Western-blotting. In line with the results observed upon ENTR1 siRNA transfection, there was a clear decline of Fas expression levels over time in wild-type HCT116 cells, whereas there was only a minor degradation of Fas observable in cells lacking expression of ENTR1 (Figure 33).

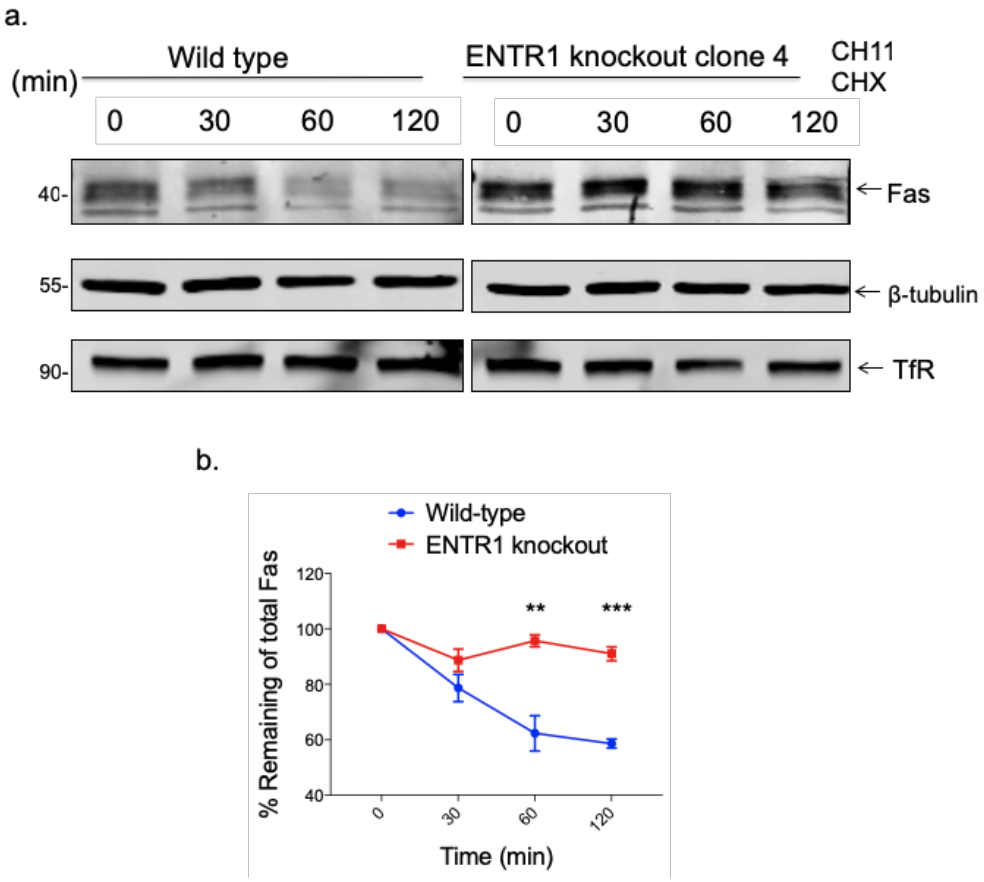

Figure 33. ENTR1 knock-out HCT-116 cells show delayed degradation of Fas (a) Immunoblot analysis of the kinetics of degradation of endogenous Fas activated by agonistic anti-Fas (CH-11)

antibody (500 ng/ml) in the presence of cycloheximide (150 µg/ml) for the indicated time points. ß-tubulin was used as a loading control. (b) Relative receptor abundance expressed as a percentage where 0 min is 100% in wild-type or ENTR1 knock-out HCT-116 cells, respectively. Data was collected from three independent experiments (n=3) and analysed by multiple comparisons test, *p<0.05, error bars represent ± SEM.

In order to add extra physiological relevance to our observations we demonstrated that this is not only specific for CH11-induced Fas apoptosis. Therefore, we analysed Fas degradation in HCT116 wild-type versus ENTR1 knockout cells treated with the soluble version of Fas-ligand and no cycloheximide (-CHX). Consistent to the previous data, Fas degradation was still delayed in the ENTR1 knockout cells in comparison to wild-type (Figure 34).

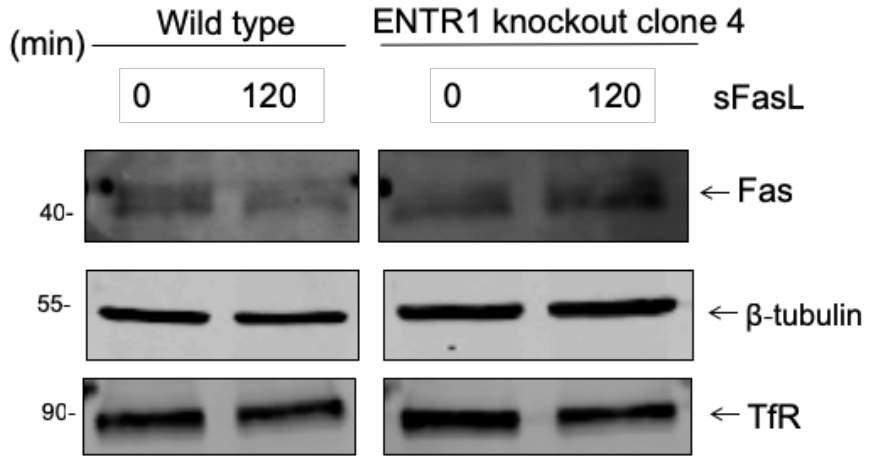

Figure 34. ENTR1 knock-out HCT-116 cells show delayed degradation of Fas (stimulation of Fas-mediated apoptosis with sFasL and no CHX). Immunoblot analysis of the kinetics of degradation of endogenous Fas activated with soluble Fas ligand (0.5 µg/ml) in the absence of cycloheximide for the indicated time points (n=2). ß-tubulin was used as a loading control.

Finally, we treated wild-type and ENTR1 knock-out cells with leupeptin (inhibitor of lysosomal degradation) and analysed the resulting degradation

kinetics upon CH11 stimulation. Fas degradation was blocked by leupeptin treatment in both wild-type and ENTR1 knock-out cells, indicating that ENTR1 is regulating Fas degradation via lysosomal pathway (Figure 35).

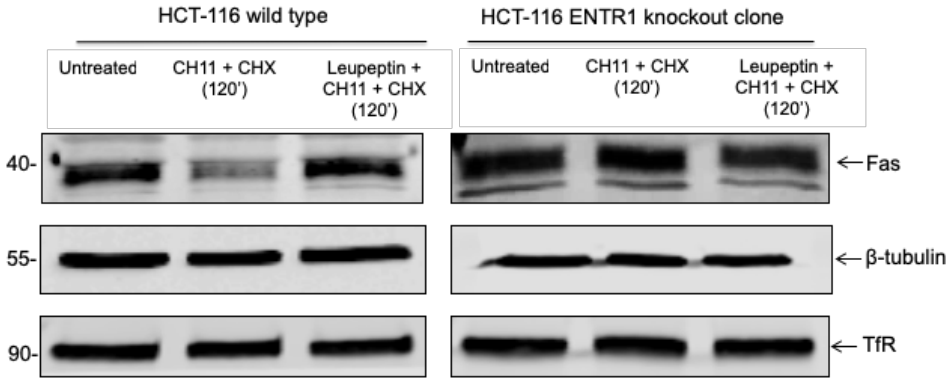

Figure 35. Fas degradation is blocked by treatment with Leupeptin. Immunoblot analysis of the kinetics of degradation of endogenous Fas in wild-type and ENTR1 knockout HCT-116 cells treated with agonistic anti-Fas (CH-11) (500 ng/ml) and cycloheximide (150µg/ml) and with or without the pre-treatment with Leupeptin (100 nM) at the indicated time points. ß-tubulin was used as a loading control and transferrin receptor (TfR) was used as a control receptor and remain unaffected upon Leupeptin treatment.

5. Recycling via Rab11 plays an important role in increased Fas cell surface levels upon ENTR1 depletion

We have demonstrated that ENTR1 depletion impairs sorting of internalized Fas receptors which leads to a delayed degradation and increased expression of Fas in the cell surface. It has previously been observed that cargo accumulation at the level of early endosomes can lead to enhanced recycling[178-180]. Thus, we hypothesized that enhanced recycling of Fas back to the plasma membrane was responsible of the increased Fas cell surface levels observed upon

ENTR1 downregulation. Our attention was focused on the two main recycling pathways: the so-called "classic" pathway (Rab-11 GTPase dependent) and the fast recycling pathway (Rab4 GTPase dependent)[69].

In order to test the hypothesis, HeLa cells were co-transfected with ENTR1 siRNA and either Rab11 or Rab4a wild-type, Rab11 or Rab4a dominant negative mutants (DN) or the Rab binding domain of the Rab coupling protein (RBD). Subsequently, Fas expression in the cell surface was measured by flow cytometry. It is important to note that Rab dominant negative mutants and RBD block Rab-dependent recycling without affecting receptor uptake or degradation[181].

Overexpression of Rab11 DN and RBD upon ENTR1 siRNA transfection inhibited Fas receptor recycling and completely rescued Fas cell surface levels (Figure 36 a). Transfection of Rab11 wild-type was unable to rescue the phenotype, indicating intact recycling process. Conversely, transfection of Rab4a dominant negative did not rescue cell surface Fas, ruling out the involvement of the Rab4a-dependent fast recycling pathway (Figure 36 b). Hence, we concluded that the increase of Fas in the cell surface observed upon ENTR1 downregulation is mostly due to enhancement of the Rab11-dependent classic recycling pathway.

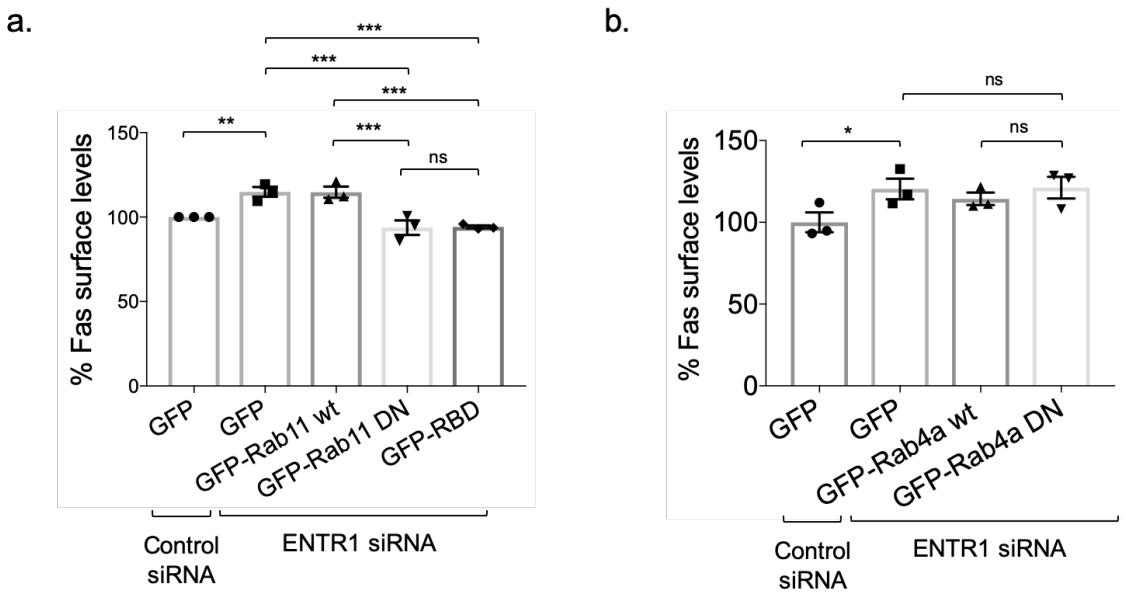

Figure 36. Enhanced Fas recycling is responsible for increased cell surface expression levels in ENTR1 depleted cells. (a) Flow cytometry quantification of Fas surface levels after transfection of GFP-Rab11 wt, GFP-Rab11 DN (dominant negative) or GFP-RBD (Rab11 binding domain) constructs ENTR1 siRNA depleted HeLa cells. (b) Flow cytometry quantification of Fas surface levels after transfection GFP-Rab4a wt or GFP-Rab4a S22N DN constructs in HeLa cells. Bar graphs represent percentage of the Alexa Fluor 633 nm median intensities. Data was collected from three independent experiments (n=3), One-way ANOVA was performed, **p<0.01, error bars represent ± SEM.

6. ENTR1 mediates endolysosomal sorting of Fas receptors via dysbindin-Hrs axis

The novel endocytic complex composed by PTPN13 and ENTR1 is able to regulate the sorting of Fas from the early endosomes to the degradation pathways once Fas receptor is activated and internalized. However, neither PTPN13 or ENTR1 are able to mediate the transport to the lysosomes by themselves. Thus, an association of ENTR1 or PTPN13 with the core endosomal sorting machinery was required. Dysbindin drew our attention as it interacts

directly with the core sorting machinery component HRS1 (hepatocyte growth factor regulated tyrosine kinase substrate), also known as ESCRT-0[182]. Moreover, two independent large-scale proteomic studies suggested a potential interaction of ENTR1 with dysbindin[183, 184]. Dysbindin regulates the post-endocytic trafficking of a variety of receptors including the chemokine receptor type 4 (CXCR4)[184]. Actually, depletion of dysbindin correlated with increased cell surface levels of CXCR4 and delayed degradation kinetics, very similar to what we have observed for Fas after ENTR1 depletion. Thus, the complex formed by ENTR1 and dysbindin could provide a potential molecular link between ENTR1 and the endosomal sorting machinery.

6.1 A novel interaction: ENTR1 interacts with sorting machinery component dysbindin

Two different approaches were applied to confirm whether ENTR1 interacts with dysbindin. First, we performed a GST-pull down assay and confirmed in line with previous proteomic results that dysbindin interacts with a fusion protein of GST and ENTR1 but not with GST alone (Figure 37 a). ENTR1 has a coiled-coil domain which tends to be sticky and usually delivers unspecific interactions. To confirm that the interaction with dysbindin was specific and not due to the stickyness of ENTR1 coiled-coil domain we used GST-VAMP3 as a control, which is also a coiled-coil domain protein. We did not observe interaction of dysbindin with VAMP3, indicating that the interaction that we observe is specific for ENTR1.

Dysbindin has also been described as an obligatory component of the BLOC-1 (biogenesis of lysosome-related organelles-1) complex[186, 187]. Interestingly, we did not find any Pallidin, another obligatory component of the BLOC-1 complex, in the pull-downs, suggesting that ENTR1 does not bind to the canonical BLOC-1 complex (Figure 37 a) and in this case functions independently from the BLOC-1 complex activities.

We further validated the interaction by GFP-trap pull down and were able to co-immunoprecipitate GFP-ENTR1 with Flag-Dysbindin but not with GFP alone (Figure 37 b, work performed by Agnieszka Skowronek).

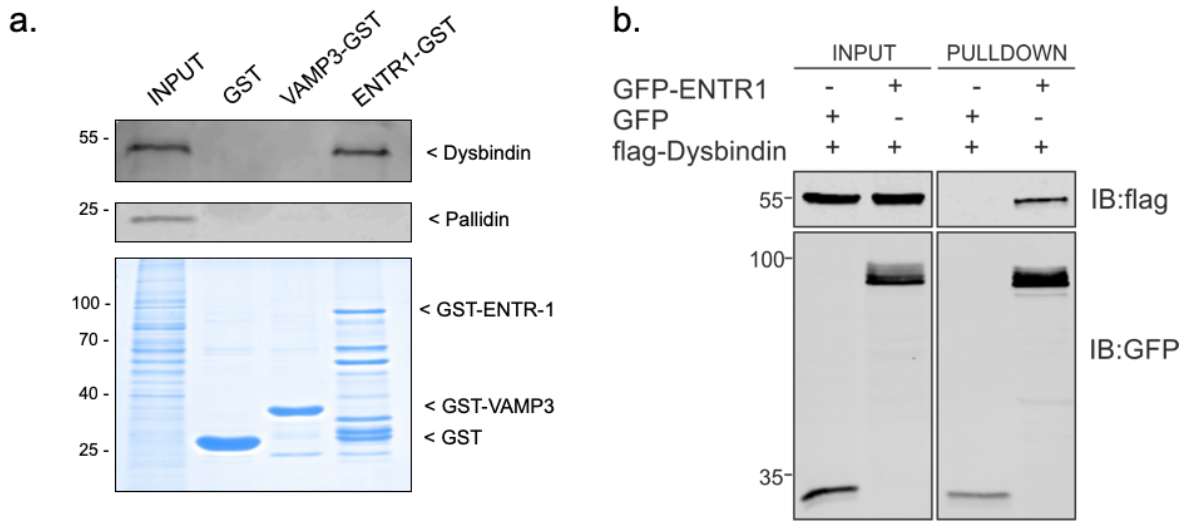

Figure 37. ENTR1 interacts with dysbindin. (a) Immunoblot and corresponding Coomassie staining for GST pull down assay of endogenous Dysbindin interacting with N-terminus GST tagged ENTR1 and not with GST alone or VAMP3-GST in HeLa cells. Endogenous pallidin is not able to interact with GST-tagged ENTR1 (b) GFP-Trap pulldown of flag-Dysbindin and N-terminal GFP-tagged ENTR1. HEK293 cells were transiently transfected with expression constructs for flag-Dysbindin and the indicated GFP proteins. Cells were lysed and subsequently subjected to GFP-TrapA pulldown. Bound proteins were detected via western blotting with anti-flag and anti-GFP antibody *(GFP-trap pull down performed by Agnieszka Skowronek).*

Extra evidence of this interaction was provided by immunofluorescence studies, that revealed a clear co-localisation of dysbindin with endogenous ENTR1 in subdomains of enlarged endosomes (work performed by Shruti Sharma[175]). Taken together, this supports our idea that both proteins might act together in the early endosomes regulating cargo sorting to the degradation pathways.

6.2 Depletion of dysbindin/Hrs expression levels correlates with increased Fas induced apoptosis

Next, we aimed a deeper investigation of the role of dysbindin in the regulation of Fas cell surface levels and its impact in the sensitivity to Fas-mediated apoptosis. If dysbindin and HRS form a complex that regulates the trafficking of Fas receptors the silencing of any of them would cause an effect on Fas cell surface levels, as we observed when depleting ENTR1. Consequently, Sharma analysed cell surface levels of Fas upon transfection with control, dysbindin, HRS and dysbindin+ENTR1 siRNA by flow cytometry[175]. In similar fashion to ENTR1, the analysis revealed that that depletion of dysbindin or HRS also increased Fas cell surface expression when compared to the control. As expected, double knockdown of dysbindin and ENTR1 showed elevated levels of cell surface Fas. However, the increase upon double knockdown was comparable to dysbindin only knockdown[175, 176], which suggested that ENTR1 and dysbindin act together in the same pathway regulating Fas trafficking.

As a complement to the above, we used the Active caspase 3 immunofluorescence assay to test if knockdown of dysbindin or HRS sensitized

HeLa cells to Fas-mediated apoptosis. In line with the results observed upon ENTR1 depletion, we identified a significant enhancement of the sensitivity to Fas-induced apoptosis in the siRNA transfected cells (Figure 38), indicated by an increase in the percentage of apoptotic cells (positive for active caspase 3). These data strongly suggested that dysbindin and HRS (ESCRT-0 sorting machinery) act together with ENTR1 to regulate cell surface levels of Fas receptors which in turn affects cell sensitivity to Fas-mediated apoptosis.

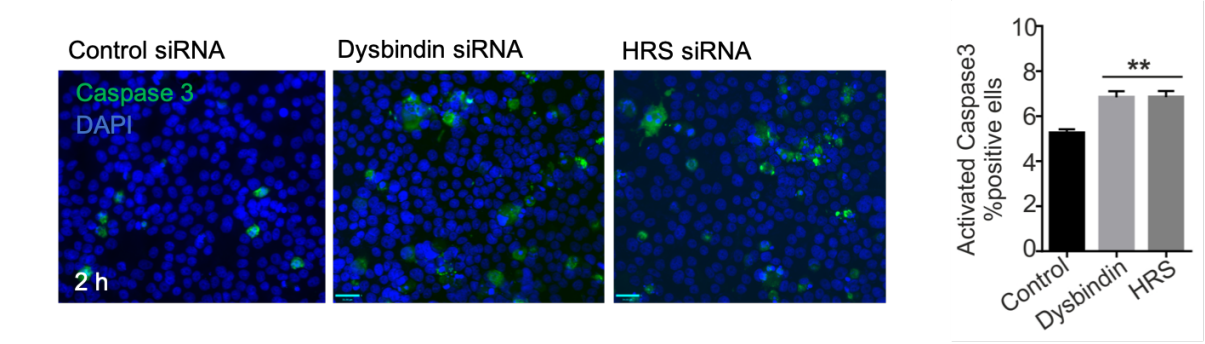

CH11 (500 ng/ml) + CHX (50 ug/ml) treatment for 2 h (HeLa cells)

Figure 38. Dysbindin and HRS knockdown enhance the sensitivity of HeLa cells towards Fas-mediated apoptosis. Representative pictures and quantification of active caspase 3 positive cells in control and Dysbindin or HRS siRNA treated cells stimulated with CH11 and CHX. Data was collected from three independent experiments (n=3), One-way ANOVA was performed, **p<0.01, error bars represent ± SEM. Validation of the indicated siRNAs in HeLa cells can be found in Sharma et al. (2019)[176].

6.3 ENTR1 association with dysbindin is key in the regulation of Fas trafficking and its cell surface expression.

We demonstrated that dysbindin plays and important role in cell surface Fas expression. Nevertheless, we needed more evidence supporting that association of ENTR1 to dysbindin is indeed essential in regulating Fas trafficking.

In order to address that question we performed a rescue experiment using a mutant version of ENTR1 with significantly reduced binding to dysbindin.

First, we generated a series of truncated versions of ENTR1 to map dysbindin's binding site and demonstrated that an ENTR1 version lacking the last C-terminal 16 amino acids abolishes interaction with dysbindin (Supplementary Figure 1, work performed by Agnieszka Skowronek).

Once we mapped dysbindin's binding site within the C-terminus of ENTR1 (397-412 aa) we performed the rescue experiment itself by co-transfecting ENTR1 siRNA with either full length GFP-ENTR1 or Δ397-412 GFP-ENTR1 and analysed cell surface Fas by flow cytometry. We could not observe any rescue when transfecting the mutant version of ENTR1 with reduced dysbindin binding whereas wild-type ENTR1 could rescue Fas cell surface to control levels (Figure 39). This result highlighted that ENTR1/dysbindin association is also contributing to the presentation of Fas at the cell surface.

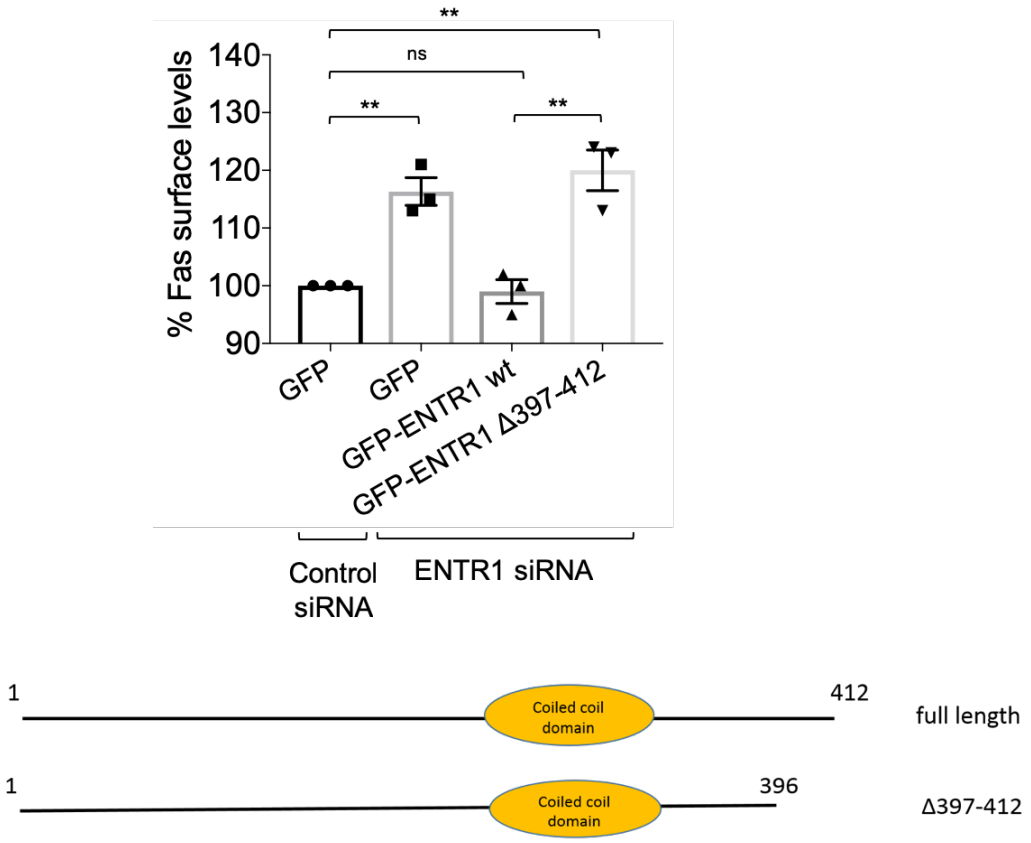

Figure 39. ENTR1 association with dysbindin affects the regulation of Fas trafficking and its cell surface expression. Flow cytometry analysis of Fas surface levels upon ENTR1 knock-down and transfection with GFP-ENTR1 wild type or a truncated version Δ397-412 (see cartoon below) in HeLa cells. Bar graphs represent the mean of the Alexa Fluor 633 nm median intensities. Data was collected from three independent experiments (n=3), One-way ANOVA was performed, **p<0.01, error bars represent ± SEM.

7. Blocking recycling upon ENTR1 depletion partially rescues Fas-mediated apoptosis

How much of the increase in apoptosis upon ENTR1 depletion is due to the actual enhancement of Fas recycling to the cell surface? To find out we measured the apoptosis rate in ENTR1 siRNA transfected cells stimulated with CH11 and

simultaneously blocked recycling using dominant negative Rab11. Strikingly, we only observed a partial rescue of apoptosis when recycling is blocked (Figure 36 a and b) although we were able to rescue cell surface expression completely (Figure 40 a). This suggests that an increased expression of Fas in the cell surface is not the only mechanism for the observed enhanced apoptosis upon ENTR1 downregulation.

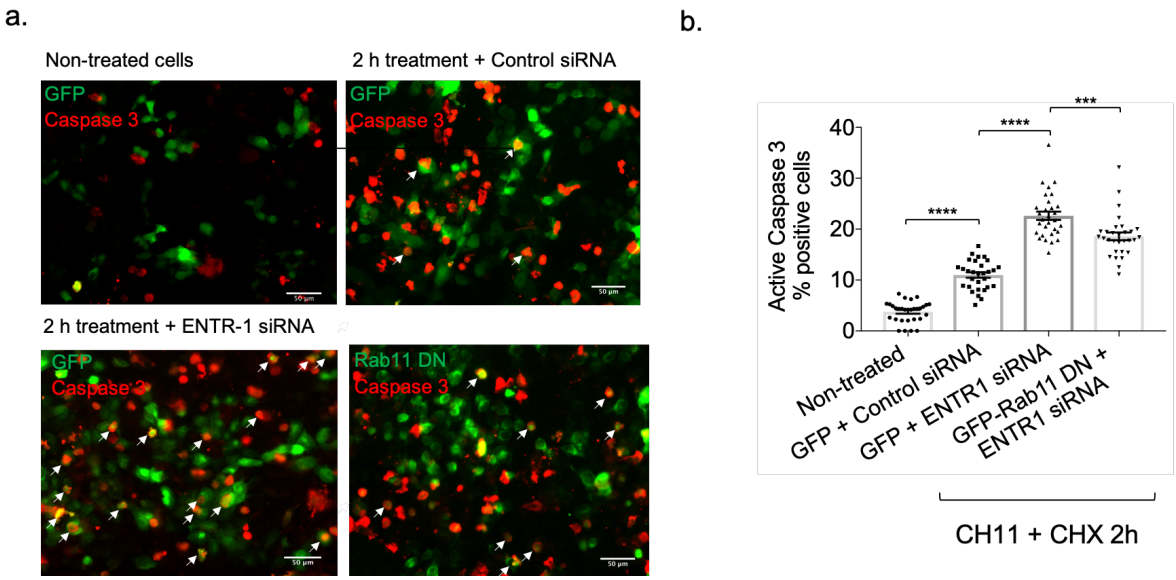

Figure 40. Enhanced Rab-11 dependent recycling is partially responsible of the increased apoptosis upon ENTR1 downregulation. Quantification of the activated caspase 3 in untreated or treated (CH11 500 ng/ml and CHX 150 μg/ml) HeLa cells transfected with the indicated expression constructs and either control or ENTR1 siRNA. Data was collected from three independent experiments (n=3), One-way ANOVA was performed, **p<0.01, error bars represent ± SEM.

8. ENTR1 is cleaved in a caspase-dependent manner during Fas-induced apoptosis

As suggested in the previous section, increased cell surface Fas is not the only mechanism responsible of the increase of Fas-mediated apoptosis upon

ENTR1 downregulation. We propose that caspase-mediated cleavage of ENTR1 upon Fas activation might be another mechanism owing to the observed enhanced apoptosis. Recent literature determined that ENTR1 is a substrate for caspase 6[188], an effector protease that can be activated downstream of caspase 8 activation. Consequently, we hypothesized that ENTR1 could be cleaved during Fas mediated apoptosis, as both caspase 8 and 6 are activated after Fas activation. Previous work in our lab monitored the expression of myc-tagged ENTR1 in HeLa cells after induction of Fas-mediated apoptosis in order to facilitate detection of potential Fas cleavage products of ENTR1 (Supplementary Figure 2, *work performed by Fangyan Yu*). Strikingly, it was observed that the band of full-length myc-ENTR1 became weaker over time and simultaneously a shorter new band appeared at around 35 KDa. This band did not appear upon adding CH11 together with the pan-caspase inhibitor z-Vad-FMK suggesting that ENTR1 is cleaved in a caspase-dependent manner (Supplementary Figure 2, *work performed by Fangyan Yu*[176]).

A negative regulator of Fas cell surface expression like ENTR1 being targeted by the Fas apoptotic signaling itself has major mechanistic implications, adding another layer of complexity to the regulation of Fas induced apoptosis by ENTR1. Thus, cleavage of ENTR1 could enhance Fas apoptotic signaling in a similar fashion to what we previously described for the ENTR1 knock down. Next, we focused our efforts on mapping the specific caspase cleavage site in ENTR1. We identified potential cleavage sites based on previously identified caspase cleavage sites in other proteins[189]. In each of these sites we mutated the conserved

aspartate to alanine; in total we tested five different mutants in our apoptosis assay and identified a single cleavage site at position amino acid 236 (D236A) of ENTR1 isoform 1 (Supplementary Figure 3, *work performed by Agnieszka Skowronek*)[176]. Finally, we introduced the same point mutation in the ENTR1 isoform 2 (D213A) by site-directed mutagenesis and confirmed that this leads to caspase-resistance (Figure 41). Although we initially mapped the caspase cleavage site using ENTR1 isoform 1 (cleavage site D236), we decided to generate the caspase resistant mutants in ENTR1 isoform 2 (cleavage site D213) to be consistent with all our previous experiments, which were performed with ENTR1 isoform 2.

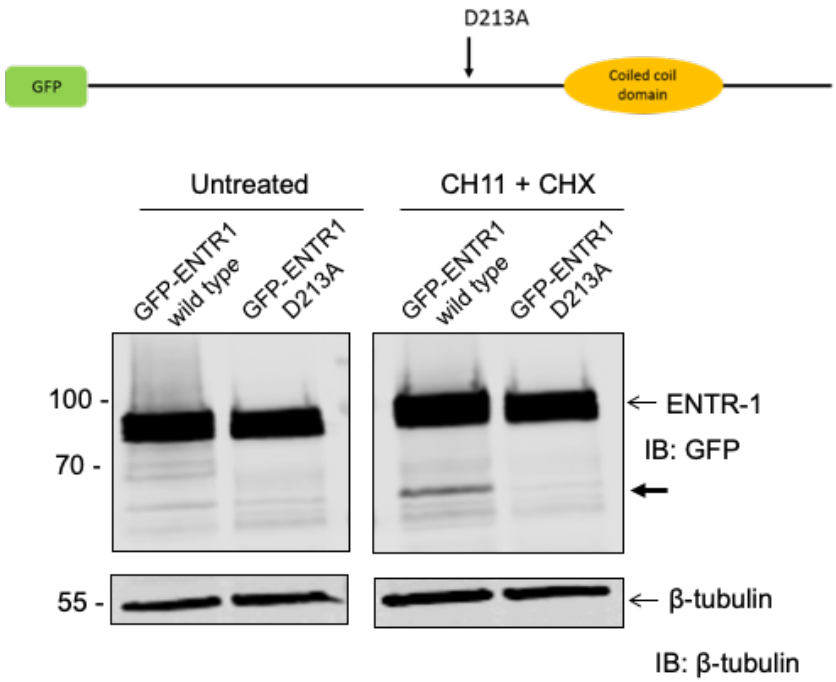

Figure 41. Validation of the caspase cleavage resistant mutant D213A (ENTR1 isoform 2) in HeLa cells. Scheme of the GFP-ENTR1 D213A mutant, exhibiting a point mutation that exchanges aspartate to alanine in the position 213 aa. Immunoblot showing equal protein expression of the ENTR1 constructs and appearance of the cleaved product in GFP-ENTR1 wild-type transfected cells but not in the GFP-ENTR1 D213A caspase-resistant mutant. Cleaved ENTR1 product indicated with an arrow. β-tubulin was used as a loading control.

Finally, the impact of ENTR1 caspase cleavage in the Fas-mediated apoptosis was evaluated. To achieve that aim we tested the ability of ENTR1 D213A mutant to rescue enhanced apoptosis in ENTR1 knock-out cells. ENTR1 knock-out HeLa cells demonstrated an increased sensitivity to Fas induced apoptosis as we observed before. Transfection of wild-type ENTR1 completely rescued the enhanced apoptosis. Interestingly, caspase-resistant D213A ENTR1 was significantly more effective in rescuing apoptosis compared to wild-type ENTR1 (Figure 42). This result suggests that blocking caspase-induced cleavage of ENTR1 reduces Fas apoptotic signaling.

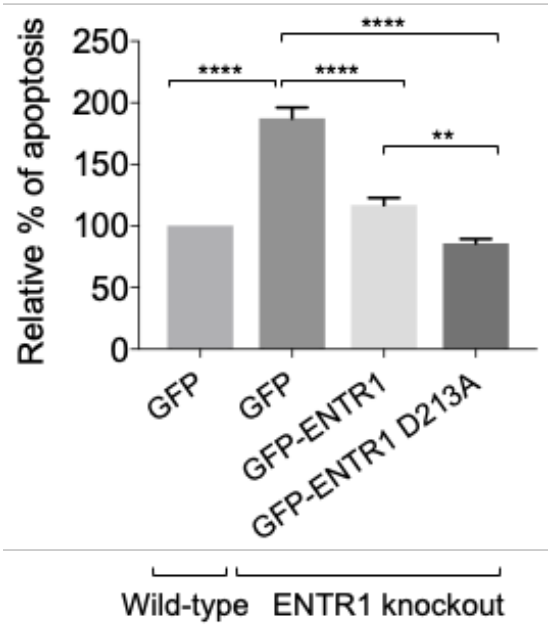

Figure 42. Cleavage-resistant ENTR1 displays enhanced anti-apoptotic activity. A caspase resistant ENTR1 has increased anti-apoptotic activity compared to wild-type ENTR1. Quantification of the immunofluorescence analysis of activated caspase 3 in CH11 (500 ng/ml) and CHX (100 μg/ml) treated wild-type HeLa cells or ENTR1 knock-out cells transfected as indicated in the graph. Relative percentage of apoptosis (in GFP+ cells only) is showed and HeLa wild-type GFP transfected cells is considered as 100%. Data was collected from three independent experiments (n=3), One-way ANOVA was performed, **p<0.01, error bars represent ± SEM.

To summarize, in normal cells with intact ENTR1 initial apoptotic events lead to caspase activation downstream of Fas and subsequent caspase-dependent cleavage of ENTR1. This prevents ENTR1 to negatively regulate Fas signaling by promoting lysosomal degradation, increases Fas at the cell surface available to trigger apoptotic events and generates a self-amplifying loop that partially depletes ENTR1. The exponential activation of caspases and deactivation of ENTR1-dependent negative regulation of Fas eventually leads to an accelerated apoptotic cell death.

However, the experiment above was based on transient transfection of the rescue constructs, which provides a more limited context. To support the previous results, we wanted to examine apoptosis in a more suitable model: stable cell lines. Accordingly, we successfully generated HeLa rescue cell lines that stably express GFP-ENTR1 wt or GFP-ENTR1 D213A in an ENTR1 knockout background (Figure 43). Unfortunately, we did not have time to examine apoptosis in these rescue cell lines, so this experiment will be done in the future (the study of these stable cell lines will be part of a future project in our lab).

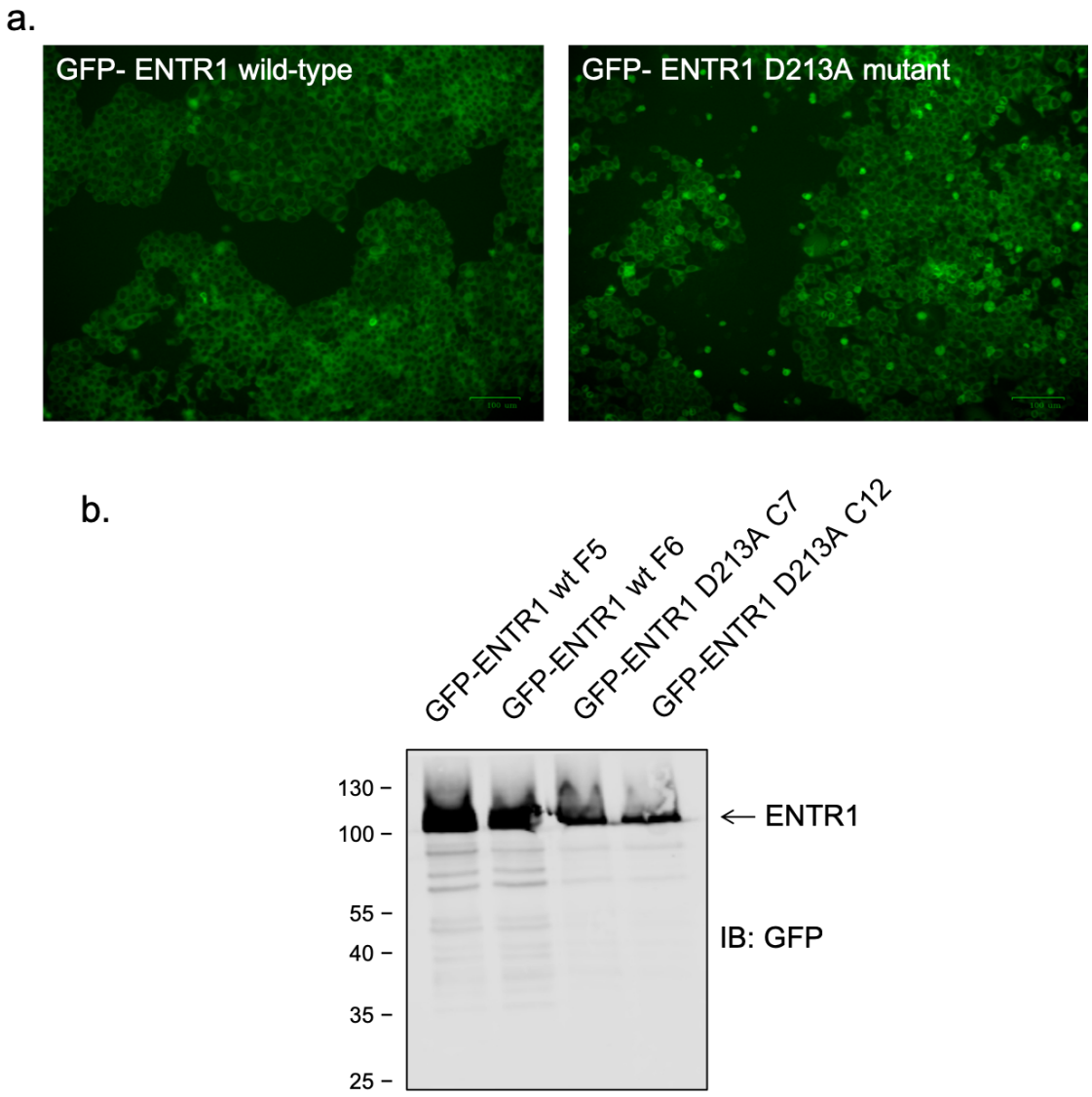

Figure 43. Validation of HeLa rescue cell lines generated upon selection with G418 and FACS sorting. HeLa rescue cell lines that stably express GFP-ENTR1 wt or GFP-ENTR1 D213A in an ENTR1 knockout background were validated by checking GFP expression under fluorescence microscope (a) and by Western blotting (b). The totality of the cells was expressing GFP fused to either ENTR1 wild-type or D213A mutant as seen in the pictures and the size of the fusion proteins matches with what we expect from GFP-ENTR1.

9. ENTR1/PTPN13 overexpression and Fas downregulation are identified in colon cancer in vivo

In order to add evidence that our model is of physiological relevance in vivo we investigated the expression of PTPN13, ENTR1 and Fas in colon cancer. An earlier publication in our lab showed that ENTR1 is upregulated in colon cancer tissue[152]. This prompted us to analyse the expression levels of PTPN13, ENTR1 and Fas in a tissue microarray containing primary colon carcinomas and paired adjacent normal tissue, expecting to find a connection between PTPN13/ENTR1 and Fas expression in vivo as we have previously found in vitro.

Our in vitro model suggests that PTPN13 and ENTR1 work in a complex that negatively regulates cell surface Fas. Consequently, cancer cells which often express low levels of Fas in the cell surface to evade apoptosis would show a higher expression of PTPN13 and ENTR1. Consistently to our hypothesis, Oncomine database[190] identified higher levels of PTPN13 and ENTR1 mRNA in colon cancers than in normal colon tissue from several datasets including Skrzypczak Colorectal[191] (Figure 44 a and b). In contrast, Fas mRNA expression was often decreased in colon cancer datasets such as Skrzypczak Colorectal (Figure 44 c).

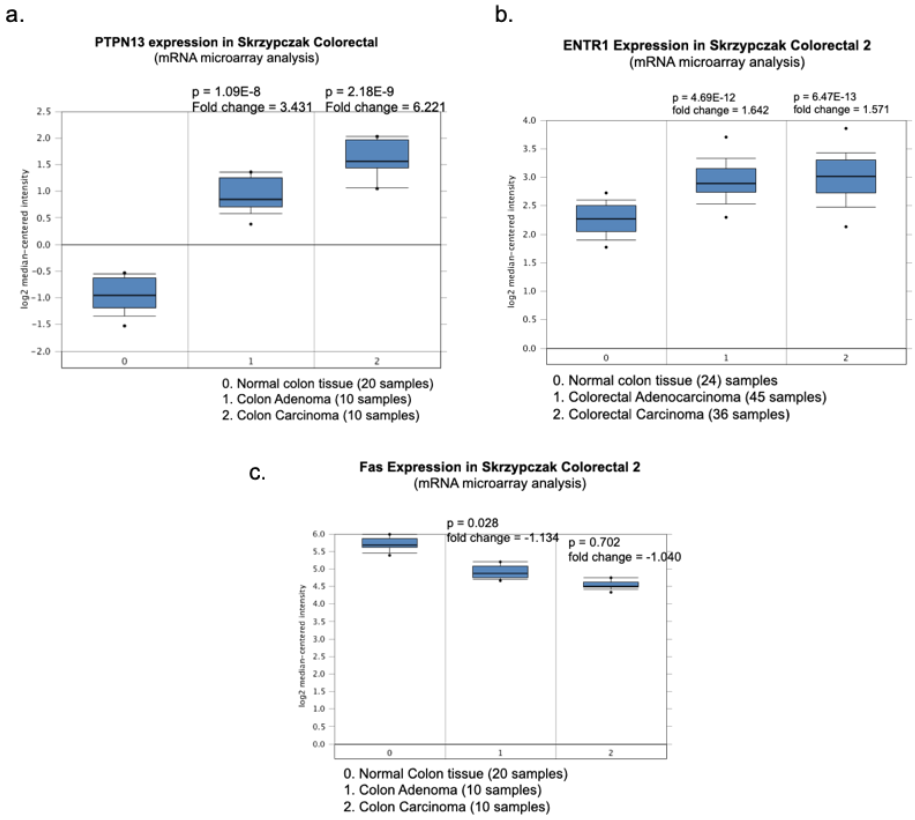

Figure 44. Expression of PTPN13, ENTR1 and Fas mRNA in colon cancer patients. Oncomine datasets are composed of samples represented as microarray data measuring mRNA expression on primary tumours from published literature. Skrzypczak Colorectal dataset containing gene expression data for both normal colon tissue and colon adenomas and carcinomas were identified by interrogation of the Oncomine database and PTPN13/ENTR1/Fas expression levels compared. mRNA expression of PTPN13 (a) and ENTR1 was significantly increased, whereas Fas mRNA expression (c) was decreased. Box plot indicates median and 25th/ 75th percentiles with error bars indicating 10th and 90th percentile.

Moreover, we determined the relationship between PTPN13/ENTR1/Fas expression and survival by generating Kaplan-Meier survival plots in a cohort of 876 gastric cancer patients (http://kmplot.com/analysis/). The Km plots indicate that patients with high PTPN13 or ENTR1 expression have a poorer gastric cancer specific survival, whereas patients with a higher expression of Fas have a better

survival rate (from 25 months onwards) (Figure 45). This is also in line with our hypothesis, as lower expression levels of either PTPN13 or ENTR1 would correlate with higher levels of Fas and increased Fas-mediated apoptosis in cancer cells, improving the rate of survival of those patients.

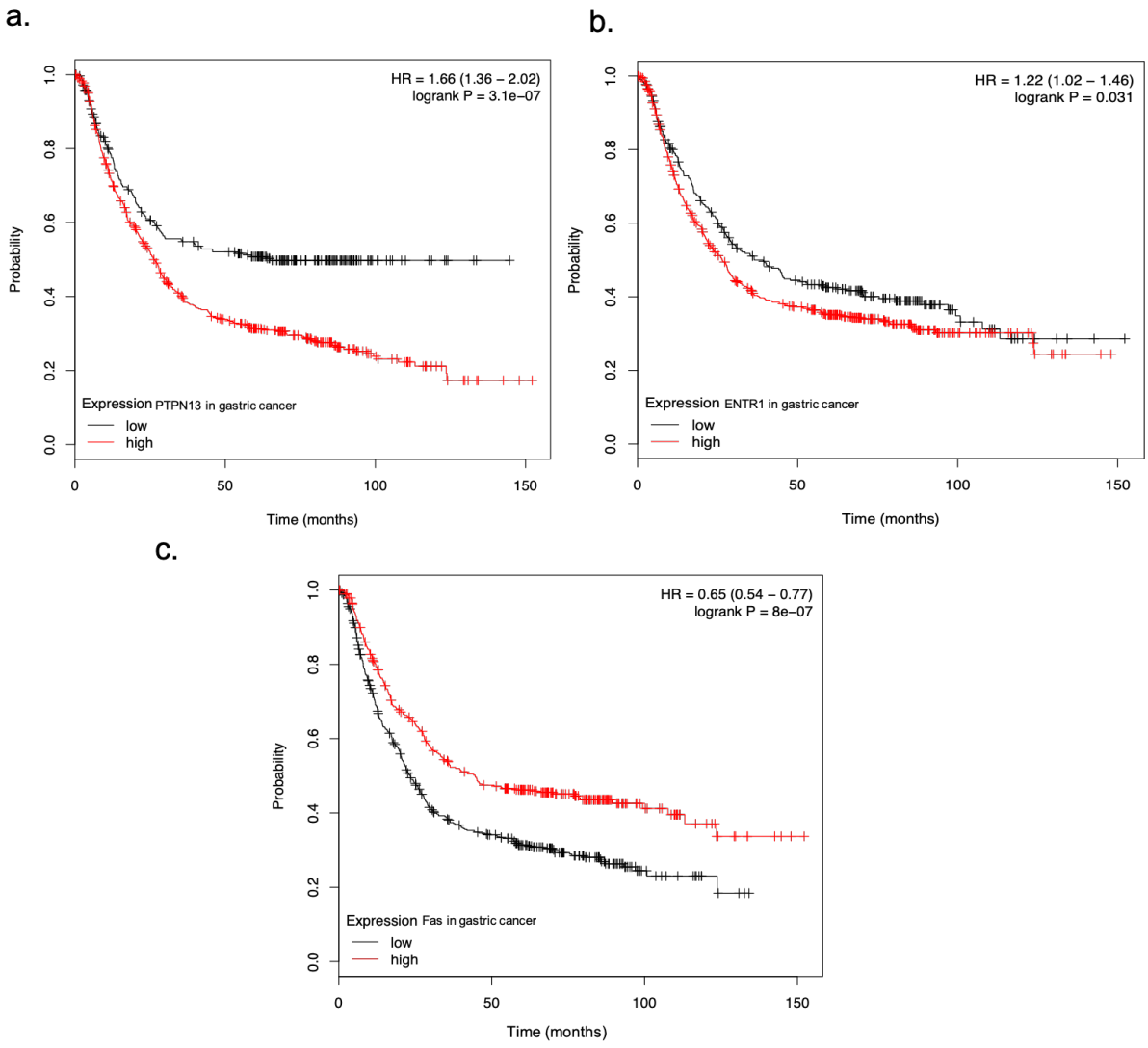

Figure 45. Expression of PTPN13, ENTR1 and Fas is correlated to gastric cancer patient survival. Kaplan-Meier survival plots indicating the probability of survival of gastric cancer patients over time with low or high expression of PTPN13 (a), ENTR1 (b) and Fas (c). The corresponding log rank P values (calculated with a log rank test) indicate that the difference in probability of survival between patients with low vs. high expression of PTPN13, ENTR1 and Fas is significant in the analysed cohort (876 gastric cancer patients). HR (hazard rate). Data obtained from KM plot database[192].

Next, immunohistochemistry was performed on small-scale colon cancer tissue microarrays (TMAs) comprising 24 histocores (20 colon cancer tissue samples and 4 normal adjacent colon tissue samples). We found that ENTR1 is upregulated in colon cancer tumours compared to non-tumourous tissue, confirming our previous findings[152]. Similarly, we observed increased PTPN13 expression in colon cancer tissue samples, whereas Fas expression was downregulated (Figure 46).

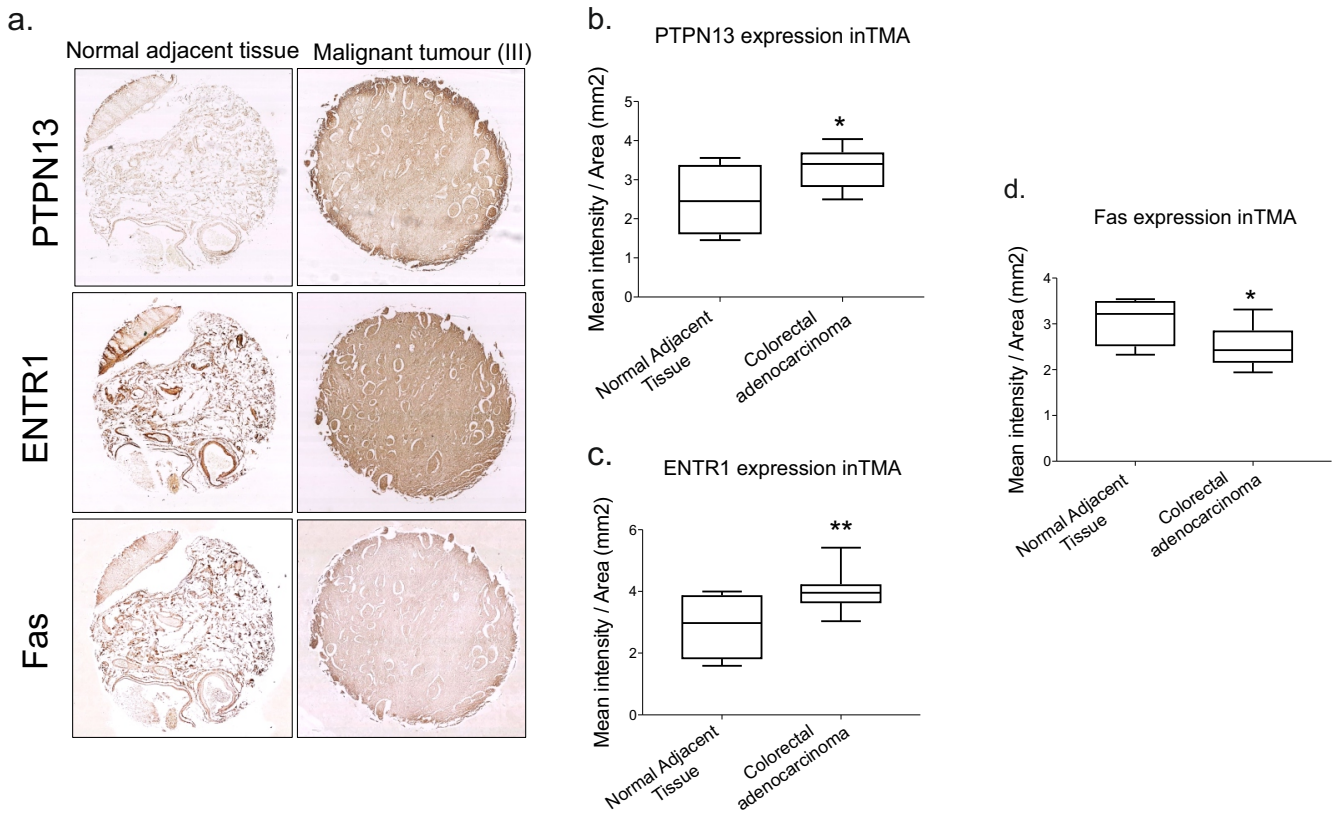

Figure 46. Immunohistochemical analysis of PTPN13, ENTR1 and Fas expression in colon cancer tissue microarrays. (a) Examples of immunohistochemical staining of PTPN13, ENTR1 and Fas in a colon cancer TMA (CO242b, Biomax US) indicating weak expression of the markers in normal adjacent colon tissue and a moderate/strong staining for PTPN13 and ENTR1 in the colon cancer histocore whereas weak staining for Fas in the same colon cancer histocore. (b-d) Box and whiskers plots displaying the expression of PTPN13 (b), ENTR1 (c) and Fas (d) in colorectal cancer TMAs. Expression of the markers in normal adjacent tissue (n=4) is compared to colorectal

adenocarcinoma histocores (n=19) in terms of mean intensity of staining in each core / area of the core (mm2). Data was collected from three independent experiments (n=3) and statistical significance was analysed by t-test. Box represents the interquartile range and the middle line represents the median, whiskers represent minimum to maximum values.

The overexpression of both PTPN13 and ENTR1 was also observed in a large-scale TMA comprising 80 total histocores: 40 colon cancer samples and 40 matching normal colon tissue samples. We identified a majority of colon cancer histocores with a higher expression of PTPN13/ENTR1 when compared to normal colon tissue controls, corroborating the results obtained in the small-scale TMAs (Figure 47).

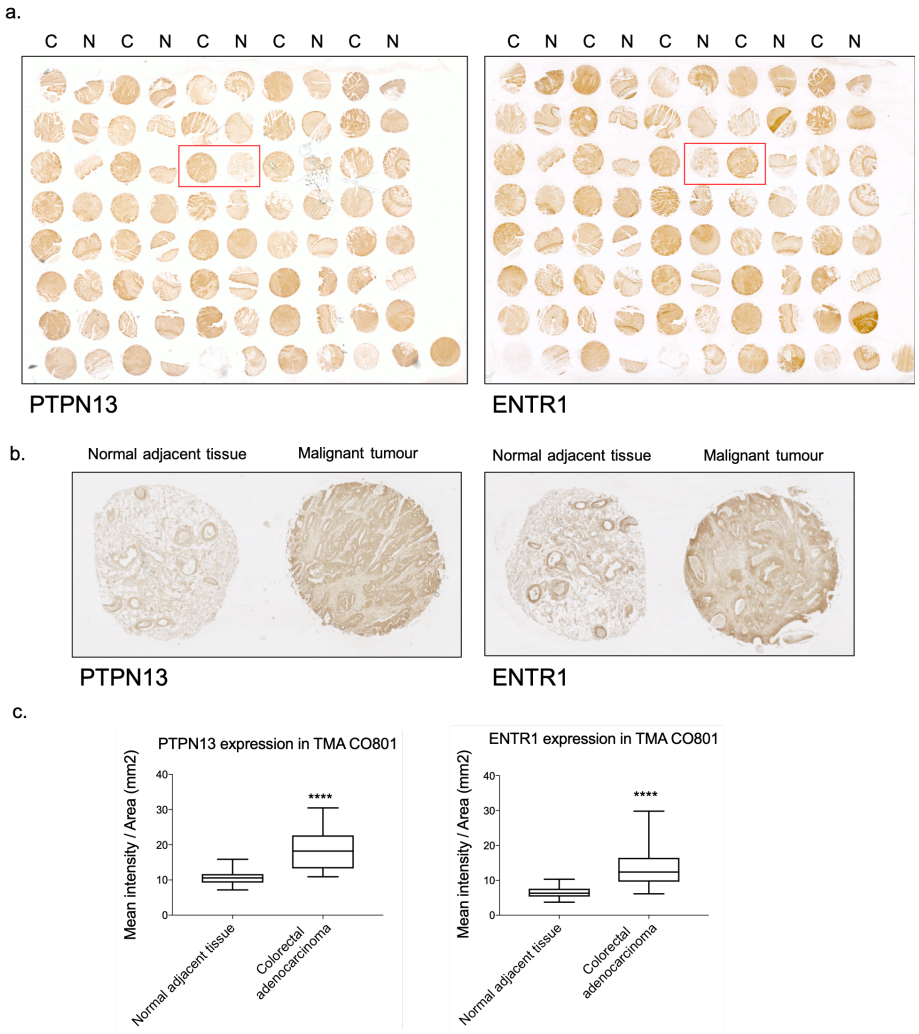

Figure 47. Immunohistochemical analysis of PTPN13 and ENTR1 in a large-scale colon cancer tissue microarray. (a) Image from the whole TMA showing differential expression of PTPN13 and ENTR1 in colon cancer vs. normal colon tissue histocores (n=80) (b) Examples of immunohistochemical staining of PTPN13 and ENTR1 in a colon cancer TMA (CO801a, Biomax US) indicating weak expression of the markers in normal adjacent colon tissue and a moderate/strong staining for PTPN13 and ENTR1 in the colon cancer histocores. (c) Box and whiskers plots displaying the expression of PTPN13 and ENTR1 in colorectal cancer TMAs. Expression of the markers in normal adjacent tissue is compared to colorectal adenocarcinoma histocores in terms of mean intensity of staining in each core / area of the core (mm2). Statistical significance was analysed by t-test. Box represents the interquartile range and the middle line represents the median, whiskers represent minimum to maximum values.

Interestingly, when comparing the expression of ENTR1/PTPN13 with Fas a significant proportion of colon cancer samples exhibit upregulated ENTR1 or PTPN13 and concomitantly a downregulation of Fas expression levels (Figure 48, data obtained from the small-scale TMAs). A 78% of the ENTR1 and 73% of the PTPN13 colon cancer histocores met the previous criteria. It is important to note that this statistical parameter is just indicating the proportion of histocores that meet our criteria and not a correlation between expression of ENTR1/PTPN13 and Fas.

To summarize, we can find a majority of histocores with overexpressed ENTR1 and PTPN13 and a lower expression of Fas. This is in line with our findings that ENTR1 and PTPN13 are negatively regulating Fas in colon cancer and provides further evidence that our model is of physiological relevance in vivo.

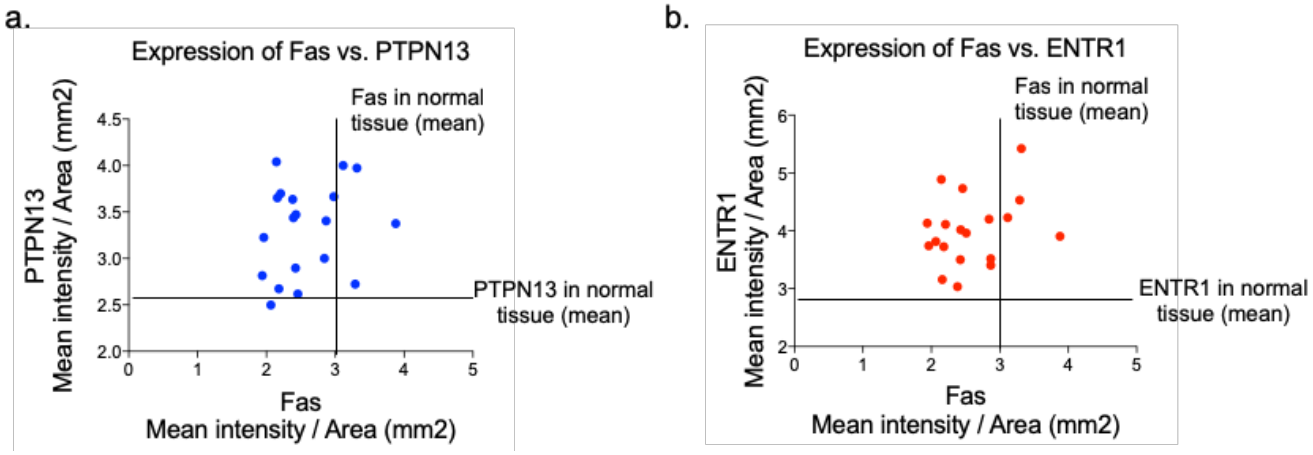

Figure 48. PTPN13, ENTR1 and Fas compared expression in colon cancer tissue microarrays. Dot plots displaying the expression of Fas and either PTPN13 (a) or ENTR1 (b) in colorectal adenocarcinoma samples (n=19). p-value (ENTR1 vs Fas) = 0,00587 (**); p-value (PTPN13 vs Fas) = 0,01970 (*) were calculated by one-tailed proportion test (z). Internal axis correspond to the mean expression of the corresponding markers in normal adjacent colon tissue. Imaging data were collected from three independent experiments (n=3).

10. Discussion

10.1 PTPN13/ENTR1 complex regulates post-endocytic sorting of the death receptor Fas

In the previous chapter we have focused on investigating the role of PTPN13 and ENTR1 in the regulation of the post-endocytic trafficking of Fas receptors and how they are able to modulate Fas-mediated apoptosis. We have described a novel endocytic complex composed by PTPN13 and ENTR1 that negatively regulates Fas cell surface levels. This complex has proved itself to be a major player in Fas endocytic trafficking by contributing to the sorting Fas receptors towards lysosomal degradation and consequently shutting down Fas-dependent signal transduction.

We first established that expression levels of ENTR1 affect the surface presentation of Fas receptors. (Figures 20, 21, 24). Moreover, downregulation of ENTR1 not only increased the levels of Fas in the cell surface but made cells more sensitive to Fas-mediated apoptosis (Figures 26-28). In other words, regulation of Fas receptor trafficking by ENTR1 had a clear outcome in the sensitivity of cells to undergo apoptosis. This is of great relevance, as several cancer cells express low surface levels of Fas evading potential surveillance mechanisms that use Fas-mediated apoptosis as their main weapon[56, 57, 143, 144, 193, 194].

In a similar fashion to ENTR1, downregulation of PTPN13 also increased cell surface levels of Fas (Figure 29) suggesting that PTPN13 and ENTR1 could act

together in a complex to mediate regulation of Fas trafficking. Not only PTPN13 is interacting with Fas, but ENTR1 was earlier shown to interact directly PTPN13[152]. Interestingly, previous research in the Erdmann lab showed that upon Fas-mediated apoptosis stimulation both PTPN13 and ENTR1 co-localise with Fas in the early endosomes. The localisation of the three proteins in the early endosomes place them in the correct location for regulating Fas sorting and we hypothesized that PTPN13 was the molecular bridge that connected Fas with ENTR1 in the early endosomes.

To further confirm the involvement of PTPN13 in the complex we performed a rescue experiment based on flow cytometry and established that ENTR1 and PTPN13 act together to regulate Fas cell surface levels (Figure 31). The discovery provided a deeper mechanistic insight into how PTPN13 can regulate Fas sensitivity in cancer, as it has been unclear so far. Extensive literature reported that there is a negative correlation between PTPN13 expression and Fas induced apoptosis in cancer cell lines[57, 131, 143, 148, 160, 164, 194] and in colon cancer in vivo[161, 195]. For instance, a recent study demonstrated that uncoupling binding of Fas to PTPN13 by adding a peptide derived from the PDZ binding motif of Fas (SLV tripeptide) restores Fas sensitivity and decreased the growth of colon cancer xenografts in a mouse cancer model[195].

The increase in cell surface Fas observed upon ENTR1 depletion pointed to a potential role of ENTR1 in tuning Fas trafficking (either internalization or sorting from the endosomes to the degradation pathways). On one hand, we could not

detect any effect of ENTR1 depletion at the step of internalisation of Fas, which is in line with our previous finding that ENTR1 localises to early and recycling endosomes[152, 175]. On the other hand, we analysed the degradation kinetics of Fas upon ENTR1 depletion and found a delayed rate of degradation of Fas receptors in both ENTR1 knockdown and knockout cells (Figures 32-35). The endosomal compartment serves as a major site for Fas-mediated DISC formation and caspase activation, being directly responsible of amplifying the apoptotic signaling. Thus, the longer retention time of Fas in the endosomal compartment upon ENTR1 depletion is likely to contribute to enhanced apoptotic signaling.

In addition, previous confocal microscopy work done in our lab revealed that depletion of ENTR1 traps Fas into early endosomes that are internalized following stimulation with an agonistic antibody and delays their transport to lysosomes[175, 176]. Altogether this confirmed that ENTR1 regulates the degradation of internalized Fas, that is the transition of the receptor from the early endosomal compartment to lysosomes. More specifically, ENTR1 was shown to regulate the sorting of Fas from the limiting endosomal membrane into intraluminal vesicles of multivesicular bodies[176]. The influence of ENTR1 in the sorting of Fas receptors into the endolysosomal degradation pathway has a direct impact on the cellular apoptosis response, as it leads to the attenuation of the apoptotic signaling.

Neither HeLa nor HCT-116 cells undergo type I apoptosis, which does not involve the mitochondrial pathway upon Fas stimulation in the cell surface. In contrast, they both exhibit type II apoptosis, which requires the mitochondrial

pathway for full activation of the caspase cascade and might provide a more limited context than type I cells. Although our experiments were performed with type II apoptosis cells, our proposed model is also of relevance for type I cells, as it has been demonstrated that receptor internalisation is a crucial step for DISC formation and apoptotic signaling for several type I cell lines[31]. We indeed tried to extend our results to type I apoptosis cells BJAB (Human Burkitt lymphoma B cell line) but after many struggles we finally ruled them out due to their low efficiency of transfection and overall difficult manipulation.

Furthermore, increased Fas cell surface expression upon ENTR1 depletion is explained by a defective endolysosomal sorting that leads to the accumulation of Fas at early endosomes and enhanced Rab11-dependent recycling pathway (Figure 36). In other words, part of the excess of Fas trapped in the early endosomes in the absence of ENTR1 is diverted to the Rab11 recycling endosomes and subsequently added to the pool of Fas receptors in the membrane. In line with our data, it has also been demonstrated that knocking out dysbindin, which is as well involved in endolysosomal sorting, increases the recycling of dopamine D2 receptor[182].

10.2 ENTR1 mediates endolysosomal sorting of Fas receptors via dysbindin-HRS axis

This section provided a better molecular insight into the mechanism by which ENTR1 regulates lysosomal sorting of Fas. ESCRT complexes are the main endocytic machinery that tune sorting of cargo from early/sorting endosomes to the endolysosomal pathway[196, 197]. We identified dysbindin, a protein involved in cargo delivery to endosomes, as a potential candidate to link our ENTR1/PTPN13 complex to the ESCRT machinery. ENTR1 was suggested as an interacting partner of dysbindin by two independent proteomic screenings[183, 184] but only in our study we demonstrated that dysbindin is directly interacting with ENTR1 by two different approaches: GST pull down and by GFP-trap co-immunoprecipitation (Figure 37). Additionally, overexpressed dysbindin co-localised with endogenous ENTR1 in the limiting membrane of enlarged endosomes[175]. This is in line with dysbindin forming a complex with ENTR1 and contributing to the regulation endolysosomal sorting.

Previous literature supports our hypothesis, as dysbindin has previously been involved in the lysosomal sorting of G-protein coupled receptors (GPCRs) like the δ-opioid receptor (DOP), the dopamine-2 receptor (D2R) and the chemokine receptor type 4 (CXCR4)[182, 185]. There is an uncanny resemblance between the phenotypes observed upon depletion of dysbindin shown in the previous studies and those identified in ENTR1 depleted cells. For example, surface levels of the aforementioned receptors were upregulated in dysbindin

depleted cells. Dysbindin is also a well-described interacting partner of HRS, a key member of the ESCRT-0 sorting machinery[182]. Thus, it can be understood that dysbindin is an accessory protein of the ESCRT-0 via HRS, acting in the early steps of the endolysosomal sorting and facilitating the connection between Fas endosomal regulators and the ESCRT machinery.

If our hypothesis is correct and dysbindin/HRS/ENTR1 form a complex that regulates sorting of Fas receptors, depletion of dysbindin and HRS should affect the intracellular trafficking of Fas in a similar manner as ENTR1. We indeed observed an upregulation of cell surface Fas in HeLa cells upon dysbindin and HRS knockdown suggesting that they acted in a similar pathway as ENTR1[175, 176]. Notably, transfection of ENTR1 and dysbindin siRNA in parallel did not further increase the levels of cell surface Fas as compared to only ENTR1 or only dysbindin depleted cells[175]. Sensitivity towards Fas-mediated apoptosis was also increased when dysbindin or HRS were depleted with siRNA (Figure 38). These results provided good evidence that both dysbindin and HRS are in line with ENTR1 in the same pathway to regulate Fas receptor post-endocytic trafficking.

To confirm the importance of dysbindin in Fas receptor trafficking, we performed a rescue experiment of Fas cell surface levels upon ENTR1 depletion. As ENTR1 mutant with significantly reduced binding to dysbindin could not rescue Fas cell surface to ENTR1 wild-type levels (Figure 39) we propose that ENTR1 interaction with dysbindin is important in Fas sorting from the early endosomes to the endolysosomal pathway.

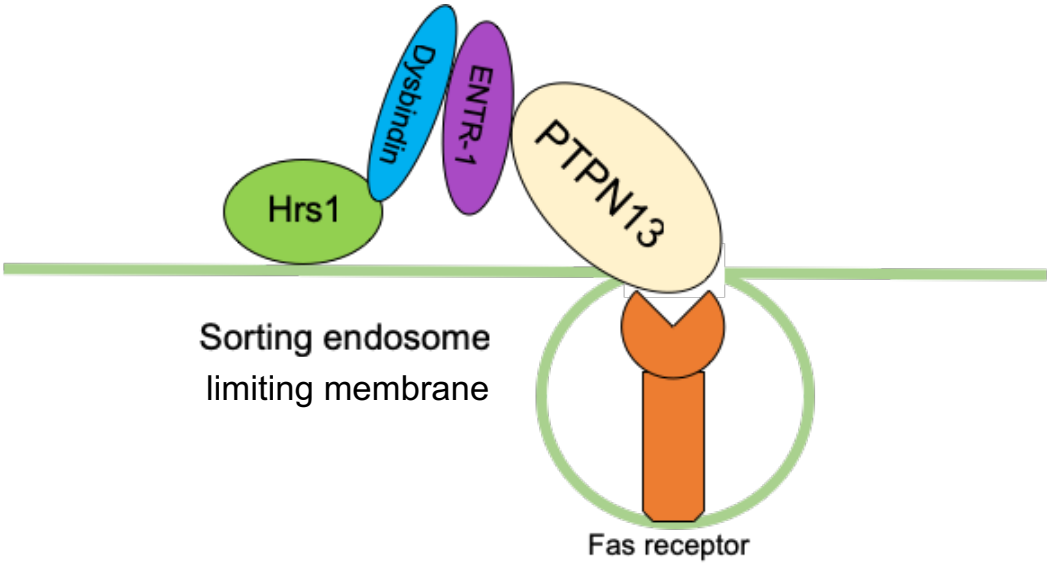

Figure 49. Closer look to the PTPN13/ENTR1/dysbindin complex. The model depicts the molecular machinery involved with ENTR1 in sorting of the internalized Fas receptors as suggested by the current study. ENTR1 binds to Fas through PTPN13 and connects to the ESCRT-0 machinery (Hrs) via dysbindin in the limiting membrane of early/sorting endosomes. The complex regulates post-endocytic sorting of Fas, more precisely the transport into intraluminal vesicles that finally lead to the degradation of cargo in the lysosomes.

As an alternative to the model depicted above (Figure 49), PTPN13/ENTR1/dysbindin might not be associated in a single complex, but in two complexes that act sequentially. In the first step, ENTR1/PTPN13 complex would bind to Fas during early stages of sorting and locate Fas receptors in specific endosomal compartments for cargo destined for degradation. Next, dysbindin would associate with ENTR1 and in collaboration with Hrs would aid sorting of Fas to the endolysosomal pathway.

10.3 ENTR1 is cleaved in a caspase-dependent manner during Fas-induced apoptosis

Last but not least, we determined that ENTR1 is cleaved during Fas-induced apoptosis revealing a novel positive feedback loop of apoptotic signaling. Several proteins involved in intracellular trafficking have been shown to be substrates for caspases[189]. Surprisingly, we identified ENTR1 as a target for caspase-mediated cleavage upon Fas activation (Supplementary Figures 2 and 3, work performed by Agnieszka Skowronek and Fangyan Yu). If we combine this finding with the ENTR1 depletion results described above, we could hypothesize that proteolytic decrease of endogenous ENTR1 (due to caspase-dependent cleavage) impairs Fas degradation and increases apoptotic signaling which in turn induces even more caspase mediated cleavage of ENTR1 and other downstream targets resulting in a positive feedback loop of apoptotic signaling. In line with this, we observed enhanced anti-apoptotic activity with a caspase-resistant version of ENTR1 compared to wild-type ENTR1 (Figures 42). This discovery highlights the importance of endogenous ENTR1 in the regulation of Fas-mediated apoptosis.

10.4 The whole picture: ENTR-1/PTPN13/dysbindin complex regulates post-endocytic sorting of the death receptor Fas

The current study describes a novel mechanism for post-endocytic trafficking of Fas (Figure 50). In summary, depletion of ENTR1 increased surface levels of Fas without inhibiting its rate of endocytosis but delaying the rate of degradation of Fas receptors suggesting that ENTR1 might interfere in the

endosomal sorting of Fas. A fraction of Fas receptors that remain stuck in the early endosomes upon ENTR1 depletion is diverted to the Rab11-mediated classic recycling pathway and therefore increases the presentation of Fas in the cell surface. Yet delayed, we also observe Fas degradation upon ENTR1 depletion, which means that a fraction of Fas is eventually destined for degradation by alternative proteins of the endolysosomal sorting machinery.

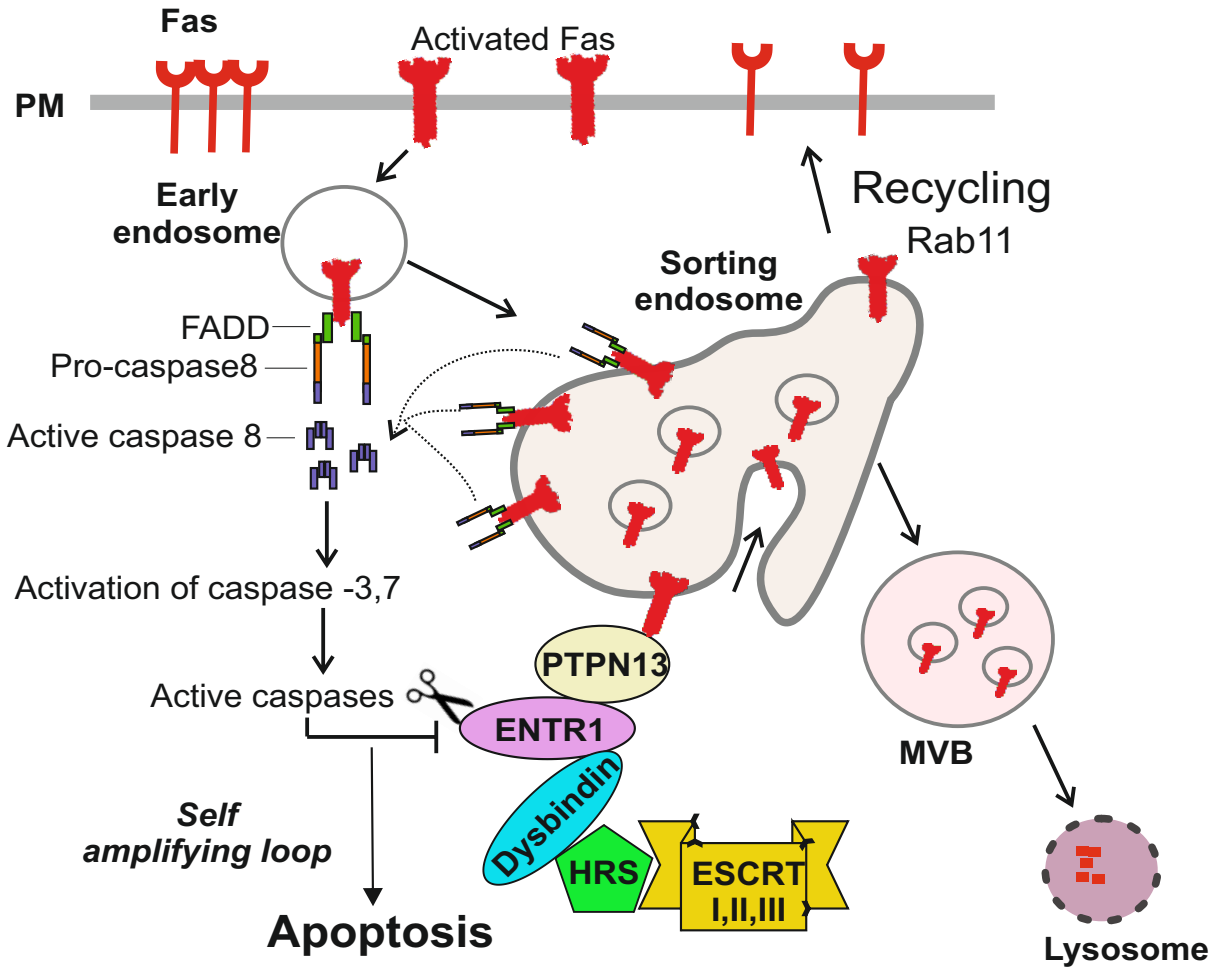

Figure 50. Proposed model for ENTR1 and PTPN13 role in Fas-mediated apoptosis. The PTPN13/ENTR1 endocytic complex regulates Fas-mediated apoptotic signaling by regulating the delivery of internalized Fas receptors from the early endosomes to the endolysosomal degradation pathway via dysbindin-HRS axis thereby controlling termination of Fas signal transduction. Deregulation of any of the components of the complex affects the expression of Fas receptor in the cell surface.

According to our model, once Fas is internalized upon ligand binding, DISC complex is assembled in the early endosomes and launches apoptotic signaling. DISC triggers the activation of the caspase cascade which subsequently cleaves ENTR1 and prevents sorting of Fas towards lysosomes to sustain apoptotic signaling by a positive feedback loop. The accumulation of Fas in the early endosomes upon ENTR1 cleavage enables the assembly of a larger amount of DISC complex (or for a longer time) and faster accumulation of active caspase 8. In addition, the excess of Fas receptors stuck in the endosomes is recycled back to the cell surface, increasing available Fas receptors in membrane and sensitivity to Fas-mediated apoptosis. The amplification of the apoptotic loop finally leads to cell death by mitochondrial and nuclear fragmentation. In this scenario, sorting of Fas by ENTR1 might act as a checkpoint for further sustaining or blocking apoptotic signaling. On the other hand, when ENTR1 is artificially depleted (either by siRNA or by CRISPR-Cas9 technology) the self-amplifying loop is boosted and the observed effects on trafficking and sensitivity to apoptosis are more striking. This is because ENTR1 depletion by these techniques is more efficient than endogenous caspase cleavage.

In the case of cancer cells, deregulation of either ENTR1 or PTPN13 might lead to reduced levels of Fas receptor in the cell surface, which would translate into an unusual resistance to Fas-mediated apoptosis and a higher resilience to be efficiently cleared from tumours. These findings shed light on how cancer cells lower surface Fas expression to evade the surveillance mechanisms that our immune system uses against them.

Consistently to our model, databases for mRNA expression (Oncomine)[190] identified higher levels of PTPN13 and ENTR1 expression in colon cancers with respect to normal colon tissue, whereas Fas mRNA expression was decreased (Figure 44). In addition, Km survival plots in gastric cancer patients revealed that patients with high PTPN13 or ENTR1 expression have a poorer gastric cancer specific survival, whereas patients with a high expression of Fas have a better survival rate (Figure 45). Finally, we added further evidence that our model is of physiological relevance in vivo by investigating the expression of PTPN13, ENTR1 and Fas in colon cancer tissue microarrays. Our immunohistochemical data corroborated that higher expression levels of either PTPN13 or ENTR1 in colorectal cancer are often accompanied with lower levels of Fas, which is in consonance with our proposed model (Figures 46-48).

Taken together, this study describes a novel function of ENTR1 and PTPN13 in Fas mediated apoptotic signaling where it regulates intracellular sorting of Fas towards lysosomal degradation and shuts off the apoptotic signaling. Identification of both PTPN13 and ENTR1 as targets of apoptotic signaling has revealed insights into key aspects of the endolysosomal sorting of Fas and how this regulates sensitivity to Fas-induced apoptosis; however further investigations are necessary to fully understand the complex interplay of Fas membrane trafficking and its signal transduction.

10.5 Future directions

First, it will be very interesting to determine whether PTPN13/ENTR1 complex is only participating the sorting of Fas or if it also participates in the sorting of other cargoes. With the tools developed in the present thesis it will be feasible to test whether depletion of ENTR1 or PTPN13 is also affecting cell surface expression of other receptors or transmembrane proteins.

Moreover, an extensive flow cytometry-based screening might reveal new players involved in Fas trafficking, which might add further complexity to the proposed model. The identification of novel players in the endocytic sorting of Fas receptor might be of great value to understand how other cell surface receptors are trafficked.

Finally, our ENTR1 caspase resistant stable cell lines will be used in a future project for a deeper study of the caspase-dependent ENTR1 cleavage. Further rescue experiments with stable cell lines expressing ENTR1 wild-type or ENTR1 caspase resistant version would be required to corroborate the findings in experiments based on transient transfections.

5. Chapter II: Investigating the role of PTPN13 and ENTR1 in the Hippo pathway and cell proliferation

1. ENTR1 forms a complex with LATS2, a key component of the Hippo pathway

PTPN13 and ENTR1 were found in close proximity to LATS kinases in an extensive proteomic screening by Couzens[151]. This pointed to a potential interaction of PTPN13 and ENTR1 with LATS kinases. In order to establish a connection of PTPN13 with the Hippo pathway, we first examined the potential interaction of PTPN13 with LATS1 and LATS2. We were unable to confirm the interaction of full length PTPN13 with LATS kinases using GFP and myc trap co-immunoprecipitations (data not shown).

We previously found that PTPN13 and ENTR1 work together to regulate Fas-mediated apoptosis. In a similar fashion, we thought that ENTR1 could interact directly with LATS kinases and form a complex with PTPN13. Thus, we tested the interaction of overexpressed GFP-ENTR1 with myc-LATS2 by GFP-trap co-immunoprecipitation. Interestingly, we found a positive interaction of GFP-ENTR1 with myc-LATS2, as a clear band for LATS2 can be observed in the myc pull down blot but not in the negative control (Figure 51). This result confirmed that ENTR1 is associated with the LATS 2 kinase, central kinase of the Hippo pathway.

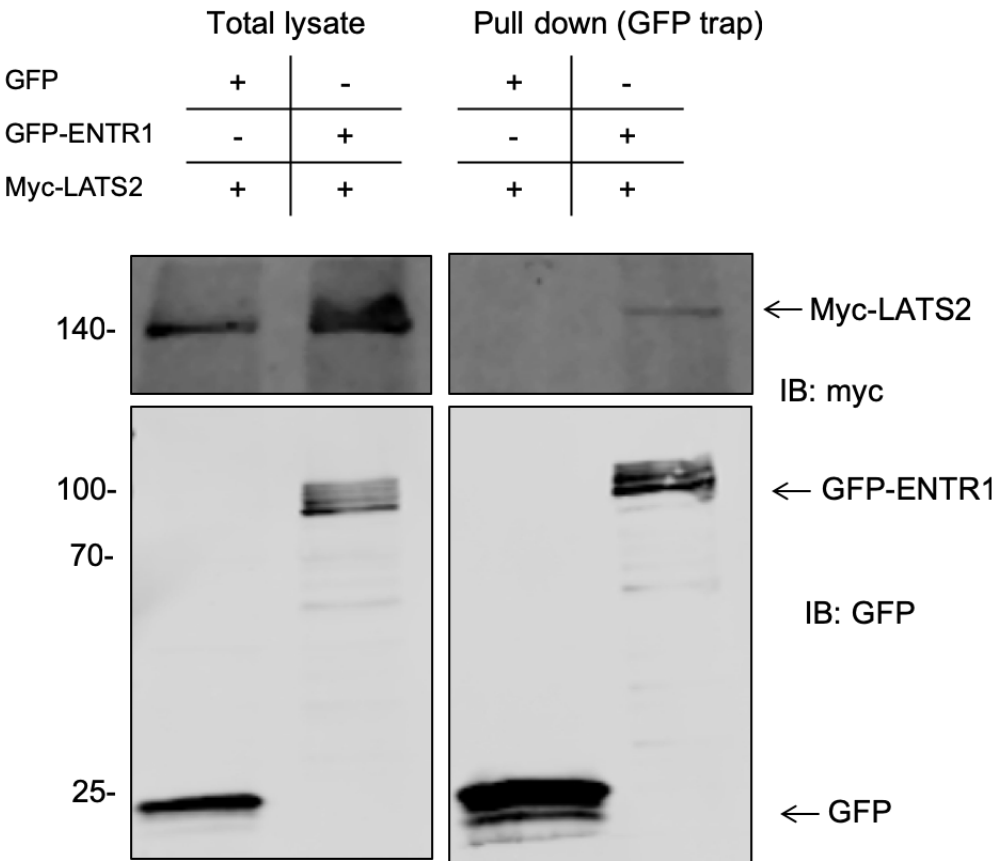

Figure 51. ENTR1 interacts with Hippo pathway's LATS2 kinase. Co-immunoprecipitation analysis of the interaction of overexpressed GFP alone and GFP-ENTR1 with myc-LATS2. HEK293 cells were transfected with the indicated constructs followed by GFP-trap and Western Blotting.

The BioID data from Couzens indicated that both PTPN13 and ENTR1 were in close proximity to LATS kinases, suggesting that they might form a multiprotein complex. In this case, ENTR1 would be directly mediating the association with LATS kinases, whereas PTPN13 would be indirectly connected to them through the complex.

As previous pull-down experiments with the full-length PTPN13 did not work, we decided to try a pull-down experiment with the FERM and PDZ domains of PTPN13 individually. HEK293 cells were co-transfected with GFP constructs

comprising different protein domains of PTPBL (Figure 52 a) and myc-LATS2. Cell lysates were subjected to GFP-trap co-immunoprecipitation. As a result, bands corresponding to myc-LATS2 were detected by myc immunoblot in pull down samples, both in PDZ and FERM domains, but not in the GFP negative control (Figure 52 b).

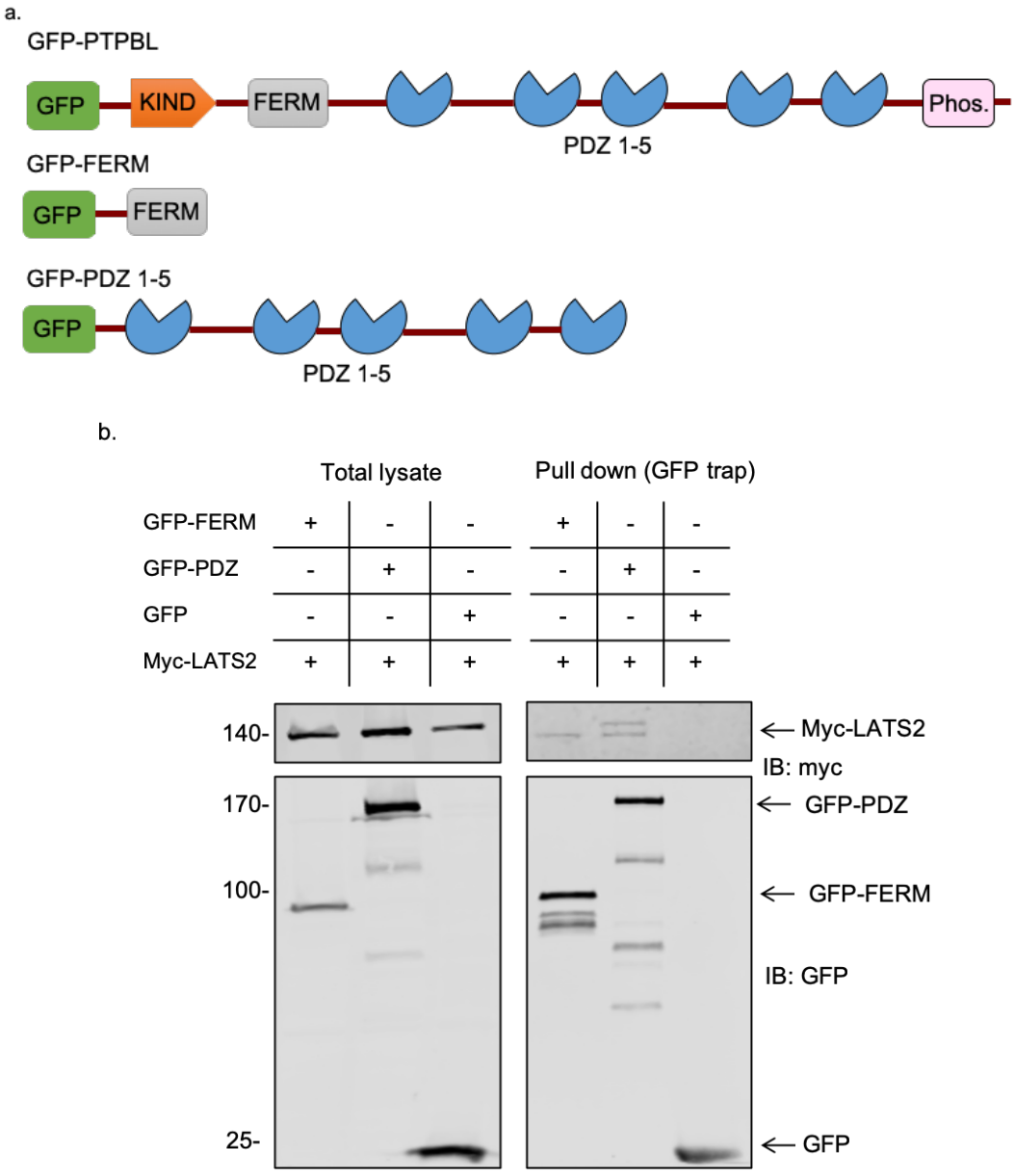

Figure 52. Pull down of PTPN13 FERM and PDZ with LATS2 by GFP trap co-immunoprecipitation. (a) PTPN13 domain constructs used in the experiment (GFP-FERM domain, GFP-PDZ 1 to 5 domains) (b) Co-immunoprecipitation analysis of the interaction of overexpressed GFP alone, GFP-FERM, GFP-PDZ with myc-LATS2. HEK293 cells were transfected

with the indicated constructs followed by GFP-trap and Western Blotting. Note: bands in the anti-myc pull-down blot were really faint, and a high exposure in the LICOR membrane developer was required for their clear visualization.

The previous experiments provided a first connection of PTPN13 and ENTR1 with LATS kinases, key elements of the Hippo pathway. However, the subcellular localization of the ENTR1/PTPN13/LATS complex and whether it acts dependently or independently from the Hippo pathway, still requires further investigation.

2. Identification of PTPN13 in the cell-to-cell junctions.

Several Hippo pathway members, including LATS kinases, interact with membrane-associated proteins and proteins found in tight and adherens junctions. The spatial regulation of LATS kinases might be decisive for the Hippo pathway, and PTPN13/ENTR1 complex might participate in these processes through the association with LATS in the adherens or tight junctions and apical membrane complexes.

First, PTPN13 exhibits a FERM domain that plays an important role at the interface between the plasma membrane and the cytoskeleton[124] and binds to 1-phosphatidylinositol 4,5-biphosphate (PIP2), which has been suggested to be important for membrane localisation of PTN13. Second, PDZ2 domain of PTPN13 is known to interact with proteins that regulate cell adhesion: Trip6/ZRP-1[198] and APC[140]. The exact function of PTPN13 in cell adhesion is poorly understood, but

the previous evidence is suggestive of PTN13 involvement in cell adhesions. Unfortunately, previous efforts to visualize endogenous PTPN13 at the cell-cell junctions were not successful.

For the first time, we have been able to detect endogenous PTPN13 at the plasma membrane in Caco2 cells after methanol fixation instead of the 4% PFA fixation by immunofluorescence (Figure 53). We validated the specificity of the PTPN13 membrane staining by PTPN13 siRNA knockdown (Figure 54).

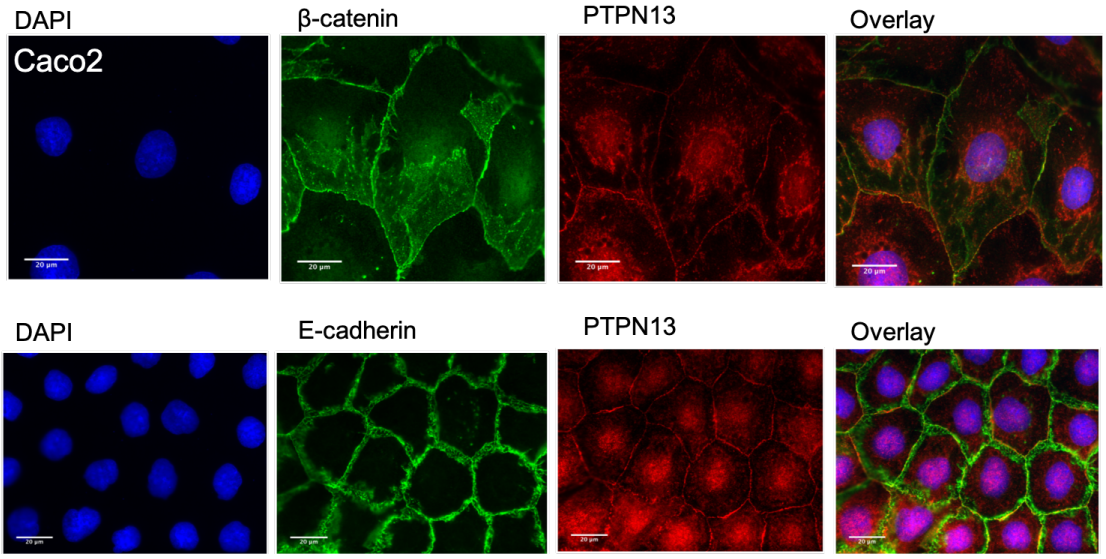

Figure 53. PTPN13 localisation in the cell membrane. Epifluorescence microscope images of Caco2 epithelial cells after methanol fixation. PTPN13 is visualized at the plasma membrane and partially co-localises with both β-catenin and E-cadherin. Images taken at 60x magnification show nuclei in blue (DAPI), β-catenin/E-cadherin in green and PTPN13 in red. Scale 20 µm.

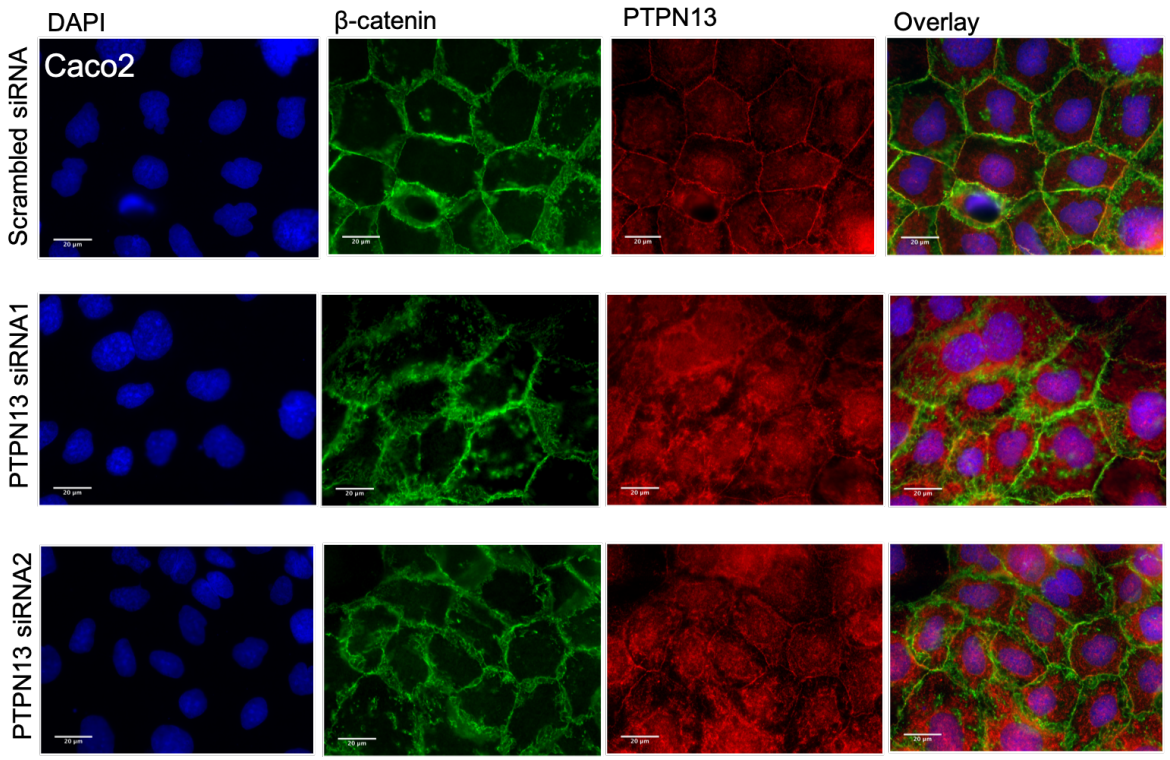

Figure 54. Validation of the specificity of PTPN13 membrane staining by siRNA knockdown. Epifluorescence microscope pictures show that PTPN13 staining in the membrane is dramatically reduced in knockdown Caco2 cells. Images taken at 60x magnification show nuclei in blue (DAPI), β-catenin in green and PTPN13 in red. Scale 20 μm.

PTPN13 exhibits an apical localisation in polarized cells and a recent proteomic screening showed that PTPN13 is enriched at the tight junctions[199]. As many elements of the Hippo pathway are also associated to proteins in the tight junctions, we were interested in confirming whether PTPN13 could be found in the tight junctions by analysing PTPN13 and ZO-1 (Zonula Occluden 1, tight junction marker) localisation in epithelial cells. Caco2 cells were grown until maturation of the tight junctions was completed. Cells were subsequently co-stained with PTPN13 and ZO-1 antibodies and visualized in the epifluorescence microscope. We observe PTPN13 in close proximity or running in parallel to ZO-1

marker (Figure 55). This supports the possibility of PTPN13 being enriched in the tight junctions but we cannot extract any definitive conclusions as the samples were visualized by epifluorescence microscopy (so the potential co-localization spots are likely to be in different planes within the Y-axis). Consequently, we would need to perform a similar experiment but with confocal microscopy to confirm that PTPN13 co-localizes to the tight junctions.

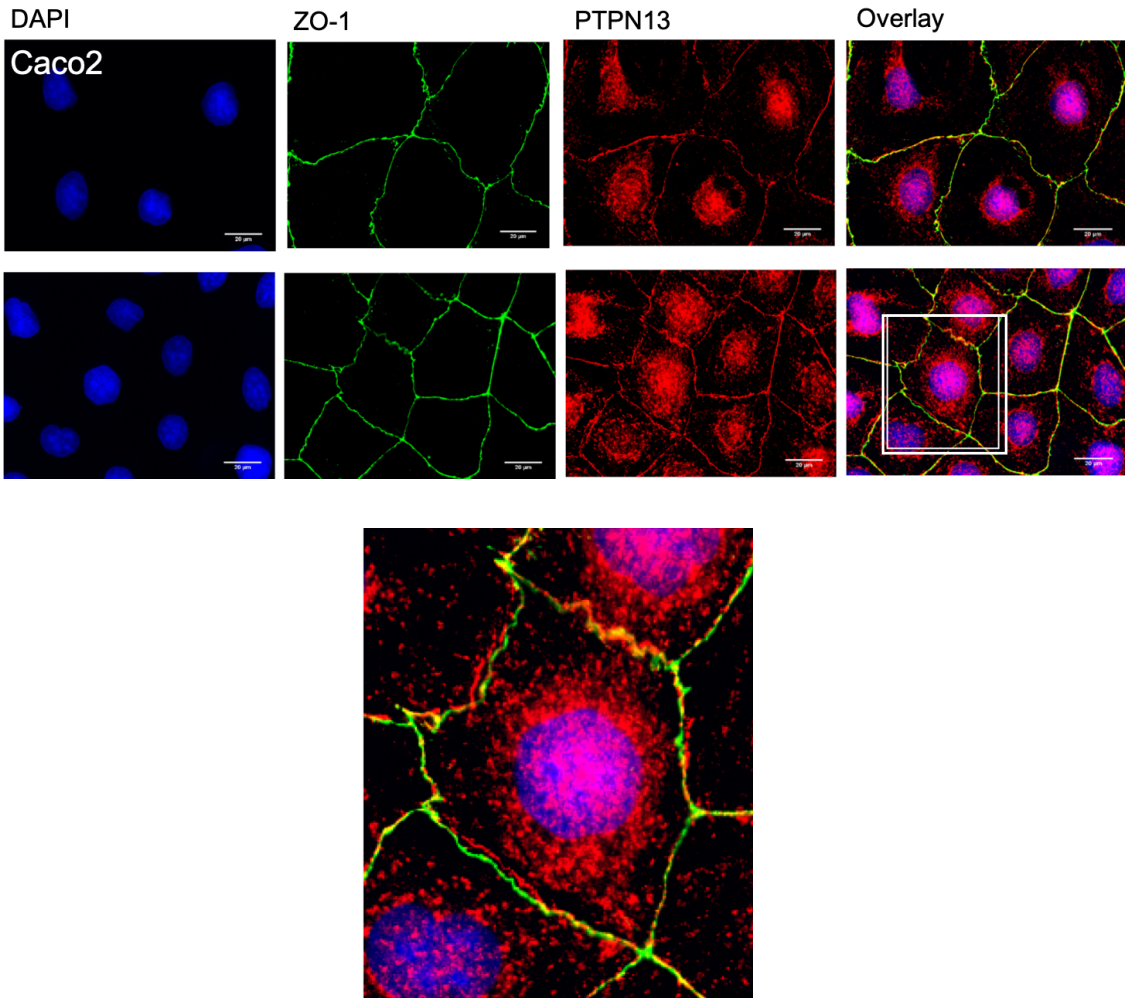

Figure 55: PTPN13 is in close proximity to the tight junctions. Epifluorescence microscopy images showing PTPN13 and ZO-1 staining in Caco2 cells. Images taken at 60x magnification show nuclei in blue (DAPI), ZO-1 in green and PTPN13 in red. Scale 20 μm *(experiments performed by Despoina Chrysostomou).*

3. PTPN13 subcellular localisation is affected by cell density

YAP, central effector of the Hippo pathway, shuttles from the nucleus to the cytoplasm in response to cell density. Previous literature and our data pointed to a potential involvement of PTPN13 and its interacting partner ENTR1 in the Hippo pathway. Therefore, we investigated whether PTPN13 might act similarly to YAP and respond to changes in cell density. First, as a basic tool for subcellular localisation studies, we validated a previously published[122] readout assay for YAP localisation based on immunofluorescence. We tested the assay in HEK293 (Figure 56 a) and Caco2 cells (Figure 56 b) and our results were in line with the expected YAP localisation at low and high density. When cells reach confluence, YAP is found excluded from the nucleus. Conversely, at low density, YAP is translocated to the nucleus.

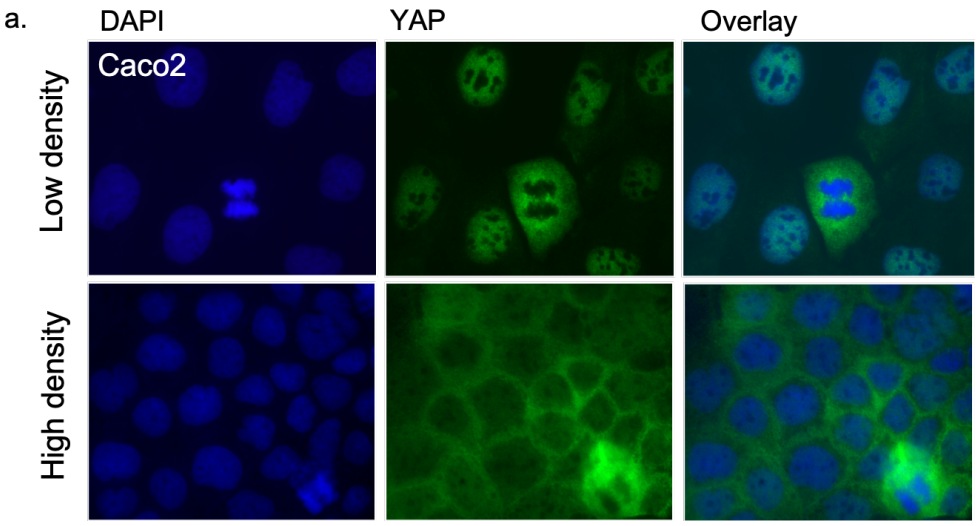

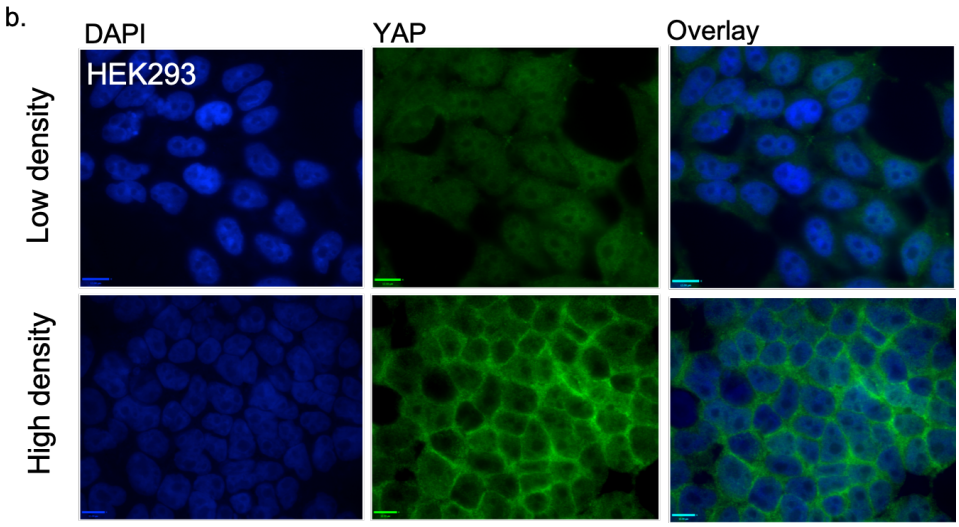

Figure 56. Validation of YAP localisation readout assay at different cell densities. Cell density immunofluorescence-based assay in Caco2 (a) and HEK293 cells (b). YAP is excluded from the nucleus at high density but exhibits nuclear pattern at low density. Olympus Epifluorescence microscopy images shows nuclei in blue (DAPI) and YAP in green (60X magnification). Scale bar 12 μm.

Interestingly, when we performed this assay with PTPN13 itself we found a similar cell density dependent-behaviour. Our data showed that PTPN13 localises in the nucleus at low cell density and is mainly cytoplasmic at high density in epithelial cells. The changes in PTPN13 subcellular localisation at different cell densities were confirmed in Caco2, DLD-1 and MCF-10A (Figure 57) but not in MDCKII, probably due to the lack of a suitable antibody for canine cells (Figure 58). Moreover, in Caco2 and DLD-1 cells PTPN13 is completely excluded from the nucleus at high density, resembling the behaviour of YAP. We were not able to find exclusion from the nucleus in confluent MCF-10A cells, although a predominantly cytoplasmic localisation is observed if compared with the nuclear PTPN13 distribution in cells at low density (Figure 57).

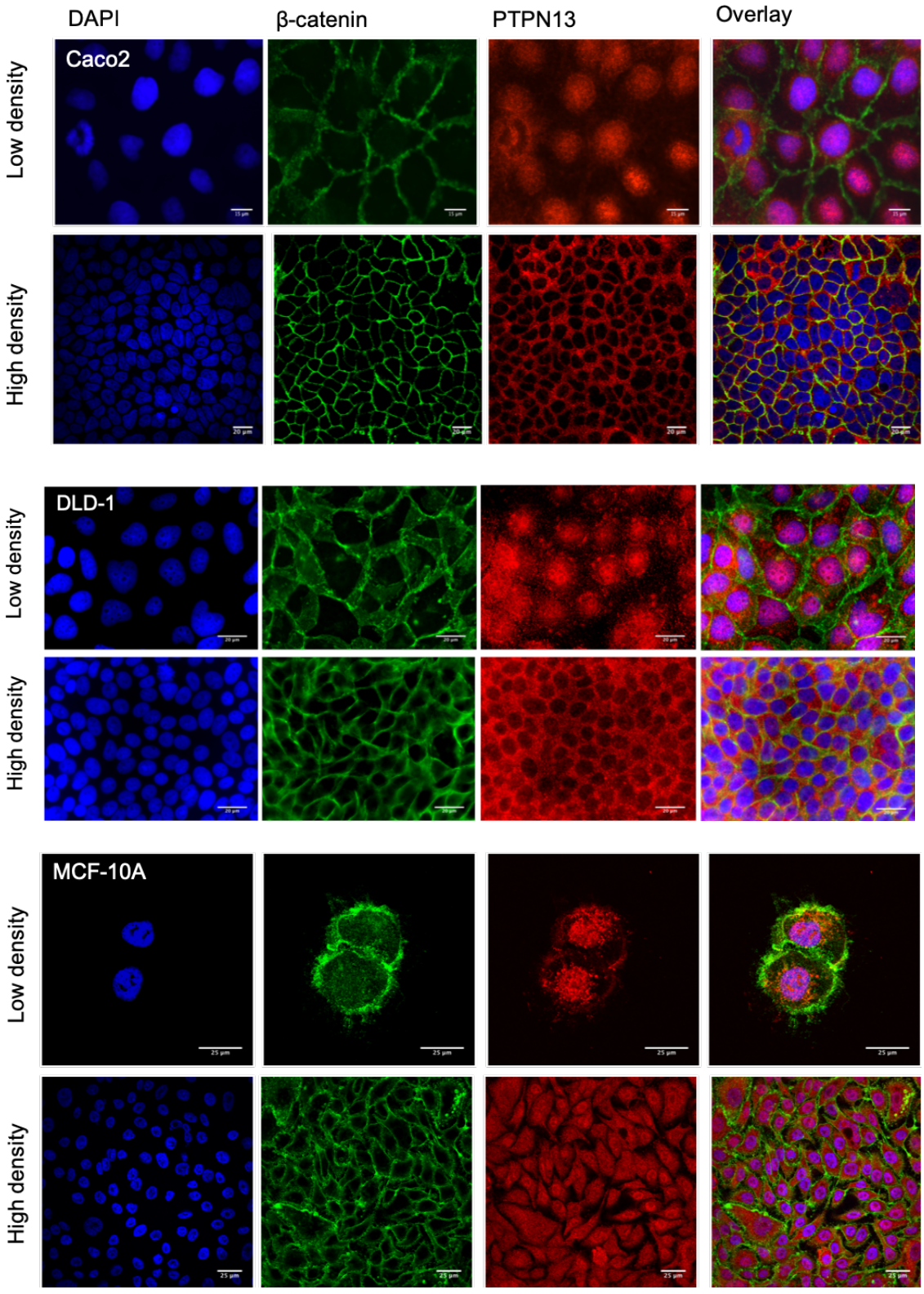

Figure 57. PTPN13 is predominantly localised in the nucleus at low density and is mostly cytoplasmic at high density in epithelial cells (a) Confocal pictures in Caco2 cells (b) Confocal pictures in DLD-1 cells. (c) Confocal pictures in MCF-10A cells. Confocal microscopy images show nuclei in blue (DAPI), β-catenin in green and PTPN13 in red (60X magnification).

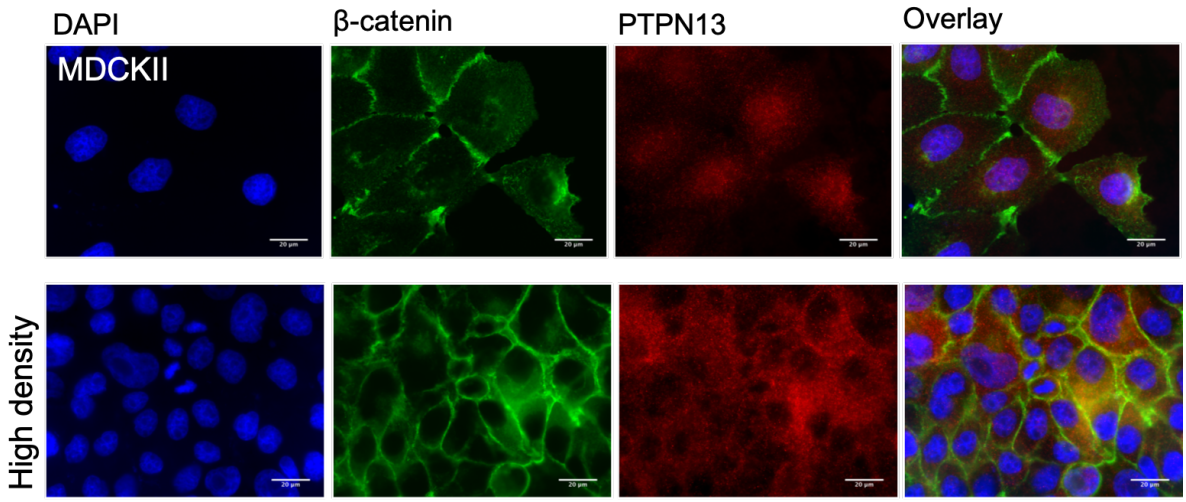

Figure 58. PTPN13 moderately respond to cell density in MDCKII cells. Localisation of PTPN13 within the nucleus at low density is clear. However, a rather diffused cytoplasmic and nuclear localisation is observed at high density. Epifluorescence microscopy images show nuclei in blue (DAPI), β-catenin in green and PTPN13 in red (60X magnification). Scale 20 μm

The nuclear localisation of PTPN13 was suggested by previous literature, but never properly validated. As the observed nuclear staining could be non-specific, further validation of the nuclear localisation of PTPN13 was carried out. First, we used a different PTPN13 antibody (provided by Santa Cruz) to validate the cell density-dependent changes in PTPN13 subcellular localisation in Caco2 cells (Figure 59 a). Again, PTPN13 was clearly excluded from the nucleus at high density, but mostly nuclear at low density.

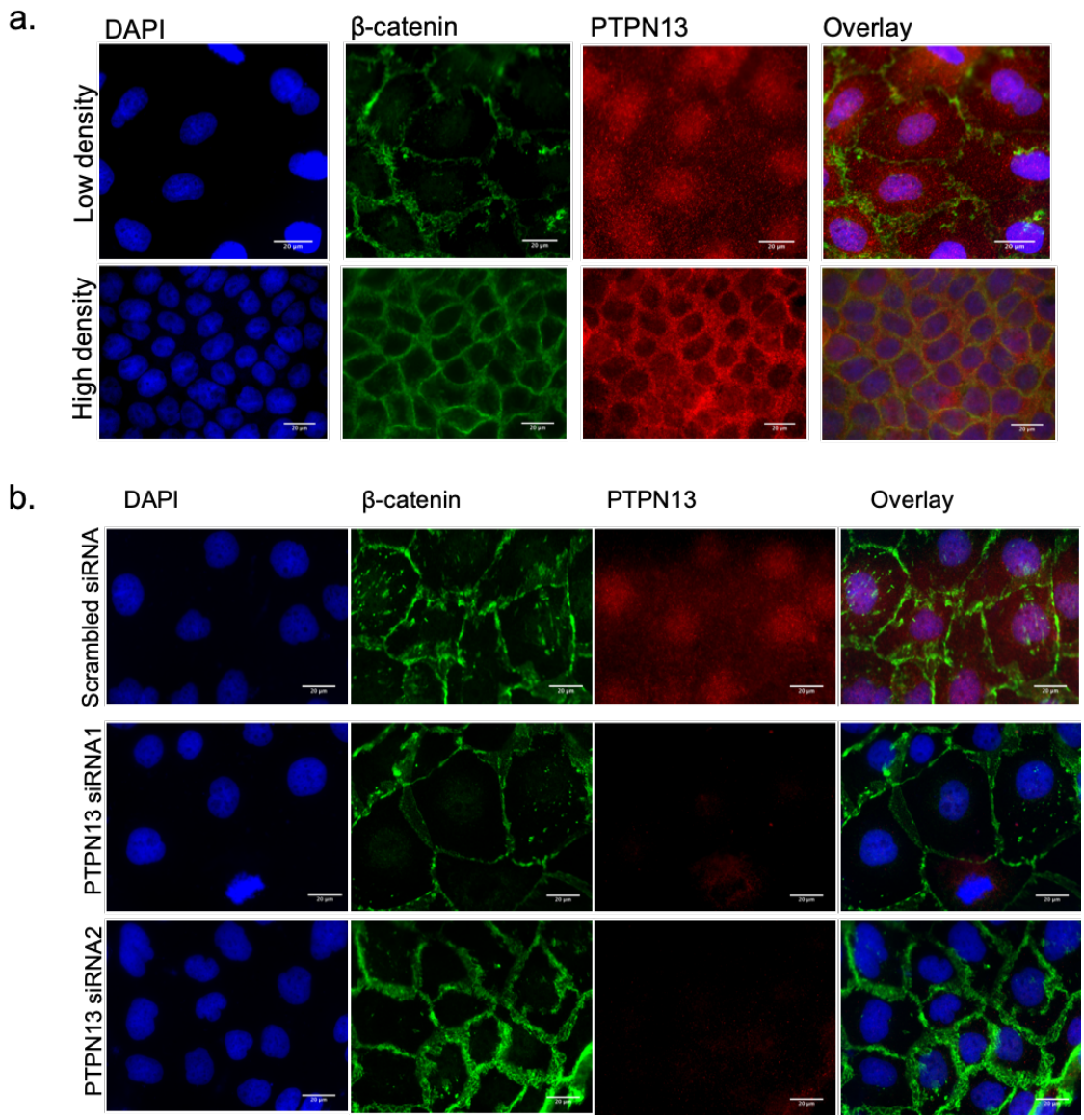

Figure 59. Validation of nuclear PTPN13 staining with an alternative PTPN13 antibody (Santa Cruz) in Caco2 cells. (a) PTPN13 localises to the nucleus at low density but is excluded from the nucleus and exhibits a cytoplasmic pattern at higher density **(b)** Validation of PTPN13 nuclear staining by siRNA knockdown with an alternative PTPN13 antibody (from Santa Cruz) in Caco2 cells. Epifluorescence microscope images taken at 60x magnification show nuclei in blue (DAPI), β-catenin in green and PTPN13 in red. Scale 20 μm

Second, we tested the specificity of the nuclear PTPN13 staining upon siRNA knockdown with two different PTPN13 antibodies. We transfected Caco2 cells with a pair of siRNAs specifically designed to knock down PTPN13 and

performed immunofluorescence (Figure 60 a and Figure 59 b). Caco2 cells transfected with PTPN13 siRNAs showed a substantial reduction of PTPN13 nuclear staining, indicating that the pair of antibodies are indeed specific for PTPN13 and are not recognizing other nuclear epitopes. We also validated the knock down efficiency of the siRNAs used in Caco2 cells by Western blotting (Figure 60 b).

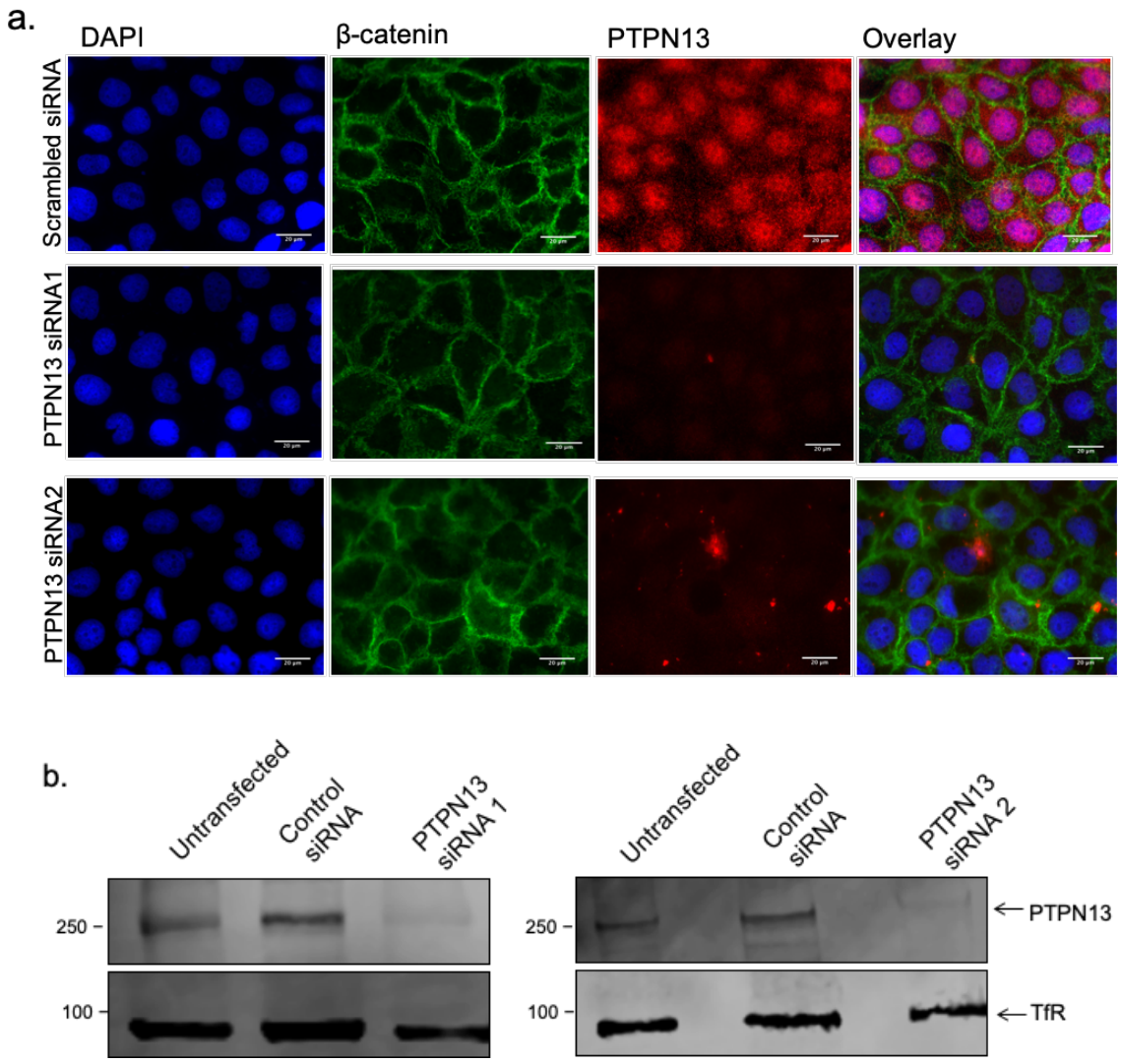

Figure 60. PTPN13 nuclear staining observed at low density is specific for the indicated Novus antibody (a) Validation of PTPN13 nuclear staining by siRNA knockdown with Novus PTPN13 antibody in Caco2 cells. Epifluorescence microscope images taken at 60x magnification

show nuclei in blue (DAPI), β-catenin in green and PTPN13 in red. Scale 20 μm (**b)** Validation of PTPN13 siRNA1 and siRNA2 in Caco2 cells by Western Blotting. Transferrin receptor used as a loading control due to high molecular weight of PTPN13.

4. Discussion

In the present thesis we describe a potential involvement of PTPN13 and ENTR1 with elements of the Hippo pathway, more specifically with LATS kinases. Moreover, we showed that PTPN13 subcellular localization is affected by cell density, in a similar fashion to YAP, central effector of the Hippo pathway. At a first glance, our data support the participation of PTPN13 in a pathway that regulates cell proliferation such as Hippo. However, it is attractive to hypothesize that PTPN13 and ENTR1 might be part of a novel pathway, parallel to the Hippo, that also takes advantage of the activity of LATS kinases.

Previous proteomic studies that hinted the interaction of PTPN13 with LATS kinases were only indicating that PTPN13 was in close proximity to LATS, not necessarily directly interacting. This proteomic study also identified ENTR1, a well-described interacting partner of PTPN13 as a potential candidate for the interaction. Our data indicated that ENTR1 is directly interacting with LATS2 (Figure 51), but not with full length PTPN13. We have only been able to identify a potential interaction of the FERM and PDZ domains of PTPN13 with LATS2 (Figure 52). This could be explained by PTPN13 interacting with LATS2 in two different sites simultaneously. Moreover, a positive interaction of LATS2 with the FERM domain of PTPN13 suggests that PTPN13 might be forming a complex with ENTR1

that interacts with LATS2. As ENTR1 also interacts with the FERM domain of PTPN13, the observed interaction could be an indication of the association of LATS2 with ENTR1 in the multiprotein complex.

As we observed in the regulation of Fas-mediated apoptosis, PTPN13 and ENTR1 could form a complex that interacts with LATS kinases. In this case, PTPN13 would indirectly interact with LATS via ENTR1, being ENTR1 the direct interacting partner with LATS kinases. Future work will focus on whether the complex acts dependently or independently from the Hippo pathway.

Little is known about the influence of endocytic trafficking in the Hippo pathway and how LATS kinases activity might be regulated by promoting, for instance, their endolysosomal degradation. Thus, it is appealing to speculate that given the identification of ENTR1 as a post-endocytic trafficking regulator, it could participate in the regulation of LATS trafficking, having a direct impact on its activity. This speculation opens a window for a novel field of investigation: the cross-talk between Hippo pathway and trafficking.

However, the precise subcellular localization where the interaction between ENTR1/PTPN13 and LATS kinases takes place is unknown. The localization of the complex in the cell adhesions is worth considering. Several Hippo pathway elements, including LATS kinases, interact with membrane-associated proteins (e.g. NF2) and proteins found in tight and adherens junctions, as well as in apical polarity complexes. The spatial regulation of LATS kinases is a

major regulator of the Hippo pathway[89, 200] and PTPN13/ENTR1 complex might participate in these processes through the association with LATS in the cell junctions.

Several studies suggested the presence of PTPN13 in the cell junctions[140,198, 201,199]. However, previous attempts of detecting membrane PTPN13 by immunofluorescence failed as paraformaldehyde fixation was preventing a proper visualization of PTPN13 in the plasma membrane. We have successfully identified PTPN13 in the plasma membrane (Figures 53-54) by immunofluorescence upon methanol fixation. It is likely that paraformaldehyde fixation was masking PTPN13 epitopes that allow its membrane visualization, but these are conserved upon methanol fixation. It will be interesting to design new experiments aiming the co-localization of PTPN13 with ENTR1 and LATS kinases within the cell junctions to support our idea that the complex is associating in the cell junctions.

An alternative role of PTPN13 in the tight junctions could be through PRK2. PRK2 is a well-established interacting partner of PTPN13 and participates in the formation and maturation of tight junctions in epithelial cells. Previous work in the Erdmann lab has shown that FRMPD2, a similar protein to PTPN13, recruits PRK2 to the cell-cell contacts. We hypothesize that PTPN13 could act redundantly to FRMPD2 and also recruit PRK2 to the tight junctions, regulating its formation and/or maturation. In fact, PRK2 and FRMPD2 knockdown had an effect in tight junction formation and maturation (unpublished data). Thus, it will be interesting

to investigate the effects that a PTPN13 knockdown and a double knockdown of PTPN13 and FRMPD2 might induce on tight junction formation and maturation.

A potential localization of PTPN13 within the nucleus would provide further evidence on the involvement of PTPN13 in cell proliferation, dependently or independently to the Hippo pathway. During decades, PTPN13 has been considered a cytoplasmic protein and only few papers suggested a nuclear localisation[140, 202]. Cuppen et al. showed that PTPN13 PDZ1 domain is able to interact with BRD7, a bromodomain-containing nuclear protein[202]. BRD7 is involved in PI3K signaling[203], transforming growth factor-β signaling pathway[204], chromatin remodelling and the regulation of p53 dependent replicative senescence[205], all of them functions that take place within the nucleus. Thus, there was some evidence pointing out to a nuclear localisation of PTPN13.

For instance, YAP, central effector of the Hippo pathway is localised in the nucleus at low cell density, where it regulates the transcription of genes that ultimately increase cell proliferation. In contrast, YAP is excluded from the nucleus and is retained in the cytoplasm at high density, stopping cell proliferation (Figure 56). Surprisingly, we found that PTPN13 has a similar behaviour and shuttles from the nucleus to the cytoplasm in response to an increase in cell density (Figure 57).

The description of PTPN13 localization in the nucleus together with the potential interaction of PTPN13/ENTR1 complex with LATS kinases open an

interesting line of research as these results suggest that PTPN13 might be an alternative effector parallel to the Hippo pathway that could control cell proliferation in response to external signals such as cell density.

Moreover, the fact that PTPN13 is shuttling from the nucleus to the cytoplasm in response to cell density might connect PTPN13 with mechanotransduction components which are responsible of sensing external cues. So far, we have described a potential response to cell density, but in a similar fashion to YAP, it is feasible that PTPN13 could also respond to extracellular matrix stiffness or cell polarity. Hence, future experiments will be focused on elucidating how PTPN13 responds to other mechanical cues. However, it is essential to determine first if the PTPN13 subcellular localisation is solely dependent on cell density or if the state of proliferation of the cell is also influential.

In summary, we suggest a model in which PTPN13 interacts with LATS kinases and either acts as an effector in an alternative pathway to Hippo or as a regulatory element in the Hippo pathway itself. First, we propose that PTPN13 and ENTR1 would localize to the cell junctions and associate with membrane-associated proteins involved in mechanotransduction. PTPN13 would then receive information about changes in cell density and maybe other mechanical cues. Next, LATS kinases would come into play and the interaction with PTPN13 via ENTR1 would have different outcomes:

- LATS kinases phosphorylate PTPN13 and regulate its localization, facilitating shuttling from the cytoplasm to the nucleus. Within the nucleus, PTPN13 could potentially modulate cell proliferation or cytoskeleton dynamics.
- PTPN13 might dephosphorylate LATS kinases and have an impact in the Hippo pathway and YAP regulation. It has been published that LATS kinases are also regulated by Src tyrosine phosphorylation[206]. Thus, it is reasonable to think that PTPN13 through dephosphorylation of LATS could be able to switch ON or OFF the Hippo pathway which will ultimately influence cell proliferation.

These options are not mutually exclusive and might be happening simultaneously. Hence, PTPN13 is a strong candidate to participate in the spatial regulation of LATS kinases through interaction with ENTR1 and have an effect on cell proliferation in a Hippo dependent or independent manner. However, our suggested model needs to be supported with further experimental data and requires extensive work.

As a matter of fact, there are alternative models that are also worth considering. One possibility is that PTPN13/ENTR1 complex is interacting with LATS kinases and carrying out a function which is not dependent on the Hippo signalling. LATS is actually known to also be involved in mitotic progression[207], cytokinesis[208] and in the control of p53 expression[209]. It is reasonable to think that PTPN13/ENTR1 might participate in these processes in association with LATS2. Particularly, both PTPN13 and ENTR1 regulate cytokinesis[130], so there is indeed a

functional connection between LATS and the ENTR1/PTPN13 complex which is independent to the Hippo signalling.

Another possible model would argue that PTPN13 is translocated to the nucleus under certain conditions and interact with cell proliferation regulators not involved in the Hippo signalling. Interestingly, PTPN13 is a well-established interacting partner of BRD7, a nuclear bromodomain-containing protein[202]. So far, no evidence of the function of the PTPN13 and BRD7 complex has been found. BRD7 is a transcription co-factor of p53-dependent genes that activates the oncogenic-induced senescence via interaction with p53 and p300[205]. Thus, PTPN13 could interact with BRD7 within the nucleus and modulate the transcription of p53-dependent genes, having an effect in cell proliferation.

Investigating the role of PTPN13 in cell proliferation and its implications in tumour development will provide a better insight into the potential role of PTPN13 as a tumour suppressor or promoter. Expanding the investigation on the involvement of PTPN13 within the Hippo pathway and further characterizing PTPN13 as a Hippo-independent regulator of cell proliferation will provide a more detailed understanding of the molecular mechanisms of tumour progression. This valuable knowledge might allow a better evaluation of suitable targets and biomarkers in the fight against cancer disease.

6. Appendix 1: Supplementary figures

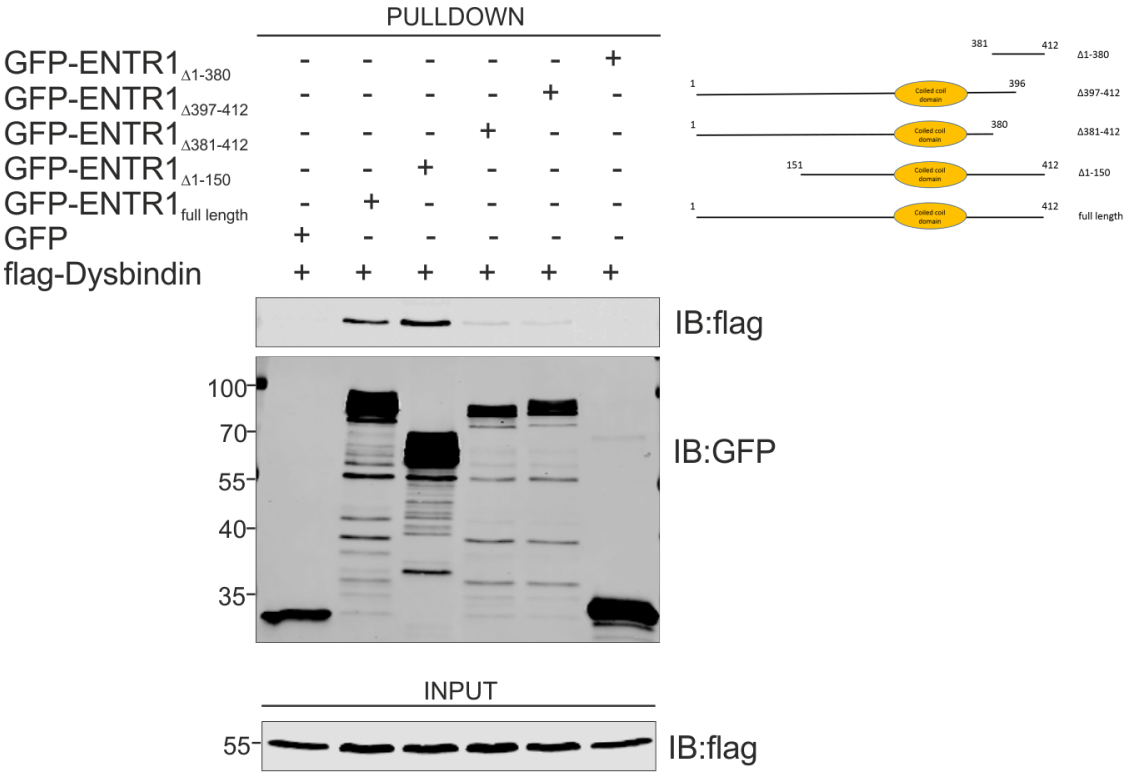

Supplementary Figure 1. ENTR1 mapping of dysbindin's interaction site. HEK293 cells were transiently transfected with the indicated GFP-ENTR1 wild-type or deletion expression constructs tagged with FLAG. After 48h cell lysates were subjected to GFP-Trap®_A pulldown. Bound proteins were detected via western blotting with anti-flag and anti-GFP antibody. E*xperiment performed by Agnieszka Skowronek*.

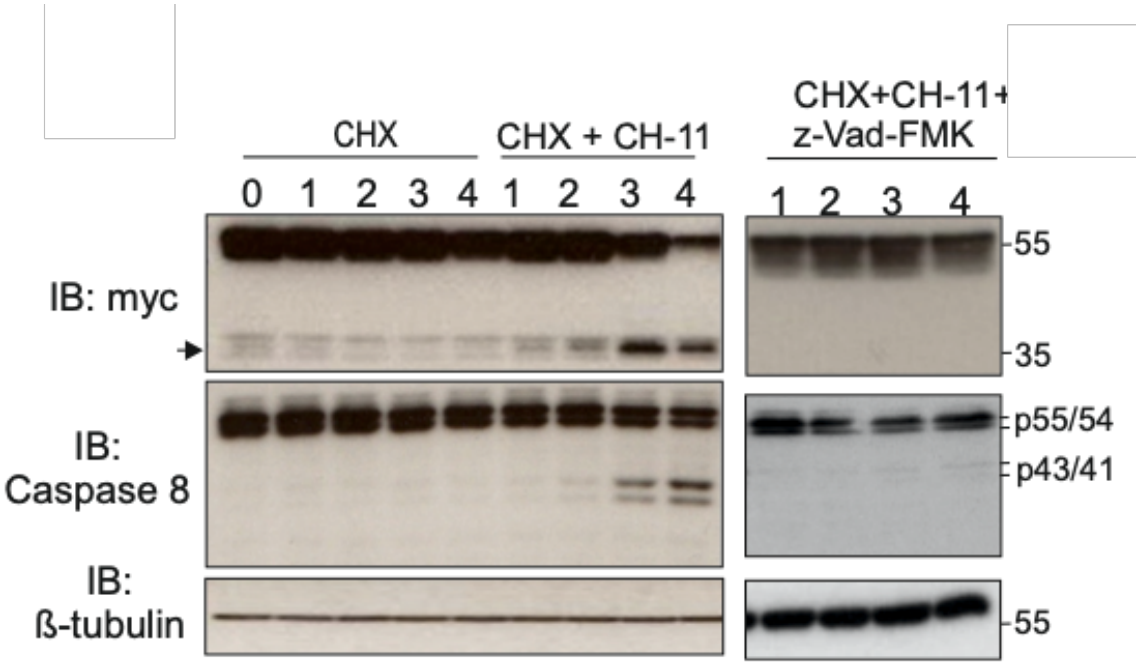

Supplementary Figure 2. ENTR1 is cleaved during Fas induced apoptosis. Overexpressed myc-ENTR1 (55kDa) is cleaved upon activation of Fas mediated apoptotic signaling to a produce a 35-40 kDa band after 3 hours of treatment (indicated by an arrow) with anti-Fas (CH-11) and cycloheximide in HeLa cells. Cleavage of Caspase 8 (p18) was also observed only upon activation with anti-Fas (CH-11). Myc-ENTR1 was not cleaved upon activation by cycloheximide only or in the presence of pan-caspase inhibitor (z-vad-FMK). *Experiment performed by Fangyan Yu.*

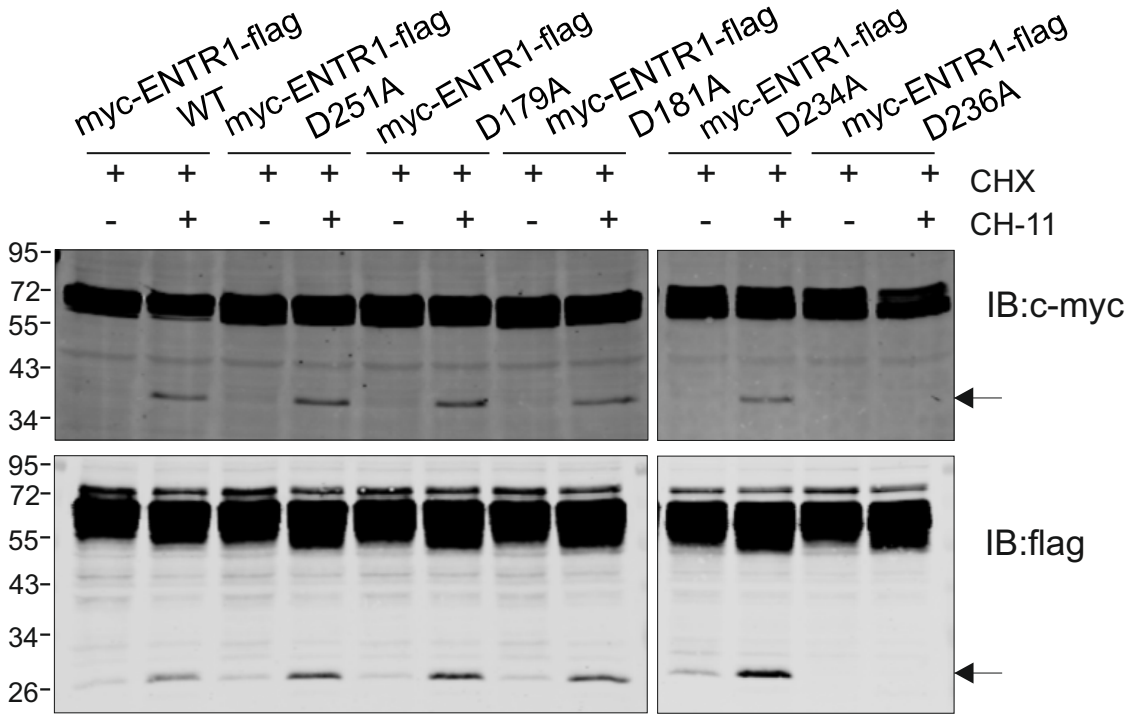

Supplementary Figure 3. Mapping of ENTR1 caspase cleavage site in HeLa cells. ENTR1 is cleaved by caspase at position aa236 (isoform1) into two fragments (indicated by arrows). Myc- and flag-tagged ENTR1 mutants D179A, D181A, D234A and D236A were created by site-directed mutagenesis using D251A mutant as a template. *Experiment performed by Agnieszka Skowronek.*

7. Appendix 2: Abbreviations

BLOC-1: biogenesis of lysosome-related organelle complex-1

CCV: clathrin-coated vesicles

CHX: cycloheximide

CME: clathrin mediated endocytosis

DAB: 3,3'-diaminobenzidine

DAPI: 4',6-diamidino-2-phenylindole

DISC: death-inducing signaling complex

DMEM: Dulbecco's Modified Eagle Medium

DN: dominant negative

DR: death receptor

ECM: extra cellular matrix

EE: early endosomes

EEA1: early endosome antigen 1

ENTR1: endosomal associated trafficking regulator 1

ER: endoplasmic reticulum

ERC: endocytic recycling compartment

ESCRT: endosomal sorting complexes required for transport

FACS: fluorescence-activated cell sorter

FADD: Fas associated death domain protein

FC: flow cytometry

FERM: 4.1 protein, ezrin, radixin, moesin

FW: forward

g: grams

GFP: green fluorescent protein

gRNA: guide RNA

GST: glutathione S-transferase

HRS: hepatocyte growth factor-regulated tyrosine kinase substrate

IF: immunofluorescence

IHC: immunohistochemistry

ILV: intra-luminal vesicles

ko: knock-out

l: litres

LAMP1: lysosomal associated membrane protein 1

LATS: large tumour suppressor

LB: Luria-Bertani broth

LE: late endosomes

m: metres

MOMP: mitochondrial outer membrane permeabilization

MVB: multi-vesicular body

PAM: protospacer adjacent motif

PBS: phosphate-buffered saline

PCR: polymerase chain reaction

PDZ: post synaptic density protein (PSD95), Drosophila disc large tumour suppressor (Dlg1) and zonula occludens-1 protein (ZO-1)

PM: plasma membrane

PTM: post translational modifications

PTPBL: protein tyrosine phosphatase basophil-like

PTPN13: protein tyrosine phosphatase non-receptor type 13

RV: reverse

SDS-PAGE: sodium dodecyl sulfate polyacrylamide gel electrophoresis

SEM: standard error of the mean

sFasL: soluble Fas ligand

siRNA: silencing RNA

SNXs: sorting nexins

TAZ: transcriptional coactivator with PDZ-binding motif

TEN: tubular endosomal network

TGN: trans Golgi network

TMA: tissue microarray

WB: Western blotting

wt: wild-type

YAP: yes-associated protein

8. Bibliography

1. Elmore, S. Apoptosis: a review of programmed cell death. *Toxicol Pathol* **35**, 495-516 (2007).
2. Norbury, C.J. & Hickson, I.D. Cellular responses to DNA damage. *Annu Rev Pharmacol Toxicol* **41**, 367-401 (2001).
3. Kerr, J.F., Wyllie, A.H. & Currie, A.R. Apoptosis: a basic biological phenomenon with wide-ranging implications in tissue kinetics. *Br J Cancer* **26**, 239-257 (1972).
4. Strasser, A., Jost, P.J. & Nagata, S. The many roles of FAS receptor signaling in the immune system. *Immunity* **30**, 180-192 (2009).
5. Krammer, P.H. CD95's deadly mission in the immune system. *Nature* **407**, 789-795 (2000).
6. Barnhart, B.C., Alappat, E.C. & Peter, M.E. The CD95 type I/type II model. *Semin Immunol* **15**, 185-193 (2003).
7. Peter, M.E. & Krammer, P.H. The CD95(APO-1/Fas) DISC and beyond. *Cell Death Differ* **10**, 26-35 (2003).
8. Chipuk, J.E. & Green, D.R. Dissecting p53-dependent apoptosis. *Cell Death Differ* **13**, 994-1002 (2006).
9. Nagata, S. Apoptosis by death factor. *Cell* **88**, 355-365 (1997).
10. Bodmer, J.L., Schneider, P. & Tschopp, J. The molecular architecture of the TNF superfamily. *Trends Biochem Sci* **27**, 19-26 (2002).
11. Ware, C.F. The TNF superfamily. *Cytokine Growth Factor Rev* **14**, 181-184 (2003).
12. Ashkenazi, A. & Dixit, V.M. Death receptors: signaling and modulation. *Science* **281**, 1305-1308 (1998).
13. Schneider-Brachert, W., Heigl, U. & Ehrenschwender, M. Membrane trafficking of death receptors: implications on signalling. *Int J Mol Sci* **14**, 14475-14503 (2013).
14. Li, J. & Yuan, J. Caspases in apoptosis and beyond. *Oncogene* **27**, 6194-6206 (2008).
15. Hirata, H. *et al.* Caspases are activated in a branched protease cascade and control distinct downstream processes in Fas-induced apoptosis. *J Exp Med* **187**, 587-600 (1998).
16. Lakhani, S.A. *et al.* Caspases 3 and 7: key mediators of mitochondrial events of apoptosis. *Science* **311**, 847-851 (2006).
17. Slee, E.A., Adrain, C. & Martin, S.J. Executioner caspase-3, -6, and -7 perform distinct, non-redundant roles during the demolition phase of apoptosis. *J Biol Chem* **276**, 7320-7326 (2001).
18. Sadowski-Debbing, K., Coy, J.F., Mier, W., Hug, H. & Los, M. Caspases--their role in apoptosis and other physiological processes as revealed by knock-out studies. *Arch Immunol Ther Exp (Warsz)* **50**, 19-34 (2002).
19. Itoh, N. *et al.* The polypeptide encoded by the cDNA for human cell surface antigen Fas can mediate apoptosis. *Cell* **66**, 233-243 (1991).
20. Cheng, J., Liu, C., Koopman, W.J. & Mountz, J.D. Characterization of human Fas gene. Exon/intron organization and promoter region. *J Immunol* **154**, 1239-1245 (1995).
21. Huang, B., Eberstadt, M., Olejniczak, E.T., Meadows, R.P. & Fesik, S.W. NMR structure and mutagenesis of the Fas (APO-1/CD95) death domain. *Nature* **384**, 638-641 (1996).

22. Starling, G.C. *et al.* Identification of amino acid residues important for ligand binding to Fas. *J Exp Med* **185**, 1487-1492 (1997).
23. Edmond, V. *et al.* Precise mapping of the CD95 pre-ligand assembly domain. *PLoS One* **7**, e46236 (2012).
24. Itoh, N. & Nagata, S. A novel protein domain required for apoptosis. Mutational analysis of human Fas antigen. *J Biol Chem* **268**, 10932-10937 (1993).
25. Kamitani, T., Nguyen, H.P. & Yeh, E.T. Activation-induced aggregation and processing of the human Fas antigen. Detection with cytoplasmic domain-specific antibodies. *J Biol Chem* **272**, 22307-22314 (1997).
26. Schütze, S., Tchikov, V. & Schneider-Brachert, W. Regulation of TNFR1 and CD95 signalling by receptor compartmentalization. *Nat Rev Mol Cell Biol* **9**, 655-662 (2008).
27. Fu, Q. *et al.* Structural Basis and Functional Role of Intramembrane Trimerization of the Fas/CD95 Death Receptor. *Mol Cell* **61**, 602-613 (2016).
28. Peter, M.E. *et al.* The CD95 receptor: apoptosis revisited. *Cell* **129**, 447-450 (2007).
29. Chinnaiyan, A.M., O'Rourke, K., Tewari, M. & Dixit, V.M. FADD, a novel death domain-containing protein, interacts with the death domain of Fas and initiates apoptosis. *Cell* **81**, 505-512 (1995).
30. Scaffidi, C. *et al.* Two CD95 (APO-1/Fas) signaling pathways. *EMBO J* **17**, 1675-1687 (1998).
31. Lee, K.H. *et al.* The role of receptor internalization in CD95 signaling. *EMBO J* **25**, 1009-1023 (2006).
32. Donepudi, M., Mac Sweeney, A., Briand, C. & Grütter, M.G. Insights into the regulatory mechanism for caspase-8 activation. *Mol Cell* **11**, 543-549 (2003).
33. Chang, D.W., Xing, Z., Capacio, V.L., Peter, M.E. & Yang, X. Interdimer processing mechanism of procaspase-8 activation. *EMBO J* **22**, 4132-4142 (2003).
34. Martin, D.A., Siegel, R.M., Zheng, L. & Lenardo, M.J. Membrane oligomerization and cleavage activates the caspase-8 (FLICE/MACHalpha1) death signal. *J Biol Chem* **273**, 4345-4349 (1998).
35. Chang, D.W. *et al.* c-FLIP(L) is a dual function regulator for caspase-8 activation and CD95-mediated apoptosis. *EMBO J* **21**, 3704-3714 (2002).
36. Zhao, Y. *et al.* Promotion of Fas-mediated apoptosis in Type II cells by high doses of hepatocyte growth factor bypasses the mitochondrial requirement. *J Cell Physiol* **213**, 556-563 (2007).
37. Würstle, M.L., Laussmann, M.A. & Rehm, M. The central role of initiator caspase-9 in apoptosis signal transduction and the regulation of its activation and activity on the apoptosome. *Exp Cell Res* **318**, 1213-1220 (2012).
38. Vaux, D.L. & Silke, J. Mammalian mitochondrial IAP binding proteins. *Biochem Biophys Res Commun* **304**, 499-504 (2003).
39. Sun, X.M., Bratton, S.B., Butterworth, M., MacFarlane, M. & Cohen, G.M. Bcl-2 and Bcl-xL inhibit CD95-mediated apoptosis by preventing mitochondrial release of Smac/DIABLO and subsequent inactivation of X-linked inhibitor-of-apoptosis protein. *J Biol Chem* **277**, 11345-11351 (2002).
40. Takahashi, T. *et al.* Human Fas ligand: gene structure, chromosomal location and species specificity. *Int Immunol* **6**, 1567-1574 (1994).
41. Janssen, O., Qian, J., Linkermann, A. & Kabelitz, D. CD95 ligand--death factor and costimulatory molecule? *Cell Death Differ* **10**, 1215-1225 (2003).

42. Blott, E.J., Bossi, G., Clark, R., Zvelebil, M. & Griffiths, G.M. Fas ligand is targeted to secretory lysosomes via a proline-rich domain in its cytoplasmic tail. *J Cell Sci* **114**, 2405-2416 (2001).
43. Schneider, P. *et al.* Conversion of membrane-bound Fas(CD95) ligand to its soluble form is associated with downregulation of its proapoptotic activity and loss of liver toxicity. *J Exp Med* **187**, 1205-1213 (1998).
44. Ehrenschwender, M. & Wajant, H. The role of FasL and Fas in health and disease. *Adv Exp Med Biol* **647**, 64-93 (2009).
45. Desbarats, J. & Newell, M.K. Fas engagement accelerates liver regeneration after partial hepatectomy. *Nat Med* **6**, 920-923 (2000).
46. Jarad, G. *et al.* Fas activation induces renal tubular epithelial cell beta 8 integrin expression and function in the absence of apoptosis. *J Biol Chem* **277**, 47826-47833 (2002).
47. Reinehr, R., Sommerfeld, A. & Häussinger, D. CD95 ligand is a proliferative and antiapoptotic signal in quiescent hepatic stellate cells. *Gastroenterology* **134**, 1494-1506 (2008).
48. Desbarats, J. *et al.* Fas engagement induces neurite growth through ERK activation and p35 upregulation. *Nat Cell Biol* **5**, 118-125 (2003).
49. Cohen, P.L. & Eisenberg, R.A. Lpr and gld: single gene models of systemic autoimmunity and lymphoproliferative disease. *Annu Rev Immunol* **9**, 243-269 (1991).
50. Watanabe-Fukunaga, R., Brannan, C.I., Copeland, N.G., Jenkins, N.A. & Nagata, S. Lymphoproliferation disorder in mice explained by defects in Fas antigen that mediates apoptosis. *Nature* **356**, 314-317 (1992).
51. Peter, M.E. *et al.* The role of CD95 and CD95 ligand in cancer. *Cell Death Differ* **22**, 885-886 (2015).
52. Algeciras-Schimnich, A. *et al.* Two CD95 tumor classes with different sensitivities to antitumor drugs. *Proc Natl Acad Sci U S A* **100**, 11445-11450 (2003).
53. Fulda, S. *et al.* Sensitization for death receptor- or drug-induced apoptosis by re-expression of caspase-8 through demethylation or gene transfer. *Oncogene* **20**, 5865-5877 (2001).
54. Tourneur, L. *et al.* Loss of FADD protein expression results in a biased Fas-signaling pathway and correlates with the development of tumoral status in thyroid follicular cells. *Oncogene* **22**, 2795-2804 (2003).
55. Igney, F.H. & Krammer, P.H. Death and anti-death: tumour resistance to apoptosis. *Nat Rev Cancer* **2**, 277-288 (2002).
56. Ivanov, V.N., Ronai, Z. & Hei, T.K. Opposite roles of FAP-1 and dynamin in the regulation of Fas (CD95) translocation to the cell surface and susceptibility to Fas ligand-mediated apoptosis. *J Biol Chem* **281**, 1840-1852 (2006).
57. Ivanov, V.N. *et al.* FAP-1 association with Fas (Apo-1) inhibits Fas expression on the cell surface. *Mol Cell Biol* **23**, 3623-3635 (2003).
58. Barnhart, B.C. *et al.* CD95 ligand induces motility and invasiveness of apoptosis-resistant tumor cells. *EMBO J* **23**, 3175-3185 (2004).
59. Lee, J.K., Sayers, T.J., Back, T.C., Wigginton, J.M. & Wiltrout, R.H. Lack of FasL-mediated killing leads to in vivo tumor promotion in mouse Lewis lung cancer. *Apoptosis* **8**, 151-160 (2003).
60. Zhang, Y. *et al.* Fas signal promotes lung cancer growth by recruiting myeloid-derived suppressor cells via cancer cell-derived PGE2. *J Immunol* **182**, 3801-3808 (2009).

61. Hoogwater, F.J. *et al.* Oncogenic K-Ras turns death receptors into metastasis-promoting receptors in human and mouse colorectal cancer cells. *Gastroenterology* **138**, 2357-2367 (2010).
62. Ogasawara, J. *et al.* Lethal effect of the anti-Fas antibody in mice. *Nature* **364**, 806-809 (1993).
63. Ceppi, P. *et al.* CD95 and CD95L promote and protect cancer stem cells. *Nat Commun* **5**, 5238 (2014).
64. Hadji, A. *et al.* Death induced by CD95 or CD95 ligand elimination. *Cell Rep* **7**, 208-222 (2014).
65. Peter, M.E. DICE: A novel tumor surveillance mechanism-a new therapy for cancer? *Cell Cycle* **13**, 1373-1378 (2014).
66. Kaufmann, S.H. & Earnshaw, W.C. Induction of apoptosis by cancer chemotherapy. *Exp Cell Res* **256**, 42-49 (2000).
67. Ametller, E. *et al.* Tumor promoting effects of CD95 signaling in chemoresistant cells. *Mol Cancer* **9**, 161 (2010).
68. Gruenberg, J. The endocytic pathway: a mosaic of domains. *Nat Rev Mol Cell Biol* **2**, 721-730 (2001).
69. Grant, B.D. & Donaldson, J.G. Pathways and mechanisms of endocytic recycling. *Nat Rev Mol Cell Biol* **10**, 597-608 (2009).
70. Maxfield, F.R. Role of endosomes and lysosomes in human disease. *Cold Spring Harb Perspect Biol* **6**, a016931 (2014).
71. McMahon, H.T. & Boucrot, E. Molecular mechanism and physiological functions of clathrin-mediated endocytosis. *Nat Rev Mol Cell Biol* **12**, 517-533 (2011).
72. Algeciras-Schimnich, A. *et al.* Molecular ordering of the initial signaling events of CD95. *Mol Cell Biol* **22**, 207-220 (2002).
73. Vitetta, E.S. & Uhr, J.W. Monoclonal antibodies as agonists: an expanded role for their use in cancer therapy. *Cancer Res* **54**, 5301-5309 (1994).
74. Feig, C., Tchikov, V., Schütze, S. & Peter, M.E. Palmitoylation of CD95 facilitates formation of SDS-stable receptor aggregates that initiate apoptosis signaling. *EMBO J* **26**, 221-231 (2007).
75. Chakrabandhu, K. *et al.* The extracellular glycosphingolipid-binding motif of Fas defines its internalization route, mode and outcome of signals upon activation by ligand. *Cell Death Differ* **15**, 1824-1837 (2008).
76. Gruenberg, J., Griffiths, G. & Howell, K.E. Characterization of the early endosome and putative endocytic carrier vesicles in vivo and with an assay of vesicle fusion in vitro. *J Cell Biol* **108**, 1301-1316 (1989).
77. Jovic, M., Sharma, M., Rahajeng, J. & Caplan, S. The early endosome: a busy sorting station for proteins at the crossroads. *Histol Histopathol* **25**, 99-112 (2010).
78. Maxfield, F.R. & McGraw, T.E. Endocytic recycling. *Nat Rev Mol Cell Biol* **5**, 121-132 (2004).
79. Sönnichsen, B., De Renzis, S., Nielsen, E., Rietdorf, J. & Zerial, M. Distinct membrane domains on endosomes in the recycling pathway visualized by multicolor imaging of Rab4, Rab5, and Rab11. *J Cell Biol* **149**, 901-914 (2000).
80. Traer, C.J. *et al.* SNX4 coordinates endosomal sorting of TfnR with dynein-mediated transport into the endocytic recycling compartment. *Nat Cell Biol* **9**, 1370-1380 (2007).
81. Cendrowski, J., Mamińska, A. & Miaczynska, M. Endocytic regulation of cytokine receptor signaling. *Cytokine Growth Factor Rev* **32**, 63-73 (2016).

82. Bonifacino, J.S. & Traub, L.M. Signals for sorting of transmembrane proteins to endosomes and lysosomes. *Annu Rev Biochem* **72**, 395-447 (2003).
83. Haglund, K. & Dikic, I. The role of ubiquitylation in receptor endocytosis and endosomal sorting. *J Cell Sci* **125**, 265-275 (2012).
84. Raiborg, C. & Stenmark, H. The ESCRT machinery in endosomal sorting of ubiquitylated membrane proteins. *Nature* **458**, 445-452 (2009).
85. Hanson, P.I. & Cashikar, A. Multivesicular body morphogenesis. *Annu Rev Cell Dev Biol* **28**, 337-362 (2012).
86. Schmidt, O. & Teis, D. The ESCRT machinery. *Curr Biol* **22**, R116-120 (2012).
87. Hurley, J.H. The ESCRT complexes. *Crit Rev Biochem Mol Biol* **45**, 463-487 (2010).
88. Henne, W.M., Buchkovich, N.J. & Emr, S.D. The ESCRT pathway. *Dev Cell* **21**, 77-91 (2011).
89. Piccolo, S., Dupont, S. & Cordenonsi, M. The biology of YAP/TAZ: hippo signaling and beyond. *Physiol Rev* **94**, 1287-1312 (2014).
90. Xu, T., Wang, W., Zhang, S., Stewart, R.A. & Yu, W. Identifying tumor suppressors in genetic mosaics: the Drosophila lats gene encodes a putative protein kinase. *Development* **121**, 1053-1063 (1995).
91. Huang, J., Wu, S., Barrera, J., Matthews, K. & Pan, D. The Hippo signaling pathway coordinately regulates cell proliferation and apoptosis by inactivating Yorkie, the Drosophila Homolog of YAP. *Cell* **122**, 421-434 (2005).
92. Halder, G., Dupont, S. & Piccolo, S. Transduction of mechanical and cytoskeletal cues by YAP and TAZ. *Nat Rev Mol Cell Biol* **13**, 591-600 (2012).
93. Wilson, K.E. *et al.* PTPN14 forms a complex with Kibra and LATS1 proteins and negatively regulates the YAP oncogenic function. *J Biol Chem* **289**, 23693-23700 (2014).
94. Dupont, S. *et al.* Role of YAP/TAZ in mechanotransduction. *Nature* **474**, 179-183 (2011).
95. Azzolin, L. *et al.* YAP/TAZ incorporation in the β-catenin destruction complex orchestrates the Wnt response. *Cell* **158**, 157-170 (2014).
96. Varelas, X. *et al.* The Hippo pathway regulates Wnt/beta-catenin signaling. *Dev Cell* **18**, 579-591 (2010).
97. Konsavage, W.M., Kyler, S.L., Rennoll, S.A., Jin, G. & Yochum, G.S. Wnt/β-catenin signaling regulates Yes-associated protein (YAP) gene expression in colorectal carcinoma cells. *J Biol Chem* **287**, 11730-11739 (2012).
98. Li, Y., Hibbs, M.A., Gard, A.L., Shylo, N.A. & Yun, K. Genome-wide analysis of N1ICD/RBPJ targets in vivo reveals direct transcriptional regulation of Wnt, SHH, and hippo pathway effectors by Notch1. *Stem Cells* **30**, 741-752 (2012).
99. Hiemer, S.E., Szymaniak, A.D. & Varelas, X. The transcriptional regulators TAZ and YAP direct transforming growth factor β-induced tumorigenic phenotypes in breast cancer cells. *J Biol Chem* **289**, 13461-13474 (2014).
100. Yu, F.X. *et al.* Regulation of the Hippo-YAP pathway by G-protein-coupled receptor signaling. *Cell* **150**, 780-791 (2012).
101. Mo, J.S., Yu, F.X., Gong, R., Brown, J.H. & Guan, K.L. Regulation of the Hippo-YAP pathway by protease-activated receptors (PARs). *Genes Dev* **26**, 2138-2143 (2012).
102. Sorrentino, G. *et al.* Metabolic control of YAP and TAZ by the mevalonate pathway. *Nat Cell Biol* **16**, 357-366 (2014).
103. Wang, Z. *et al.* Interplay of mevalonate and Hippo pathways regulates RHAMM transcription via YAP to modulate breast cancer cell motility. *Proc Natl Acad Sci U S A* **111**, E89-98 (2014).

104. Sudol, M. Yes-associated protein (YAP65) is a proline-rich phosphoprotein that binds to the SH3 domain of the Yes proto-oncogene product. *Oncogene* **9**, 2145-2152 (1994).
105. Bork, P. & Sudol, M. The WW domain: a signalling site in dystrophin? *Trends Biochem Sci* **19**, 531-533 (1994).
106. André, B. & Springael, J.Y. WWP, a new amino acid motif present in single or multiple copies in various proteins including dystrophin and the SH3-binding Yes-associated protein YAP65. *Biochem Biophys Res Commun* **205**, 1201-1205 (1994).
107. Vassilev, A., Kaneko, K.J., Shu, H., Zhao, Y. & DePamphilis, M.L. TEAD/TEF transcription factors utilize the activation domain of YAP65, a Src/Yes-associated protein localized in the cytoplasm. *Genes Dev* **15**, 1229-1241 (2001).
108. Ren, R., Mayer, B.J., Cicchetti, P. & Baltimore, D. Identification of a ten-amino acid proline-rich SH3 binding site. *Science* **259**, 1157-1161 (1993).
109. Wang, S., Raab, R.W., Schatz, P.J., Guggino, W.B. & Li, M. Peptide binding consensus of the NHE-RF-PDZ1 domain matches the C-terminal sequence of cystic fibrosis transmembrane conductance regulator (CFTR). *FEBS Lett* **427**, 103-108 (1998).
110. Basu, S., Totty, N.F., Irwin, M.S., Sudol, M. & Downward, J. Akt phosphorylates the Yes-associated protein, YAP, to induce interaction with 14-3-3 and attenuation of p73-mediated apoptosis. *Mol Cell* **11**, 11-23 (2003).
111. Dong, J. *et al.* Elucidation of a universal size-control mechanism in Drosophila and mammals. *Cell* **130**, 1120-1133 (2007).
112. Danovi, S.A. *et al.* Yes-associated protein (YAP) is a critical mediator of c-Jun-dependent apoptosis. *Cell Death Differ* **15**, 217-219 (2008).
113. Levy, D., Adamovich, Y., Reuven, N. & Shaul, Y. Yap1 phosphorylation by c-Abl is a critical step in selective activation of proapoptotic genes in response to DNA damage. *Mol Cell* **29**, 350-361 (2008).
114. Hergovich, A. & Hemmings, B.A. Mammalian NDR/LATS protein kinases in hippo tumor suppressor signaling. *Biofactors* **35**, 338-345 (2009).
115. Hao, Y., Chun, A., Cheung, K., Rashidi, B. & Yang, X. Tumor suppressor LATS1 is a negative regulator of oncogene YAP. *J Biol Chem* **283**, 5496-5509 (2008).
116. Zhang, J., Smolen, G.A. & Haber, D.A. Negative regulation of YAP by LATS1 underscores evolutionary conservation of the Drosophila Hippo pathway. *Cancer Res* **68**, 2789-2794 (2008).
117. Li, Y. *et al.* Lats2, a putative tumor suppressor, inhibits G1/S transition. *Oncogene* **22**, 4398-4405 (2003).
118. McPherson, J.P. *et al.* Lats2/Kpm is required for embryonic development, proliferation control and genomic integrity. *EMBO J* **23**, 3677-3688 (2004).
119. Yabuta, N. *et al.* Lats2 is an essential mitotic regulator required for the coordination of cell division. *J Biol Chem* **282**, 19259-19271 (2007).
120. Visser, S. & Yang, X. LATS tumor suppressor: a new governor of cellular homeostasis. *Cell Cycle* **9**, 3892-3903 (2010).
121. Oka, T., Mazack, V. & Sudol, M. Mst2 and Lats kinases regulate apoptotic function of Yes kinase-associated protein (YAP). *J Biol Chem* **283**, 27534-27546 (2008).
122. Zhao, B. *et al.* Inactivation of YAP oncoprotein by the Hippo pathway is involved in cell contact inhibition and tissue growth control. *Genes Dev* **21**, 2747-2761 (2007).
123. Hunter, T. Protein kinases and phosphatases: the yin and yang of protein phosphorylation and signaling. *Cell* **80**, 225-236 (1995).

124. Erdmann, K.S. The protein tyrosine phosphatase PTP-Basophil/Basophil-like. Interacting proteins and molecular functions. *Eur J Biochem* **270**, 4789-4798 (2003).
125. Andersen, J.N. *et al.* Structural and evolutionary relationships among protein tyrosine phosphatase domains. *Mol Cell Biol* **21**, 7117-7136 (2001).
126. Abaan, O.D. & Toretsky, J.A. PTPL1: a large phosphatase with a split personality. *Cancer Metastasis Rev* **27**, 205-214 (2008).
127. Yeh, S.H. *et al.* Genetic characterization of fas-associated phosphatase-1 as a putative tumor suppressor gene on chromosome 4q21.3 in hepatocellular carcinoma. *Clin Cancer Res* **12**, 1097-1108 (2006).
128. Stenzel, N., Fetzer, C.P., Heumann, R. & Erdmann, K.S. PDZ-domain-directed basolateral targeting of the peripheral membrane protein FRMPD2 in epithelial cells. *J Cell Sci* **122**, 3374-3384 (2009).
129. Thomas, T., Voss, A.K. & Gruss, P. Distribution of a murine protein tyrosine phosphatase BL-beta-galactosidase fusion protein suggests a role in neurite outgrowth. *Dev Dyn* **212**, 250-257 (1998).
130. Herrmann, L., Dittmar, T. & Erdmann, K.S. The protein tyrosine phosphatase PTP-BL associates with the midbody and is involved in the regulation of cytokinesis. *Mol Biol Cell* **14**, 230-240 (2003).
131. Ungefroren, H. *et al.* FAP-1 in pancreatic cancer cells: functional and mechanistic studies on its inhibitory role in CD95-mediated apoptosis. *J Cell Sci* **114**, 2735-2746 (2001).
132. Ciccarelli, F.D., Bork, P. & Kerkhoff, E. The KIND module: a putative signalling domain evolved from the C lobe of the protein kinase fold. *Trends Biochem Sci* **28**, 349-352 (2003).
133. Chishti, A.H. *et al.* The FERM domain: a unique module involved in the linkage of cytoplasmic proteins to the membrane. *Trends Biochem Sci* **23**, 281-282 (1998).
134. Hamada, K., Shimizu, T., Matsui, T., Tsukita, S. & Hakoshima, T. Structural basis of the membrane-targeting and unmasking mechanisms of the radixin FERM domain. *EMBO J* **19**, 4449-4462 (2000).
135. Kennedy, M.B. Origin of PDZ (DHR, GLGF) domains. *Trends Biochem Sci* **20**, 350 (1995).
136. Sheng, M. & Sala, C. PDZ domains and the organization of supramolecular complexes. *Annu Rev Neurosci* **24**, 1-29 (2001).
137. Zimmermann, P. *et al.* PIP(2)-PDZ domain binding controls the association of syntenin with the plasma membrane. *Mol Cell* **9**, 1215-1225 (2002).
138. Freiss, G. & Chalbos, D. PTPN13/PTPL1: an important regulator of tumor aggressiveness. *Anticancer Agents Med Chem* **11**, 78-88 (2011).
139. Maekawa, K., Imagawa, N., Nagamatsu, M. & Harada, S. Molecular cloning of a novel protein-tyrosine phosphatase containing a membrane-binding domain and GLGF repeats. *FEBS Lett* **337**, 200-206 (1994).
140. Erdmann, K.S. *et al.* The Adenomatous Polyposis Coli-protein (APC) interacts with the protein tyrosine phosphatase PTP-BL via an alternatively spliced PDZ domain. *Oncogene* **19**, 3894-3901 (2000).
141. Banville, D., Ahmad, S., Stocco, R. & Shen, S.H. A novel protein-tyrosine phosphatase with homology to both the cytoskeletal proteins of the band 4.1 family and junction-associated guanylate kinases. *J Biol Chem* **269**, 22320-22327 (1994).
142. Sato, T., Irie, S., Kitada, S. & Reed, J.C. FAP-1: a protein tyrosine phosphatase that associates with Fas. *Science* **268**, 411-415 (1995).

143. Li, Y. *et al.* Negative regulation of Fas-mediated apoptosis by FAP-1 in human cancer cells. *Int J Cancer* **87**, 473-479 (2000).
144. Ungefroren, H. *et al.* Human pancreatic adenocarcinomas express Fas and Fas ligand yet are resistant to Fas-mediated apoptosis. *Cancer Res* **58**, 1741-1749 (1998).
145. Saras, J., Engström, U., Góñez, L.J. & Heldin, C.H. Characterization of the interactions between PDZ domains of the protein-tyrosine phosphatase PTPL1 and the carboxyl-terminal tail of Fas. *J Biol Chem* **272**, 20979-20981 (1997).
146. Cuppen, E., Nagata, S., Wieringa, B. & Hendriks, W. No evidence for involvement of mouse protein-tyrosine phosphatase-BAS-like Fas-associated phosphatase-1 in Fas-mediated apoptosis. *J Biol Chem* **272**, 30215-30220 (1997).
147. Yanagisawa, J. *et al.* The molecular interaction of Fas and FAP-1. A tripeptide blocker of human Fas interaction with FAP-1 promotes Fas-induced apoptosis. *J Biol Chem* **272**, 8539-8545 (1997).
148. Foehr, E.D., Lorente, G., Vincent, V., Nikolich, K. & Urfer, R. FAS associated phosphatase (FAP-1) blocks apoptosis of astrocytomas through dephosphorylation of FAS. *J Neurooncol* **74**, 241-248 (2005).
149. Gump, J.M. *et al.* Autophagy variation within a cell population determines cell fate through selective degradation of Fap-1. *Nat Cell Biol* **16**, 47-54 (2014).
150. Liu, X. *et al.* PTPN14 interacts with and negatively regulates the oncogenic function of YAP. *Oncogene* **32**, 1266-1273 (2013).
151. Couzens, A.L. *et al.* Protein interaction network of the mammalian Hippo pathway reveals mechanisms of kinase-phosphatase interactions. *Sci Signal* **6**, rs15 (2013).
152. Hagemann, N. *et al.* The serologically defined colon cancer antigen-3 interacts with the protein tyrosine phosphatase PTPN13 and is involved in the regulation of cytokinesis. *Oncogene* **32**, 4602-4613 (2013).
153. Lambert, J.P., Tucholska, M., Go, C., Knight, J.D. & Gingras, A.C. Proximity biotinylation and affinity purification are complementary approaches for the interactome mapping of chromatin-associated protein complexes. *J Proteomics* **118**, 81-94 (2015).
154. Cai, J., Maitra, A., Anders, R.A., Taketo, M.M. & Pan, D. β-Catenin destruction complex-independent regulation of Hippo-YAP signaling by APC in intestinal tumorigenesis. *Genes Dev* **29**, 1493-1506 (2015).
155. Scanlan, M.J. *et al.* Characterization of human colon cancer antigens recognized by autologous antibodies. *Int J Cancer* **76**, 652-658 (1998).
156. Neznanov, N., Neznanova, L., Angres, B. & Gudkov, A.V. Serologically defined colon cancer antigen 3 is necessary for the presentation of TNF receptor 1 on cell surface. *DNA Cell Biol* **24**, 777-785 (2005).
157. Sakagami, H., Hara, Y. & Fukaya, M. Interaction of serologically defined colon cancer antigen-3 with Arf6 and its predominant expression in the mouse testis. *Biochem Biophys Res Commun* **477**, 868-873 (2016).
158. McGough, I.J. *et al.* Identification of molecular heterogeneity in SNX27-retromer-mediated endosome-to-plasma-membrane recycling. *J Cell Sci* **127**, 4940-4953 (2014).
159. McGough, I.J. *et al.* Retromer Binding to FAM21 and the WASH Complex Is Perturbed by the Parkinson Disease-Linked VPS35(D620N) Mutation. *Curr Biol* **24**, 1678 (2014).
160. Meinhold-Heerlein, I. *et al.* Expression and potential role of Fas-associated phosphatase-1 in ovarian cancer. *Am J Pathol* **158**, 1335-1344 (2001).

161. Yao, H., Song, E., Chen, J. & Hamar, P. Expression of FAP-1 by human colon adenocarcinoma: implication for resistance against Fas-mediated apoptosis in cancer. *Br J Cancer* **91**, 1718-1725 (2004).
162. Wieckowski, E., Atarashi, Y., Stanson, J., Sato, T.A. & Whiteside, T.L. FAP-1-mediated activation of NF-kappaB induces resistance of head and neck cancer to Fas-induced apoptosis. *J Cell Biochem* **100**, 16-28 (2007).
163. Lee, S.H. *et al.* Expression of Fas and Fas-related molecules in human hepatocellular carcinoma. *Hum Pathol* **32**, 250-256 (2001).
164. Lee, S.H. *et al.* In vivo expression of soluble Fas and FAP-1: possible mechanisms of Fas resistance in human hepatoblastomas. *J Pathol* **188**, 207-212 (1999).
165. Schickel, R., Park, S.M., Murmann, A.E. & Peter, M.E. miR-200c regulates induction of apoptosis through CD95 by targeting FAP-1. *Mol Cell* **38**, 908-915 (2010).
166. Abaan, O.D. *et al.* PTPL1 is a direct transcriptional target of EWS-FLI1 and modulates Ewing's Sarcoma tumorigenesis. *Oncogene* **24**, 2715-2722 (2005).
167. Bompard, G., Martin, M., Roy, C., Vignon, F. & Freiss, G. Membrane targeting of protein tyrosine phosphatase PTPL1 through its FERM domain via binding to phosphatidylinositol 4,5-biphosphate. *J Cell Sci* **116**, 2519-2530 (2003).
168. Hogan, A. *et al.* The phosphoinositol 3,4-bisphosphate-binding protein TAPP1 interacts with syntrophins and regulates actin cytoskeletal organization. *J Biol Chem* **279**, 53717-53724 (2004).
169. Palmer, A. *et al.* EphrinB phosphorylation and reverse signaling: regulation by Src kinases and PTP-BL phosphatase. *Mol Cell* **9**, 725-737 (2002).
170. Myagmar, B.E. *et al.* PARG1, a protein-tyrosine phosphatase-associated RhoGAP, as a putative Rap2 effector. *Biochem Biophys Res Commun* **329**, 1046-1052 (2005).
171. Bompard, G., Puech, C., Prébois, C., Vignon, F. & Freiss, G. Protein-tyrosine phosphatase PTPL1/FAP-1 triggers apoptosis in human breast cancer cells. *J Biol Chem* **277**, 47861-47869 (2002).
172. Castilla, C. *et al.* PTPL1 and PKC δ contribute to proapoptotic signalling in prostate cancer cells. *Cell Death Dis* **4**, e576 (2013).
173. Lai, Y.J., Lin, W.C. & Lin, F.T. PTPL1/FAP-1 negatively regulates TRIP6 function in lysophosphatidic acid-induced cell migration. *J Biol Chem* **282**, 24381-24387 (2007).
174. Mohseni, M. *et al.* A genetic screen identifies an LKB1-MARK signalling axis controlling the Hippo-YAP pathway. *Nat Cell Biol* **16**, 108-117 (2014).
175. Sharma, S. in Biomedical Sciences, Vol. PhD (The University of Sheffield, 2016).
176. Sharma, S. *et al.* Apoptotic signalling targets the post-endocytic sorting machinery of the death receptor Fas/CD95. *Nat Commun* **10**, 3105 (2019).
177. Ran, F.A. *et al.* Genome engineering using the CRISPR-Cas9 system. *Nat Protoc* **8**, 2281-2308 (2013).
178. Razi, M. & Futter, C.E. Distinct roles for Tsg101 and Hrs in multivesicular body formation and inward vesiculation. *Mol Biol Cell* **17**, 3469-3483 (2006).
179. Kostaras, E. *et al.* SARA and RNF11 interact with each other and ESCRT-0 core proteins and regulate degradative EGFR trafficking. *Oncogene* **32**, 5220-5232 (2013).
180. Raiborg, C., Malerød, L., Pedersen, N.M. & Stenmark, H. Differential functions of Hrs and ESCRT proteins in endocytic membrane trafficking. *Exp Cell Res* **314**, 801-813 (2008).
181. Peden, A.A. *et al.* The RCP-Rab11 complex regulates endocytic protein sorting. *Mol Biol Cell* **15**, 3530-3541 (2004).

182. Marley, A. & von Zastrow, M. Dysbindin promotes the post-endocytic sorting of G protein-coupled receptors to lysosomes. *PLoS One* **5**, e9325 (2010).
183. Huttlin, E.L. *et al.* The BioPlex Network: A Systematic Exploration of the Human Interactome. *Cell* **162**, 425-440 (2015).
184. Mead, C.L. *et al.* Cytosolic protein interactions of the schizophrenia susceptibility gene dysbindin. *J Neurochem* **113**, 1491-1503 (2010).
185. Rosciglione, S., Thériault, C., Boily, M.O., Paquette, M. & Lavoie, C. G α s regulates the post-endocytic sorting of G protein-coupled receptors. *Nat Commun* **5**, 4556 (2014).
186. Li, W. *et al.* Hermansky-Pudlak syndrome type 7 (HPS-7) results from mutant dysbindin, a member of the biogenesis of lysosome-related organelles complex 1 (BLOC-1). *Nat Genet* **35**, 84-89 (2003).
187. Mullin, A.P., Gokhale, A., Larimore, J. & Faundez, V. Cell biology of the BLOC-1 complex subunit dysbindin, a schizophrenia susceptibility gene. *Mol Neurobiol* **44**, 53-64 (2011).
188. Cho, J.H. *et al.* Identification of the novel substrates for caspase-6 in apoptosis using proteomic approaches. *BMB Rep* **46**, 588-593 (2013).
189. Duclos, C., Lavoie, C. & Denault, J.B. Caspases rule the intracellular trafficking cartel. *FEBS J* **284**, 1394-1420 (2017).
190. Rhodes, D.R. *et al.* ONCOMINE: a cancer microarray database and integrated data-mining platform. *Neoplasia* **6**, 1-6 (2004).
191. Skrzypczak, M. *et al.* Modeling oncogenic signaling in colon tumors by multidirectional analyses of microarray data directed for maximization of analytical reliability. *PLoS One* **5** (2010).
192. Szász, A.M. *et al.* Cross-validation of survival associated biomarkers in gastric cancer using transcriptomic data of 1,065 patients. *Oncotarget* **7**, 49322-49333 (2016).
193. Soubrane, C. *et al.* A comparative study of Fas and Fas-ligand expression during melanoma progression. *Br J Dermatol* **143**, 307-312 (2000).
194. Elnemr, A. *et al.* Human pancreatic cancer cells disable function of Fas receptors at several levels in Fas signal transduction pathway. *Int J Oncol* **18**, 311-316 (2001).
195. Huang, W., Bei, L. & Eklund, E.A. Inhibition of Fas associated phosphatase 1 (Fap1) facilitates apoptosis of colon cancer stem cells and enhances the effects of oxaliplatin. *Oncotarget* **9**, 25891-25902 (2018).
196. Frankel, E.B. & Audhya, A. ESCRT-dependent cargo sorting at multivesicular endosomes. *Semin Cell Dev Biol* **74**, 4-10 (2018).
197. Szymanska, E., Budick-Harmelin, N. & Miaczynska, M. Endosomal "sort" of signaling control: The role of ESCRT machinery in regulation of receptor-mediated signaling pathways. *Semin Cell Dev Biol* **74**, 11-20 (2018).
198. Cuppen, E. *et al.* The zyxin-related protein TRIP6 interacts with PDZ motifs in the adaptor protein RIL and the protein tyrosine phosphatase PTP-BL. *Eur J Cell Biol* **79**, 283-293 (2000).
199. Fredriksson, K. *et al.* Proteomic analysis of proteins surrounding occludin and claudin-4 reveals their proximity to signaling and trafficking networks. *PLoS One* **10**, e0117074 (2015).
200. Hergovich, A. Regulation and functions of mammalian LATS/NDR kinases: looking beyond canonical Hippo signalling. *Cell Biosci* **3**, 32 (2013).
201. Yi, J. *et al.* Members of the Zyxin family of LIM proteins interact with members of the p130Cas family of signal transducers. *J Biol Chem* **277**, 9580-9589 (2002).

202. Cuppen, E., van Ham, M., Pepers, B., Wieringa, B. & Hendriks, W. Identification and molecular characterization of BP75, a novel bromodomain-containing protein. *FEBS Lett* **459**, 291-298 (1999).
203. Chiu, Y.H., Lee, J.Y. & Cantley, L.C. BRD7, a tumor suppressor, interacts with p85 α and regulates PI3K activity. *Mol Cell* **54**, 193-202 (2014).
204. Zhan, H. *et al.* Tumour-suppressive role of PTPN13 in hepatocellular carcinoma and its clinical significance. *Tumour Biol* **37**, 9691-9698 (2016).
205. Drost, J. *et al.* BRD7 is a candidate tumour suppressor gene required for p53 function. *Nat Cell Biol* **12**, 380-389 (2010).
206. Si, Y. *et al.* Src Inhibits the Hippo Tumor Suppressor Pathway through Tyrosine Phosphorylation of Lats1. *Cancer Res* **77**, 4868-4880 (2017).
207. Iida, S. *et al.* Tumor suppressor WARTS ensures genomic integrity by regulating both mitotic progression and G1 tetraploidy checkpoint function. *Oncogene* **23**, 5266-5274 (2004).
208. Yang, X. *et al.* LATS1 tumour suppressor affects cytokinesis by inhibiting LIMK1. *Nat Cell Biol* **6**, 609-617 (2004).
209. Furth, N. *et al.* Down-regulation of LATS kinases alters p53 to promote cell migration. *Genes Dev* **29**, 2325-2330 (2015).